MAGNETOM Flash

Issue Number 86 · 1/2024
SCMR Edition

magnetomworld.siemens-healthineers.com

SIEMENS
Healthineers

3D Whole-Heart[1] imaging

3D Whole-Heart[1] applications:
Angiography and delayed enhancement

Ferumoxytol-enhanced[3] 4D MRI
in pediatric[2] and adult CHD

[1]Work in progress. The application is currently under development and is not for sale in the U.S. and in other countries. Its future availability cannot be ensured.
[2]MR scanning has not been established as safe for imaging fetuses and infants less than two years of age. The responsible physician must evaluate the benefits of the MR examination compared to those of other imaging procedures.
[3]Ferumoxytol is not approved for diagnostic applications and its use for MRI is off-label.

46

Non-contrast, sedation-free neonatal[2] feed and wrap cardiac MRI

54

BioMatrix Beat Sensor: Cardiac MRI exams without ECG leads

62

Compendium Medicine Cardiac Amyloidosis

Cardiac Imaging

Meet Siemens Healthineers

Claudia Prieto received her Ph.D. from the Pontificia Universidad Católica de Chile in 2007. From 2008 to 2011 she was a Postdoctoral Research Fellow in the Division of Imaging Sciences at Kings College London, UK. In 2012, she joined the School of Biomedical Engineering at Kings College London as Lecturer where she is currently Professor in Medical Imaging. She is Professor and Director for Research and Innovation at the School of Engineering at Pontificia Universidad Católica de Chile.

Dr. Prieto was a board member of the Society for Cardiovascular Magnetic Resonance from 2021 to 2023 and is the abstract co-chair of the CMR 2024. She is a board member of the Society for Magnetic Resonance Angiography (SMRA) and co-organizer of the 2024 SMRA meeting. Dr. Prieto is currently Associate Editor of the journal Magnetic Resonance in Medicine and has authored more than 150 peer-reviewed original and review articles and 10 book chapters in the field of cardiac magnetic resonance. She also holds 6 patents and is an editor of a textbook on Magnetic Resonance Image Reconstruction.

René Botnar received his Ph.D. from the ETH Zurich, Switzerland. From 1996 to 97 he was a Research Associate in the Department of Radiology at the University Zurich. In 1997, he joined the Cardiac MR Center at the Beth Israel Deaconess Medical Center and became its Scientific Director in 2003. He subsequently was appointed to Assistant Professor of Medicine at Harvard Medical School in 2004.

In 2005, Dr. Botnar accepted a Professorship of Biomedical Imaging at the Technische Universität München. At the end of 2007, he joined the School of Biomedical Engineering & Imaging Sc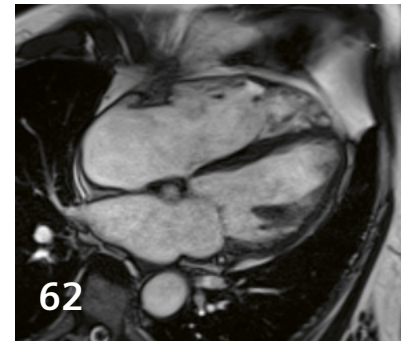iences at King's College London where he is currently Chair of Cardiovascular Imaging. In 2022 he joined Pontificia Universidad Católica de Chile where he is currently Director of the Institute of Biological and Medical Engineering. Dr. Botnar is a Fellow of the International Society of Magnetic Resonance Imaging in Medicine, the Society for Cardiovascular Magnetic Resonance, and the Institute for Advanced Study at the TU Munich. He was a board member of the Society for Cardiovascular Magnetic Resonance from 2008 to 2011 and currently is a co-organizer of the SMRA 2024 annual meeting. He is currently Associate Editor of the Journal of Cardiac Magnetic Resonance and has authored more than 320 peer-reviewed original papers, 50 review articles and 30 book chapters in the field of cardiac magnetic resonance. He also holds 12 patents and is an editor of a textbook on Cardiovascular Magnetic Resonance Imaging.

The Power of Collaboration

Dear Readers and Colleagues,

Welcome to London and this exciting new edition of MAGNETOM Flash, which is dedicated to the joint SCMR, EACVI and ESCR meeting. CMR 2024 convenes physicists, engineers, technologists, radiologists, cardiologists, and industry, under the theme 'The Global CMR Conference: Together – expanding CMR worldwide!'. This theme highlights one of the most distinct aspects of our community that has shaped the history of cardiovascular magnetic resonance imaging: the power of working together.

Since the early conceptualization of MRI in the 70's, through the acquisition of the first images of the heart anatomy in the mid 80's, to several breakthroughs to enable functional assessment and tissue characterization in the 90's and early 2000, and the further advances nowadays; the power of collaboration, interdisciplinary expertise and collective efforts has been fundamental in translating technical developments into meaningful clinical applications and wider clinical acceptance of cardiovascular MRI.

Collaboration between scientists and clinicians is fundamental to developing solutions that address technical challenges while meeting clinical needs. Long exam times, limited spatial and temporal resolution, limited 2D coverage, complex scan planning and the need for patient cooperation, are some of several remaining challenges in cardiovascular MRI. These technical and clinical challenges drive the development of exciting advances in terms of novel imaging sequences, motion correction and reconstruction approaches, novel exogenous and endogenous contrasts, efficient scans, multidimensional and multiparametric sequences, as well as image processing and analysis, among others.

This scientist-physician collaboration is also fundamental to evaluate and validate these innovations, first in academic clinical settings, providing valuable feedback on the strengths, limitations, and potential clinical impact of the new techniques. Subsequent collaboration with industry

partners enables the translation of these innovations into tangible technologies, facilitating the validation of new techniques in various clinical settings and in different countries and continents. Finally, the expertise of industry facilitates scaling up innovations, quality control, and regulatory compliance, which is essential for the successful transition of scientific discoveries into commercially viable and widely accessible cardiac MRI technologies and to the establishment of evidence-based guidelines for clinical use.

In this issue of MAGNETOM Flash, we find an exciting collection of articles showcasing the power of interdisciplinary collaboration in pushing the boundaries of cardiovascular MRI.

One of the three main topics of this issue is whole-heart MRI[1], which has been one of the remaining challenges of CMR for many years and was born in the early 90s with the desire of imaging the coronary arteries non-invasively with high-spatial resolution as a non-invasive alternative to X-ray coronary angiography. While the first demonstration by Manning and Edelman et al. in 1991 employed breath-holding in concert with ECG triggered fat suppressed 2D gradient echo imaging subsequent approaches employed free-breathing 3D coronary MR angiography (CMRA) with a thin 3D slab approach in concert with magnetization transfer contrast or T2 preparation enabling the visualisation of the proximal left and right coronary arteries without the need of a contrast agent. These free-breathing approaches were made possible using respiratory navigators first proposed by Ehman et al. in 1989 which for the first-time enabled achieving sub millimetre in-plane spatial resolution not possible with breath holding. While still being the state-of-art today on most clinical systems, unpredictable long scan times, residual motion artifacts and limited spatial resolution have limited the successes of 3D whole heart until today.

The article by Kunze et al. describes a new framework that our group at King's College London developed and that addresses the shortcomings of the diaphragmatic navigator approach. This novel 3D whole heart MRI sequence consists of an image navigator (iNAV)[1] for "model free" respiratory motion correction, a spiral like Cartesian trajectory with golden angle increment enabling respiratory data binning, and a non-rigid motion corrected image reconstruction enabling 100% respiratory scan efficiency, predictable scan times and isotropic resolution of $0.9 - 1.2 \text{ mm}^3$ in a 5 to 10-minute scan. Moreover, to further simplify the scanning procedure and selection of the inversion delay an AI assisted placement of the imaging, shim and navigator volume have been developed by a team of Siemens Healthineers scientists enabling the automated detection of the quiescent phase of the cardiac cycle. To test the robustness of the new 3D whole-heart approach in different healthcare systems validation has been performed in 3500 real world patients in 18 imaging centres on 4 continents. The article

demonstrates successful use of this novel approach to differentiate between myocardial infarction and fatty infiltration, identify potential ablation targets from 3D corridors of border zone tissue or the identification of coronary artery disease on sub-millimetre resolution 3D coronary MR angiograms. These achievements are a demonstration of the power of collaboration between MR physicists of and clinicians at the research stage, a demonstration of collaboration between academics and industry at the innovation and prototype implementation stage and finally the demonstration of collaboration between industry, academics, and clinical centres at the clinical validation stage. Despite all the greatness of modern technologies, human collaboration remains at the centre stage of any advance in knowledge and creation of innovative solutions, even more so in healthcare.

The second article of the 3D whole heart topic demonstrates the power of collaboration between Siemens Healthineers scientists and clinicians at a high-volume medical centre in Greece exploring the new whole-heart sequence for interventional planning in complex congenital heart disease patients or for pre-procedural non-invasive mapping of the arrhythmogenic substrate in patients with atrial fibrillation, in order to better guide ablations, and ultimately assessing post-procedural success. This study demonstrates that 3D whole-heart MRI not only can be used for improved diagnosis or treatment planning in CHD patients but also can simplify the scanning protocol, obviate the need for direct expert supervision and collectively shorten the scan time in these patients with often complex anatomies.

The last article on the topic 3D whole heart MRI demonstrates how the collaboration between Siemens Healthineers and the team at St. Francis Heart Hospital in New York led to a new application of the iNAV as a "fluoro trigger" where the iNAV is "misused" for monitoring the passage of contrast agent and to start the high resolution free-breathing 3D pulmonary angiography scan in which the iNAV is subsequently used in its indented form for respiratory motion correction and to achieve 100% respiratory scan efficiency. This last example demonstrates how the power of collaboration can unlock new applications by thinking out of the box. It is also a notable example of the way the MRI community has worked in the past 30–40 years, and which has kept our community so vibrant and innovative.

The second main topic of this issue is MR Angiography. From a collection of articles, I would draw attention to the article by Paul Finn and colleagues since it addresses another holy grail application in cardiac MRI, which is free-breathing multidimensional (space, time, and velocity) 3D imaging of pediatric patients[2] without sedation. Scanning these patients is very demanding due to the complex heart anatomy, the small size of the vessels and cardiac structure,

the high heart rates, and irregular breathing patterns. Typically, these exams require highly skilled teams with many years of experience, which usually are only available in advanced imaging centres in large metropolitan areas. In this study the UCLA team combines several ingredients such as

1) the use of a blood pool contrast agent, ferumoxytol[3] to prolong the imaging window and enable steady state imaging,
2) a novel free-running free-breathing self-gated 3D MRI sequence to obtain isotropic resolution multi heart phase images and
3) a compressed sensing accelerated 4D flow sequence[4] with diaphragmatic navigation.

The entire exam using this approach can be performed without breath holding and complex planning procedure and can be acquired in less than 30 minutes in comparison to the 60–90 minutes, which a complex CHD exam usually requires. What made this new exam possible is again the power of collaboration between scientists, industry, and clinicians. Each of the three ingredients of this CHD exam required several interdisciplinary teams to create innovative solutions. It also demonstrates that it takes many years of work to bring innovative ideas to fruition. Intravascular contrast agents were first proposed and demonstrated in clinical efficacy trials in the mid-90s, but it took almost 30 years until we start harvesting the fruits of this hard labour. Moreover, to fully exploit the potential of blood pool contrast agents it also required the development of free-breathing 3D whole-heart technology which equally almost took the same time to be ready for prime clinical use. One of the important lessons learned from the whole-heart articles in this MAGNETOM Flash edition is that collaboration allows us to move mountains and that we need to be persistent and patient to harvest the fruits of the challenging work, which is required to achieve ambitious goals.
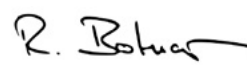
The third main topic of this issue is cardiac imaging. An article that stands out is the BioMatrix Beat Sensor which enables cardiac MRI exams without ECG Leads. The Beat Sensor started as a curious engineering project within the Siemens Healthineers cardiac predevelopment team, but quickly developed into a hot topic as there was a clear

clinical need for ECG lead less cardiac imaging due to difficulty of obtaining a good ECG trace in specific patient populations and due to the lack of highly trained cardiac MR technicians outside of academic clinical centres. The success of the BioMatrix Beat Sensor would again not have been possible without collaboration within Siemens Healthineers among engineers and the applications team and without the collaboration between Siemens Healthineers scientists and university academics and clinicians to demonstrate early in the development phase the true clinical potential of this unique and ingenious invention. The article by Mizuno and colleagues provides a good technical background into the working of the Beat Sensor and how its signal compares with the ECG signal for various cardiac diseases including hypertrophic cardiomyopathy, single ventricle, reduced LV ejection fraction, atrial fibrillation with low heart rates, atrial fibrillation with high heart rates, and pacing rhythm. The images presented are of excellent quality for a lead less scan and are very much comparable to ECG triggered cardiac scans. What makes this article special is the rapid clinical translation of a completely novel technology requiring new hardware and software in less than 10 years.

There are many more outstanding contributions in this issue of MAGNETOM Flash that we could not cover in this editorial, but we hope that the readers will enjoy this special SCMR 2024 edition, which highlights several progresses made since and thanks to the creation of our main scientific societies. This issue also highlights the power of CMR to be the ultimate cardiac imaging technology due to its unique potential to provide a fast comprehensive exam including radiation free assessment of anatomy, function, and tissue characterization in an ever-increasing spectrum of heart diseases. We hope you enjoy this issue as much as we did and hope to see you all during the CMR 2024 conference in London!

Claudia Prieto

R. Botnar

Claudia Prieto

René Botnar

---

[1] *Work in progress. The application is currently under development and is not for sale in the U.S. and in other countries. Its future availability cannot be ensured.*
[2] *MR scanning has not been established as safe for imaging fetuses and infants less than two years of age. The responsible physician must evaluate the benefits of the MR examination compared to those of other imaging procedures.*
[3] *Ferumoxytol is not approved for diagnostic applications and its use for MRI is off-label.*
[4] *The authors are using a non-product sequence, but 4D Flow has been available as a product since software version syngo MR XA30.*

3D Whole-Heart Imaging: An Innovative Collaborative Solution

Karl P. Kunze[1,2], Jens Wetzl[3], Seung Su Yoon[3], Radhouene Neji[2], Gaia Banks[3], Rene Botnar[2,4,5], Claudia Prieto[2,4], Michaela Schmidt[3]

[1]MR Research Collaborations, Siemens Healthcare Limited, Camberley, United Kingdom
[2]School of Biomedical Engineering and Imaging Sciences, King's College London, United Kingdom
[3]Cardiovascular MR Predevelopment, Siemens Healthcare GmbH, Erlangen, Germany
[4]Escuela de Ingeniería, Pontificia Universidad Católica de Chile, Santiago, Chile
[5]Institute for Biological and Medical Engineering, Pontificia Universidad Católica de Chile, Santiago, Chile

Clinical need

A broad spectrum of clinical use cases for cardiovascular magnetic resonance imaging (CMR) profit from high isotropic resolution in three dimensions to show thoracic vasculature including the small and tortious coronary artery vessels and fibrosis/myocardial viability using the late gadolinium enhancement (LGE) measurement technique. Recent clinical studies have demonstrated the value of free-breathing, high-isotropic-resolution CMR to diagnose ischemic heart disease using coronary artery and vein [1, 2] or LGE imaging [3], cardiomyopathy [4], congenital [5] and structural [6] heart disease, and ablation lesion assessment [7].

Challenges

One challenge of using a high isotropic resolution in the range of 1 mm³ to 1.3 mm³ in the context of CMR exams is the prolonged scan time when compared to other imaging methods. Although CMR has several benefits including high tissue contrast and no need for radiation, it remains a comparatively slow imaging modality. For whole-heart coverage with high isotropic resolution, a novel imaging strategy is required to complete scans in 5 to 10 minutes.

Ideally, these measurements should be acquired in free breathing. Hence, cardiac and respiratory motion must be addressed. To minimize cardiac motion, scanning should be performed during a time in the cardiac cycle when the heart is in its quiescent phase, usually at end-diastole with a window of 80–160 ms, depending on the heart rate. To find the still phase of the heart, a 4-chamber cine is usually acquired. An experienced operator needs to manually define it and then enter it correctly in the 3D measurement protocol.

To account for respiratory motion, navigators are typically used to scan during free breathing. The frequently used 1D cross-paired diaphragm navigators are manually placed on the liver dome, and imaging data are accepted only in end-expiration. Depending on the breathing pattern, the acceptance rate can be between 20% and 60%. Therefore, scan time is unpredictable upfront, and a drift in breathing pattern during the scan may further decrease acquisition efficiency.

Moreover, accepting data only in end-diastole and in end-expiration makes data sampling very inefficient. Long scan times result in high institutional costs and are a discomfort for sick patients, meaning they can result in patient movement (reduced patient compliance) and non-diagnostic images.

One method to overcome this hurdle is the "free-running" acquisition approach, which samples and uses all data irrespective of the breathing and cardiac-motion states, with separation of these during image reconstruction [8, 9]. While this single-click method has numerous benefits that have been shown in multiple publications, it has not yet been widely distributed and tested clinically because it requires high-end computing, long reconstruction times, and often the use of contrast agent.

Another way to account for respiratory motion is to use image-based navigators [10] combined with non-rigid motion-compensated reconstruction. This enables predictable scan times and an acceptance rate of 100% of data irrespective of the breathing position. When combined with novel undersampling strategies [11, 12], a scan time of 5 to 8 minutes is possible, while the reconstruction only needs to address respiratory-motion compensation and *k*-space undersampling.

3D Whole Heart is work in progress. The application is currently under development and is not for sale in the U.S. and in other countries. Its future availability cannot be ensured.

A third challenge for 3D imaging is the workflow, including positioning of multiple objects like navigators, saturation bands, and imaging volume, and determining the appropriate resting phase in the cardiac cycle as mentioned above. For the LGE measurements, correctly estimating inversion time (TI) to null healthy myocardium is yet another task for operators.
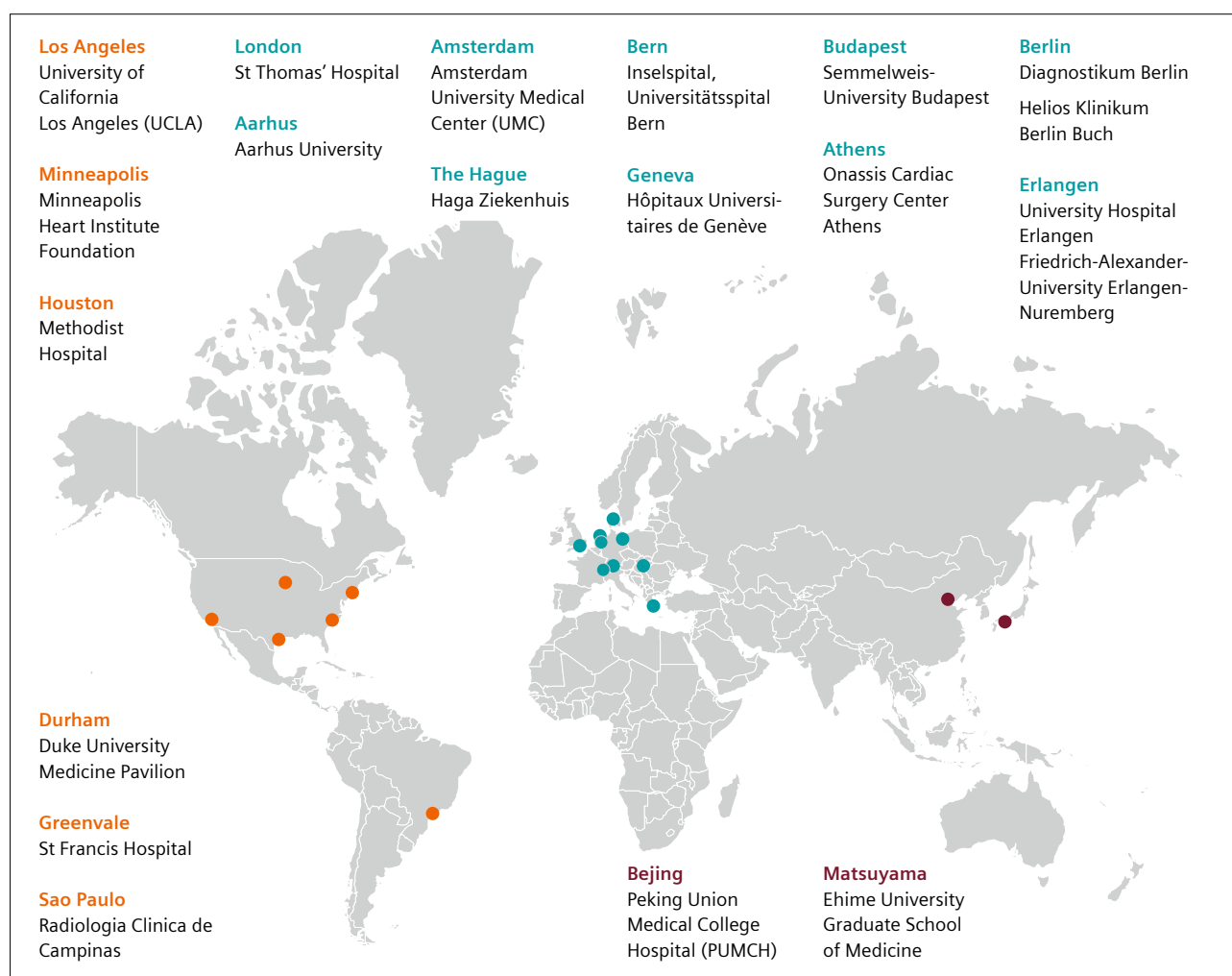
Finally, robust fat saturation is key for high-contrast display of the coronary arteries, as they are embedded in epicardial fat. For certain LGE applications, the separation of fat and water is also essential, e.g., in patients with pericarditis or small endomyocardial fibrosis, where it can be difficult to distinguish between fat and lesion.

The solution

To overcome the limitations of 1D diaphragmatic naviga-tors, 2D image navigators (iNAV) have been proposed to enable direct tracking of the impact of respiratory motion on the heart [9]. With iNAV imaging, it is possible to derive accurate quantitative motion information in two spatial dimensions. This enables retrospective motion correction rather than prospective gating, resulting in 100% respi-ratory scan efficiency and predictable scan times.

While iNAV imaging allows for direct correction of beat-to-beat translational respiratory motion in a predefined image region, accounting for non-rigid motion during the breathing cycle requires a more complex, non-rigid motion-compensated reconstruction framework. A first step in such approaches is often data binning, followed by reconstruction of different bin images repre-senting the different respiratory motion states present in the data. As each bin image only contains a small fraction of the already undersampled 3D acquisition, reconstruction of the individual bin images requires a well-designed inter-play of acquisition patterns and reconstruction algorithms.

Los Angeles
University of California
Los Angeles (UCLA)

Minneapolis
Minneapolis Heart Institute Foundation

Houston
Methodist Hospital

London
St Thomas' Hospital

Aarhus
Aarhus University

Amsterdam
Amsterdam University Medical Center (UMC)

The Hague
Haga Ziekenhuis

Bern
Inselspital, Universitätsspital Bern

Geneva
Hôpitaux Universi-taires de Genève

Budapest
Semmelweis-University Budapest

Athens
Onassis Cardiac Surgery Center Athens

Berlin
Diagnostikum Berlin

Helios Klinikum Berlin Buch

Erlangen
University Hospital Erlangen
Friedrich-Alexander-University Erlangen-Nuremberg

Durham
Duke University Medicine Pavilion

Greenvale
St Francis Hospital

Sao Paulo
Radiologia Clinica de Campinas

Bejing
Peking Union Medical College Hospital (PUMCH)

Matsuyama
Ehime University Graduate School of Medicine

1 **Clinical partners for validating the 3D Whole-Heart application**
Our clinical partners helped us by sharing their experience so we could improve the research sequence and make it robust for a wide range of clinical questions and settings.

The variable-density Cartesian trajectory with spiral profile order sampling (VD-CASPR) [11, 12] provides high overall undersampling factors while maintaining favorable undersampling properties when data is split up into respiratory bins, enabling regularized reconstruction of artifact-free respiratory bin images [13]. These bin images can then be used to estimate 3D non-rigid motion between the motion states they represent, and motion information can be used in a final, non-rigid motion-compensated reconstruction of all data [14, 15]. Despite the large number of steps involved, the computational burden in the form of reconstruction time can be minimized to orders of 1 to 2 minutes using implementations with modern GPU technology [16].

In addition to standard chemical shift-based fat saturation methods, the described approach can be combined with Dixon-based fat-water separation. This provides a means to achieve robust elimination of fat from the final water-only image [17, 18], while also providing a fat-only image that can enable, e.g., discrimination between bright myocardial scar signal and fatty infiltration (Figure 2). Dixon fat-water separation enables improved visualisation of the coronary arteries [18], especially at 3T.

Workflow automation

As previously described, whole-heart imaging has typically increased the workload and requires more experienced operators given the need for precise positioning of saturation bands, image navigator, resting phase, and potentially TI. Together with the novel whole-heart sequence, we now offer workflow support for many of the planning steps that previously required manual user input.

In the following, we describe three modules for automating common planning tasks: AutoPositioning (for placement of graphical objects, e.g., the imaging volume, navigator, saturation bands) [19]; AutoRestingPhase (to determine a suitable acquisition window during the quiescent period in the cardiac cycle) [20]; and AutoTI (to set the proper inversion time for subsequent LGE imaging) [21].

AutoPositioning is based on localizer scans in coronal and transversal orientations. It uses deep learning to detect multiple anatomical structures, including the location and size of the heart and left ventricle, as well as the location of the liver dome and the arms. These are used to automatically perform the subsequent planning steps. Based on an initial localizer, the heart is placed into the isocenter, and further localizers centered on the heart can be acquired. Slices for thorax overview imaging and the AutoAlign scout can be positioned. For the whole-heart sequence, the imaging volume including slice coverage and position of the image navigator and saturation bands can be set automatically.

AutoRestingPhase is based on a 4-chamber-view cine to determine the quiescent phases of different cardiac structures within the cardiac cycle. First, the right coronary artery (RCA) and the four chambers of the heart are automatically detected. Subsequently, their motion throughout the cardiac cycle is tracked via image registration and then quantified and displayed as a motion curve. The valleys in this motion curve serve as suggestions for the whole-heart acquisition window. Different types of whole-heart acquisition can use the resting phase results of different anatomies of interest, e.g., the RCA for T2-prepared angiography or the left ventricle for 3D LGE.
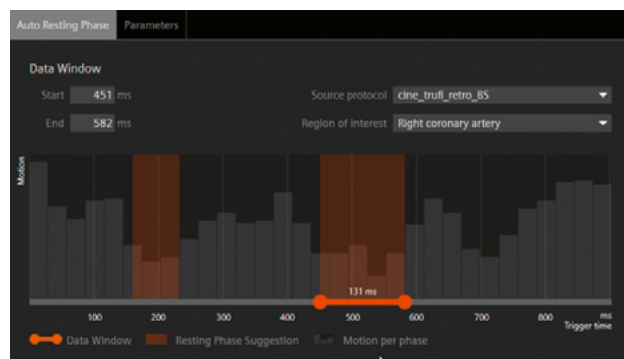
AutoTI is based on a TI scout in short-axis orientation, which is segmented to find the myocardial and blood-pool intensity values at each inversion time. The minimum of the myocardial intensity curve is first used to determine a TI with optimal myocardial nulling, then refined by finding an adjacent TI time with improved blood-myocardium contrast in case both have their zero crossings at similar times. An offset can then be applied automatically to subsequent LGE acquisitions to account for the time between TI scout and LGE acquisitions. This is applicable both to conventional 2D LGE and the novel 3D LGE acquisition.
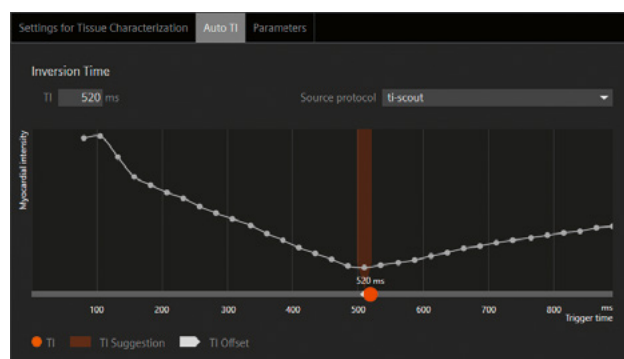
The combination of these modules significantly reduces the complexity and workload involved in performing high-quality whole-heart acquisitions, and simplifies or even improves the entire scan workflow.
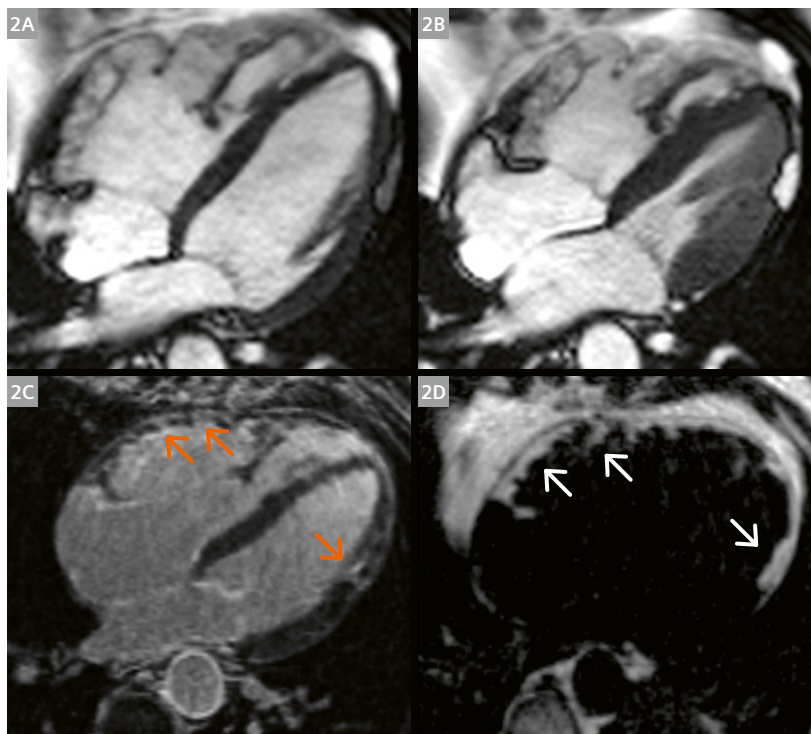
2 A 60-year-old male patient with fibrofatty replacement in LGE of the free wall of the RV and LV. Cine imaging 4-chamber view in a diastolic phase **(2A)** and systolic phase **(2B)**. The 3D whole-heart technique allows a differentiation between fibrosis **(2C)** in water-only LGE images and fat deposits **(2D)** in fat-only images. Fat deposition is depicted by the white arrows. Fibrosis is depicted by the orange arrows.

CMR imaging was performed on a 1.5 Tesla scanner (MAGNETOM Avanto fit, Siemens Healthcare, Erlangen, Germany) using cine imaging steady-state free precession (SSFP). After application of gadolinium-based contrast media (gadoteridol 0.2 mmol/kg), image-based navigated 3D whole-heart LGE sequence with fat–water separation was performed.

Images courtesy of Edyta Blaszczyk, MD[1,2,3], and Jeanette Schulz-Menger, MD[1,2,3,4]

[1]Charité – Universitätsmedizin Berlin, corporate member of Freie Universität Berlin and Humboldt-Universität zu Berlin, ECRC Experimental and Clinical Research Center, Berlin, Germany. [2]Working Group on Cardiovascular Magnetic Resonance, Experimental and Clinical Research Center, a joint cooperation between Charité Medical Faculty and the Max-Delbrück Center for Molecular Medicine. [3]DZHK (German Centre for Cardiovascular Research), partner site Berlin, Germany. [4]HELIOS Hospital Berlin-Buch, Department of Cardiology and Nephrology, Berlin, Germany.
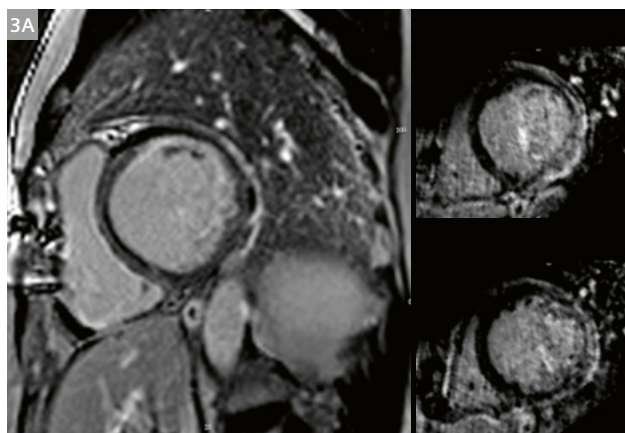
3 53-year-old male patient. **(3A)** Sustained VTs, MVR (MVP), DCM like phenotype of HF. **(3B)** Identify potential ablation targets from 3D corridors of border zone tissue and verify the detected corridors directly with the DICOM images. **(3C)** Import pre-procedural imaging into any electroanatomic mapping (EAM) system. Agreement of the structural arrhythmogenic substrate detected as corridors by CMR 3D LGE and the sites of electrical channels that may serve as the isthmus of VT. Late potentials and local abnormal ventricular activities at the areas of structural VT corridors.

CMR imaging was performed on a 1.5 Tesla MAGNETOM Sola (Siemens Healthcare, Erlangen, Germany).

Images courtesy of Evangelia Nyktari, M.D. (CMR); Athanasios Saplaouras, M.D. (EP lab); Konstantinos Letsas, M.D., Ph.D. (EP lab); Michalis Efremidis, M.D., Ph.D. (EP Lab); P Rozos and S Zarkadoulas (CMR) at Onassis Cardiac Surgery Center, Athens, Greece.
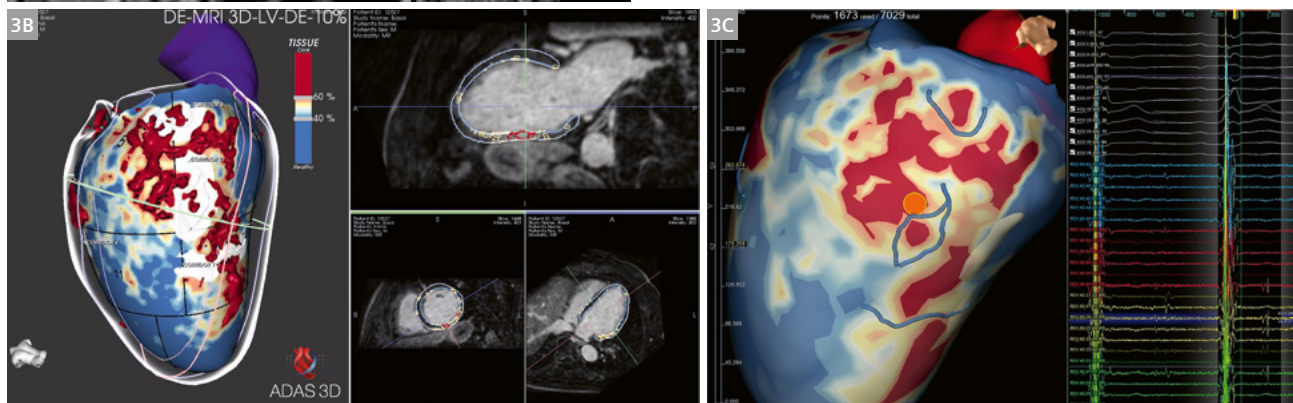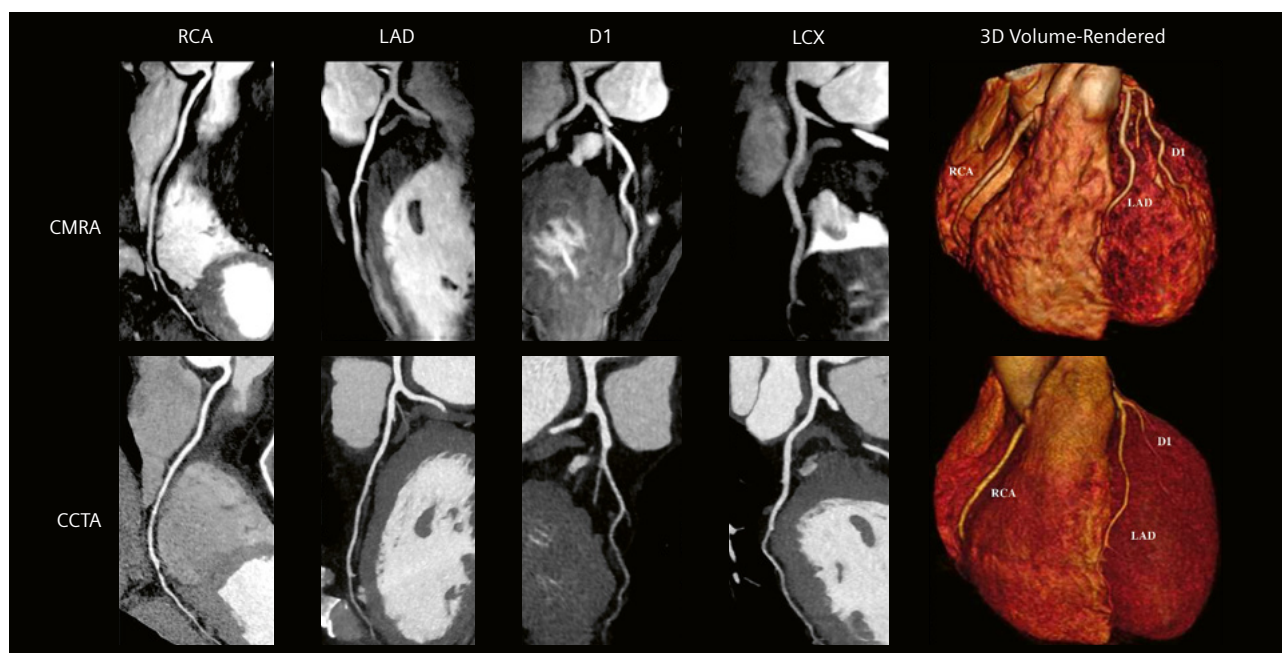
4 Curved multiplanar reformat and 3D volume-rendered non-contrast CMRA and contrast-enhanced CCTA in a 54-year-old male with no significant stenosis.
Abbreviations: CMRA = coronary magnetic resonance angiography; CCTA = coronary computed tomography angiography; RCA = right coronary artery; LAD = left anterior descending artery; D1 = first diagonal artery; LCX = left circumflex artery. CMR imaging was performed on a 1.5 Tesla MAGNETOM Aera (Siemens Healthcare, Erlangen, Germany).
Images courtesy of Reza Hajhosseiny, M.D.[1]; Aurélien Bustin, Ph.D.[1]; Imran Rashid, M.D., Ph.D., FRACP[1]; Gastao Cruz, Ph.D.[1]; Ronak Rajani, M.D., Ph.D., FACC, FRCP[2]; Claudia Prieto, Ph.D.[1]; René M. Botnar, Ph.D.[1]; et al.
Adapted and reproduced from Hajhosseiny et al. [22].

[1]*School of Biomedical Engineering and Imaging Sciences, King's College London, United Kingdom*
[2]*School of Cardiovascular Medicine and Sciences, King's College London, United Kingdom*

Technical partner for developing the 3D Whole-Heart application

The whole-heart imaging sequence, image navigator, and image reconstruction framework described here were developed in close collaboration with the research groups of Professor René Botnar and Professor Claudia Prieto at King's College London, UK.

Conclusion and outlook

Clinical validation, resp. research studies, and feedback from numerous global sites indicate that implementing the novel 3D Whole-Heart sequence from Siemens Healthineers makes scans with whole-heart coverage and high isotropic resolution routinely possible in 5 to 10 minutes. Given the high level of automation available to support operators and achieve faster scan times, we expect rapid clinical adoption.

References

1 Hajhosseiny R, Rashid I, Bustin A, Munoz C, Cruz G, Nazir MS, et al. Clinical comparison of sub-mm high-resolution non-contrast coronary CMR angiography against coronary CT angiography in patients with low-intermediate risk of coronary artery disease: a single center trial. J Cardiovasc Magn Reson. 2021;23(1):57.
2 Nazir MS, Bustin A, Hajhosseiny R, Yazdani M, Ryan M, Vergani V, et al. High-resolution non-contrast free-breathing coronary cardiovascular magnetic resonance angiography for detection of coronary artery disease: validation against invasive coronary angiography. J Cardiovasc Magn Reson. 2022;24(1):26.
3 Peters AA, Wagner B, Spano G, Haupt F, Ebner L, Kunze KP, et al. Myocardial scar detection in free-breathing Dixon-based fat- and water-separated 3D inversion recovery late-gadolinium enhancement whole heart MRI. Int J Cardiovasc Imaging. 2023;39(1):135-144.
4 Bustin A, Hua A, Milotta G, Jaubert O, Hajhosseiny R, Ismail TF, et al. High-Spatial-Resolution 3D Whole-Heart MRI T2 Mapping for Assessment of Myocarditis. Radiology. 2021;298(3):578-586.
5 Fotaki A, Pushparajah K, Hajhosseiny R, Schneider A, Alam H, Ferreira J, et al. Free-breathing, Contrast Agent-free Whole-Heart MTC-BOOST Imaging: Single-Center Validation Study in Adult Congenital Heart Disease. Radiol Cardiothorac Imaging. 2023;5(1):e220146.

6   Toupin S, Pezel T, Bustin A, Cochet H. Whole-Heart High-Resolution Late Gadolinium Enhancement: Techniques and Clinical Applications. J Magn Reson Imaging. 2022;55(4):967-987.

7   Sim I, Razeghi O, Karim R, Chubb H, Whitaker J, O'Neill L, et al. Reproducibility of Atrial Fibrosis Assessment Using CMR Imaging and an Open Source Platform. JACC Cardiovasc Imaging. 2019;12(10):2076-2077.

8   Di Sopra L, Piccini D, Coppo S, Stuber M, Yerly J. An automated approach to fully self-gated free-running cardiac and respiratory motion-resolved 5D whole-heart MRI. Magn Reson Med. 2019;82(6):2118-2132.

9   Roy CW, Di Sopra L, Whitehead KK, Piccini D, Yerly J, Heerfordt J, et al. Free-running cardiac and respiratory motion-resolved 5D whole-heart coronary cardiovascular magnetic resonance angiography in pediatric cardiac patients using ferumoxytol. J Cardiovasc Magn Reson. 2022;24(1):39.

10 Henningsson M, Koken P, Stehning C, Razavi R, Prieto C, Botnar RM. Whole-heart coronary MR angiography with 2D self-navigated image reconstruction. Magn Reson Med. 2012;67(2):437-445.

11 Prieto C, Doneva M, Usman M, Henningsson M, Greil G, Schaeffter T, et al. Highly efficient respiratory motion compensated free-breathing coronary MRA using golden-step Cartesian acquisition. J Magn Reson Imaging. 2015;41(3):738-746.

12 Bustin A, Rashid I, Cruz G, Hajhosseiny R, Correia T, Neji R, et al. 3D whole-heart isotropic sub-millimeter resolution coronary magnetic resonance angiography with non-rigid motion-compensated PROST. J Cardiovasc Magn Reson. 2020;22(1):24.

13 Correia T, Ginami G, Cruz G, Neji R, Rashid I, Botnar RM, et al. Optimized respiratory-resolved motion-compensated 3D Cartesian coronary MR angiography. Magn Reson Med. 2018;80(6):2618-2629.

14 Batchelor PG, Atkinson D, Irarrazaval P, Hill DL, Hajnal J, Larkman D. Matrix description of general motion correction applied to multishot images. Magn Reson Med. 2005;54(5):1273-1280.

15 Cruz G, Atkinson D, Henningsson M, Botnar RM, Prieto C. Highly efficient nonrigid motion-corrected 3D whole-heart coronary vessel wall imaging. Magn Reson Med. 2017;77(5):1894-1908.

16 Zeilinger MG, Kunze KP, Munoz C, Neji R, Schmidt M, Croisille P, et al. Non-rigid motion-corrected free-breathing 3D myocardial Dixon LGE imaging in a clinical setting. Eur Radiol. 2022;32(7):4340-4351.

17 Munoz C, Cruz G, Neji R, Botnar RM, Prieto C. Motion corrected water/fat whole-heart coronary MR angiography with 100% respiratory efficiency. Magn Reson Med. 2019;82(2):732-742.

18 Munoz C, Bustin A, Neji R, Kunze KP, Forman C, Schmidt M, et al. Motion-corrected 3D whole-heart water-fat high-resolution late gadolinium enhancement cardiovascular magnetic resonance imaging. J Cardiovasc Magn Reson. 2020;22(1):53.

19 Wetzl J, Yoon S, Schmidt M, Haenel A-B, Weißgerber A, Barkhausen J, et al. AI-based Single-Click Cardiac MRI Exam: Initial Clinical Experience and Evaluation in 44 Patients. International Society for Magnetic Resonance in Medicine 2023.

20 Yoon S, Preuhs E, Schmidt M, Forman C, Chitiboi T, Sharma P, et al. Automated Cardiac Resting Phase Detection Targeted on the Right Coronary Artery. Machine Learning for Biomedical Imaging. 2023;2,arXiv:2109.02342:1-26.

21 Yoon S, Schmidt M, Rick M, Chitiboi T, Sharma P, Emrich T, et al. Validation of a deep learning based automated myocardial inversion time selection for late gadolinium enhancement imaging in a prospective study. International Society for Magnetic Resonance in Medicine 2021.

22 Hajhosseiny R, Rashid I, Bustin A, Munoz C, Cruz G, Nazir M.S, et al. Clinical comparison of sub-mm high-resolution non-contrast coronary MRA against coronary CTA in patients with low-intermediate risk of CAD: A single center trial. J Cardiovasc Magn Reson. 2021;23(1):57.

Contact

Michaela Schmidt
Siemens Healthineers
SHS DI MR RCT CLS CARD
Allee am Roethelheimpark 2
91050 Erlangen
Germany
michaela.schmidt@siemens-healthineers.com

Karl P. Kunze, Ph.D.
Siemens Healthineers
SHS EMEA GBI DI PI
Riverside Way
Camberley GU15 3YL
United Kingdom
karl-philipp.kunze@siemens-healthineers.com

3D Whole-Heart Imaging in Cardiovascular MRI: Exploring the Range of Clinical Applications

Evangelia Nyktari[1], Panagiotis Rozos[1], Konstantinos Letsas[2], Athanasios Saplaouras[2], Soultana Kourtidou[1], Konstantinos Petsios[3], Spyridon Zarkadoulas[1], Michalis Efremidis[2]

[1]Cardiovascular MRI Unit, Onassis Cardiac Surgery Center, Athens, Greece
[2]Electrophysiology Unit, Onassis Cardiac Surgery Center, Athens, Greece
[3]Head of Clinical Research Office, Onassis Cardiac Surgery Center, Athens, Greece

Clinical need

Initially introduced for coronary artery visualization, three-dimensional (3D) whole-heart navigator-based acquisitions have been used routinely for over two decades, especially to delineate complex congenital anatomy and morphology [1].

The technique is superior to other imaging modalities used in congenital heart disease (CHD), as it is free from ionizing radiation and does not require breath-holding. It also allows the acquisition of full-volume data including the entire heart and thoracic vasculature at a specific point of the cardiac cycle (usually end-diastole) with high signal-to-noise ratio and isotropic voxel resolution that enables reconstruction in any plane during post processing [2].

Apart from its value in anatomy and morphology, free-breathing high-isotropic-resolution 3D whole-heart late gadolinium enhancement (LGE) imaging has been established as a valid method of tissue characterization in a wide range of ischemic and non-ischemic cardiomyopathies [3, 4].

Recent major developments in electrophysiology (EP) ablation procedures for arrhythmia treatment have raised the need for novel 3D whole-heart high-resolution LGE (HR-LGE) techniques to image thin-wall cardiac chambers such as the atria and right ventricle. Technological progress in this area has made it possible to both identify the arhythmogenic substrate and illustrate its underlying architecture.

This information has been used to aid or even guide EP procedures, increasing both safety and success rates [5].

We will focus on using 3D whole-heart imaging in adult congenital heart disease (ACHD) and arrhythmias, and on how it helps the invasive cardiologists on the Structural Heart Disease team and on the EP team in their daily practice.

3D Whole Heart is work in progress. The application is currently under development and is not for sale in the U.S. and in other countries. Its future availability cannot be ensured.
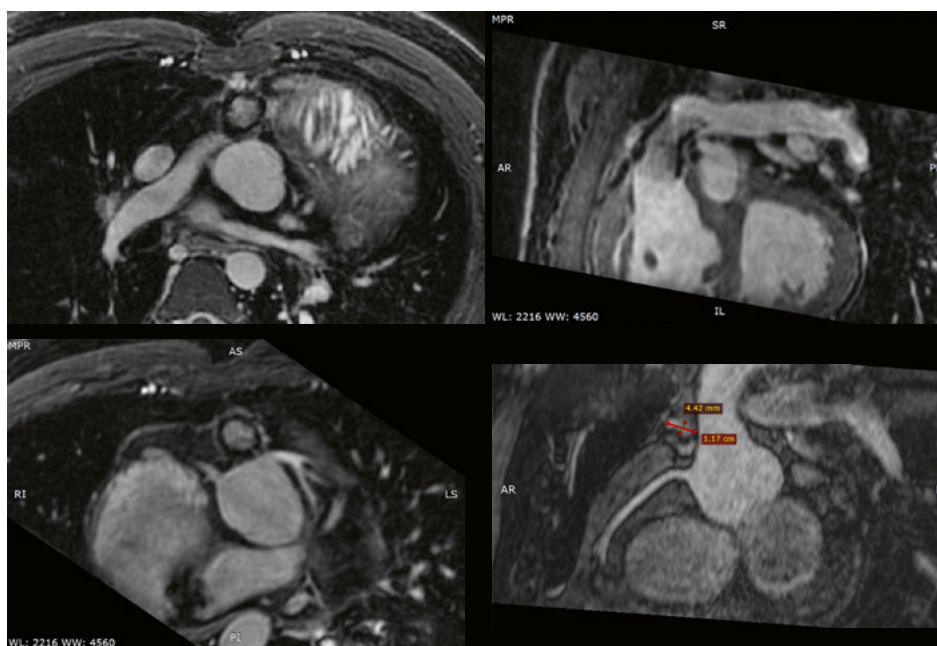
1 3D free-breathing ECG-gated navigator-based whole-heart imaging in a young patient post arterial switch for transposition of the great arteries and multiple operations for supra- and valvar stenosis of the pulmonary valve (PV). Patient had a Melody valve in the position of critical PV stenosis, and a valve-in-valve procedure was planned. Despite the presence of a prosthetic Melody valve and ASD closure device, high-quality 3D whole-heart imaging offers critical information about the origin of the coronary arteries and its relation to RVOT and pulmonary annulus. Left main coronary artery (LMCA) high origin is noted in proximity of the Melody valve. RCA is at a safe distance from the area of planned intervention.

Adult congenital heart disease

Introduction

Cardiac magnetic resonance (CMR) imaging is already an integral part of the diagnostic evaluation, risk stratification, and serial follow-up of ACHD patients [6]. This is important, as adults living with CHD currently outnumber the children [7].

CMR image quality is not affected by body habitus, there is no need for geometric assumptions, and it is radiation-free. Diagnostic imaging in ACHD aims to illustrate anatomic and functional pathology, quantify the severity, and guide clinical decision-making.

ACHD patients are a heterogeneous population, covering a wide spectrum of anatomic patterns, even within specific lesions. Furthermore, most adult patients have undergone a previous corrective or palliative surgery and other interventions, making each patient a unique case, and residual hemodynamic/anatomic abnormalities very common. In addition, as the ACHD population ages, acquired heart disease will require diagnostic evaluation.

Non-invasive visualization of accurate patient-specific cardiovascular anatomy is essential – not only for illustrating morphological complexity in ACHD cases, but also due to the difficulty of pre-surgical decision-making.

3D whole-heart applications

The non-contrast free-breathing 3D whole-heart approach with respiratory navigator gating and ECG triggering was initially introduced for dedicated coronary imaging [1] in the pediatric[1] population. Nowadays, its use has expanded to the ACHD population. It is used to describe complex anatomy and enables reliable measurements of the aortic root and aorta at the desired timepoint of the cardiac circle, obviating the need for multiple 2D cine imaging across the area of interest [8].

Many technological developments, mostly related to motion correction with the use of navigators during free breathing [9] and image-contrast improvement [10], have led to better image quality. As a result, the present technique has become integral part for intracardiac and extracardiac anatomy evaluation in complex ACHD cases, especially when there is a question of giving a gadolinium agent and in serial follow-up cases.

This is particularly important, as different cardiovascular anomalies can coexist in the same patient, posing the need for expert knowledge of the heart and vascular connections. Moreover, recent studies endeavor to show that routinely introducing a set of 3D volume data during the CMR scan for anatomy delineation and post-processing reconstruction on any plane can shorten the scan time, simplify the scanning protocol, and may obviate the need for direct expert supervision [11].

Isotropic 3D whole heart datasets are particularly useful for interventional planning in complex CHD.

Percutaneous interventions have completely changed the management of ACHD, especially the need for open heart surgery. In patients with predominant pulmonary valve regurgitation (either native or bioprosthetic, or a conduit), 3D whole-heart offers a complete evaluation of the

---

[1]Siemens Healthineers Disclaimer: MR scanning has not been established as safe for imaging fetuses and infants less than two years of age. The responsible physician must evaluate the benefits of the MR examination compared to those of other imaging procedures. Note: This disclaimer does not represent the opinion of the authors.
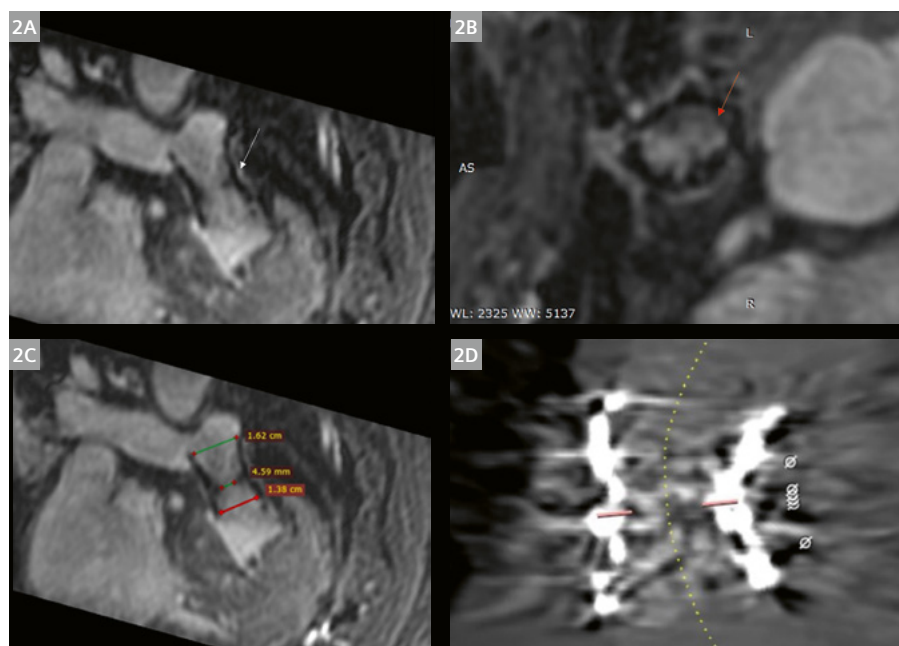

2 Same patient as in Figure 1. Reconstruction of RVOT/PV using data from 3D whole-heart imaging shows the in-stent stenosis at the mid-part of the Melody valve. Finding confirmed by CT measurement **(2D)**.

right ventricular outflow tract (RVOT), and the pulmonary artery dimensions and geometry. This is crucial for sizing and pre-planning the sitting position of the new valve/conduit even in valve-in-valve procedures [12]. Additionally, coronary anatomy is interrogated, along with higher risk anatomical features for transcutaneous pulmonary valve replacement (PVR), such as a coronary artery in close proximity to the RVOT and the risk of compression or co-existent pathology from supravalvar pulmonary stenosis, ascending aortic enlargement, or aortic coarctation [13]. Sample preprocedural images of a valve-in-valve transcutaneous PVR pre-procedure are shown in Figures 1 and 2.

Furthermore, the use of 3D volume data sets with the added advantage of gating are well suited for producing 3D-printed models to aid surgical planning in more complex cases, such as double outlet right ventricle (DORV), where the relative position of different anatomic regions is important for the surgeon when choosing the appropriate technique [14]. With 3D-printed models, it is also possible to simulate the surgical procedures in complex cases and check the results. Furthermore, the use of virtual reality platforms is expected to revolutionize the future of preprocedural planning for complex CHD [15].

All these innovations have been translated into daily clinical practice by fusing 3D whole-heart datasets with conventional fluoroscopy angiograms in the catheterization laboratory. This is to aid procedural guidance and to reduce time under radiation and the dose of iodinated contrast, both of which benefit the patient [2, 15]. It seems that the complex ACHD anatomy is the optimal paradigm in which 3D modelling and printing can permeate daily practice as augmented or virtual reality, leaving nothing to the imagination or risking misinterpretation by the clinician. Sample images of a 3D-printed model in a complex ACHD case are shown in Figure 3.

Finally, 3D LGE whole-heart imaging may have a role to play in risk stratification for sudden cardiac death, mainly caused by ventricular arrhythmias, in sub-categories of the ACHD population [16, 17]. It has been shown that right ventricular LGE burden independently predicts inducible ventricular tachycardia (VT) in repaired tetralogy of Fallot patients. However, for other types of CHD such as transposition of the great arteries (TGA) with atrial switch surgery, inducible VT appears to be of no prognostic value [18].
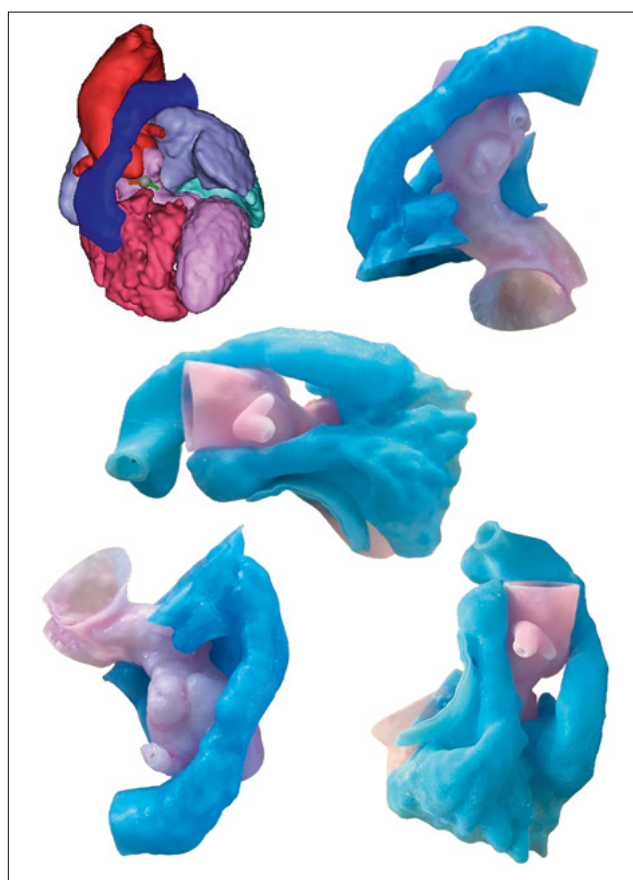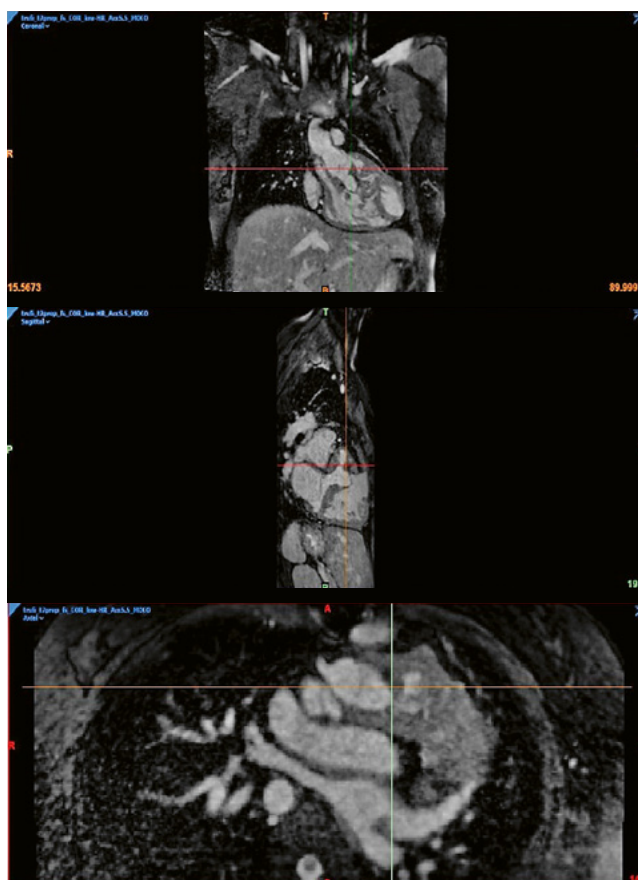
3 Young patient post-Rastelli procedure for double outlet right ventricle. 3D whole-heart imaging translated to 3D-printed model of the heart. *Courtesy of 3D Life SA, 3D4KARDIA European Funded Program, Onassis CSC, CERTH, 3D Life SA.*

Sample images of 3D LGE of the right ventricle in a patient with tetralogy of Fallot are shown in Figure 4.

Challenges

Current T2-prepared balanced steady-state free precession 3D whole-heart imaging suffers from off-resonance artifacts in small vessels, flow-related artifacts due to turbulence, and metal artifacts from stents and devices that may obscure areas of interest. Furthermore, scanning time is prolonged, especially in high-quality isotropic 3D data sets, and is often unpredictable due to the use of diaphragmatic navigators and their susceptibility to irregular respiratory patterns.

2D image navigators (iNAV) have been proposed to address the cardiac and respiratory motion problem [19]. This technique outperforms conventional diaphragmatic navigator gating and enables 100% respiratory scan efficiency, as well as shorter and predictable scan times. Dixon-based fat-water separation approaches enable superior fat suppression especially for 3D LGE applications [20] (Fig 4). Furthermore, Magnetization Transfer Contrast Bright-and-black blOOd phase SensiTive (MTC-BOOST) techniques [21] provide high luminal signal for small vessels, and optimal contrast between myocardium and blood pool, which overcomes flow artifacts.

Electrophysiology

Introduction

Advances in understanding arrhythmia and in technology for mapping and ablation have led to rapid growth in ablation techniques [22]. Ablation in atrial fibrillation (AF) and VT is an intervention with a growing need for imaging support. CMR is the gold-standard technique for tissue characterization and has made it possible to both accurately locate the abnormal tissue (scar/fibrosis) and assess its architecture and characterize the underlying arrhythmogenic substrate. Thus, CMR has been introduced to the EP lab routinely as a pre-procedural way of non-invasively mapping the underlying arrhythmogenic substrate, guiding ablations, and assessing post-procedural success.

Ventricular tachycardia

VT is the most common cause of sudden cardiac death in structural heart disease [23]. Invasive electro anatomical mapping (EAM) can, with the use of newer catheters, illustrate the presence of both scar (voltage maps) and slow conduction areas (activation maps). The most common arrhythmic substrate in patients with monomorphic VT refers to the presence of a scar-related re-entry pathway caused by slow conduction areas of intermediate tissue (so-called border zone, BZ) inside the electrically silent core scar that connects regions of healthy tissue. These areas are called conducting channels and can be accurately identified from the EAM obtained during VT ablation [24].

A high degree of concordance between EAM and images obtained by MRI has been reported [25].

Conducting channels in EAM are shown in two dimensions as an inherent disadvantage of EP mapping and this could be a reason for reduced ablation success. Therefore, there is a clinical need to improve the characterization of the VT substrate and the efficacy of VT ablation [26].
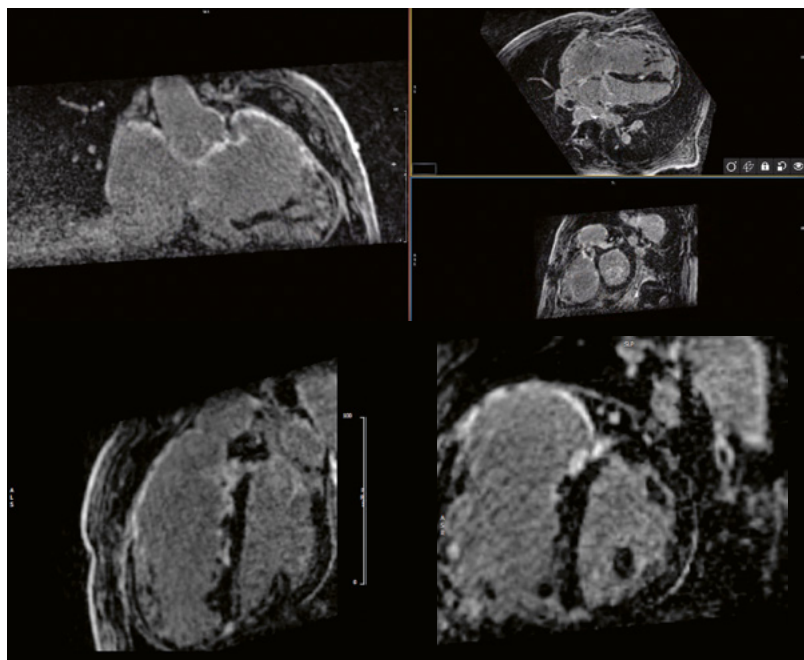
4 Middle-aged patient, post-surgical correction for tetralogy of Fallot. 3D GRE Dixon fat-water LGE imaging with image navigator.

In this context, CMR may play an important role in substrate characterization. This is especially true with the application of high-isotropic-resolution 3D whole-heart LGE imaging in the range of 1 to 1.3 mm³ that allows illustration of the BZ, healthy tissue, and core scar, and provides a 3D model of VT corridors across all layers of myocardium.

3D whole-heart applications
3D whole-heart LGE imaging can define the location of the scar tissue across the different layers of myocardium (endocardium, mid-wall, and epicardial region) with great accuracy. This information is very useful for deciding on the ablation approach (endocardial, epicardial, or both) [27].

In addition, CMR has revolutionized clinical practice by making it possible to accurately discriminate between arrhythmogenic and non-arrhythmogenic scar. The scar location, signal intensity (SI), transmurality, shape, and heterogeneity can provide a 3D model of the heart with projection of the structural equivalent of conducting channels (CC), i.e., VT corridors [26].

Using dedicated post-processing software, color-coded pixel signal intensity (PSI) maps are produced and merged with EAM during VT ablation [26].

Recent studies have shown that CMR-aided VT substrate ablation with color-coded PSI maps obtained from pre-procedural 3D LGE whole-heart imaging reduces the need for radiofrequency (RF) delivery and improves VT recurrence-free survival [27, 28].

Sample images of a patient with a previous posterolateral wall infarction and monomorphic VT pre-ablation procedure show that the VT corridors from 3D LGE whole-heart imaging using a novel iNAV Dixon 3D fat-water separation sequence agree with the conducting channels in EAM.

Atrial fibrillation

Introduction
LGE CMR imaging of left atrial (LA) fibrosis in patients with AF has been associated with impaired LA mechanics [29] and lower voltage on electroanatomic voltage maps [30]. Clinically, this translates to increased adverse cardiovascular events, persistence of AF, and treatment failure [31].

Pulmonary vein (PV) isolation has become the cornerstone technique for catheter ablation in patients with drug-refractory AF. LGE CMR imaging of the LA could offer a valuable tool to evaluate location, depth, and possible gaps in created lesions.

As low-voltage atrial areas detected by EAM correlate quite well with structural alterations on LGE CMR, using and integrating LGE imaging in current clinical practice may provide a less operator-dependent tool for quantifying LA scarring and guiding ablation. This could improve procedural success rates. Sample images of post-ablation PV lesions and respective voltage maps are seen in Figure 5.

3D whole-heart imaging applications
Over time, 3D LGE imaging has become the reference for both pre- and post-ablation atrial scar imaging. Commercial 3D free-breathing LGE acquisitions are based on respiratory navigation and an ECG-gated gradient echo pulse sequence with fat suppression and inversion recovery preparation. Data are acquired during the diastolic phase of the cardiac cycle prior to atrial kick. Scan time depends on the respiratory pattern and heart rate of the patient, and can reach up to 12 minutes. Typical voxel size is 1.25 × 1.25 × 2.5 mm (reconstructed to 0.625 × 0.625 × 1.25 mm).
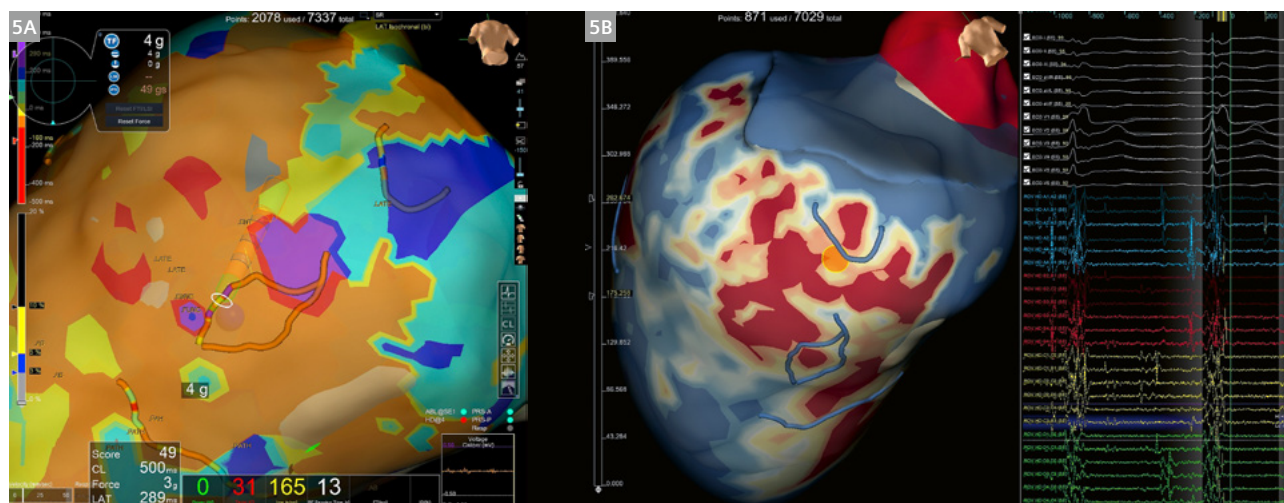

5 Middle-aged patient with posterolateral wall myocardial infarction and monomorphic VT. **5A:** Electroanatomical map showing arrhythmogenic substrate as conducting channels. **5B:** PSI map derived from 3D LGE whole-heart dataset showing the structural VT corridors in complete agreement with the EAM.

Novel techniques like the free-breathing, image-navigated isotropic high-resolution 3D LGE sequence with Dixon fat-water separation [20] introduce better spatial resolution and shorter scan times. Fat suppression improves diagnostic accuracy, which is crucial in thin structures like the atria. Sample images of post-ablation PV lesions are seen in Figures 6 and 7.

Challenges
LGE image signal intensity is very sensitive to poor ECG gating in arrhythmia, to artifacts from fat in the atrioventricular groove or epicardium, and to artifacts from respiratory motion. Additionally, volume averaging may represent a perfectly sharp but slanted scar border as "heterogeneous tissue" on LGE that affects the detection of VT corridors.
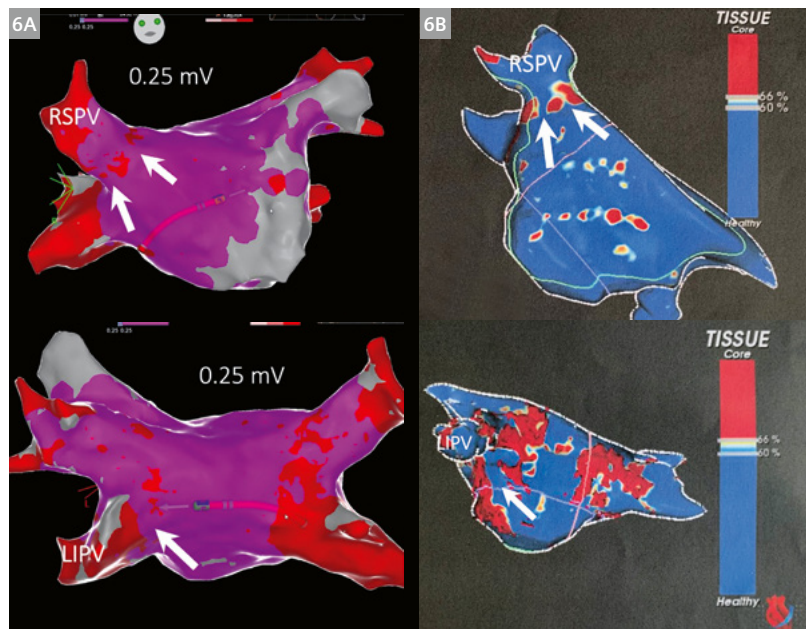
6 Post-ablation for atrial fibrillation imaging.
6A: Electroanatomical voltage maps showing the gaps in pulmonary vein isolation.
6B: PSI maps derived from 3D LGE whole-heart datasets showing complete agreement.
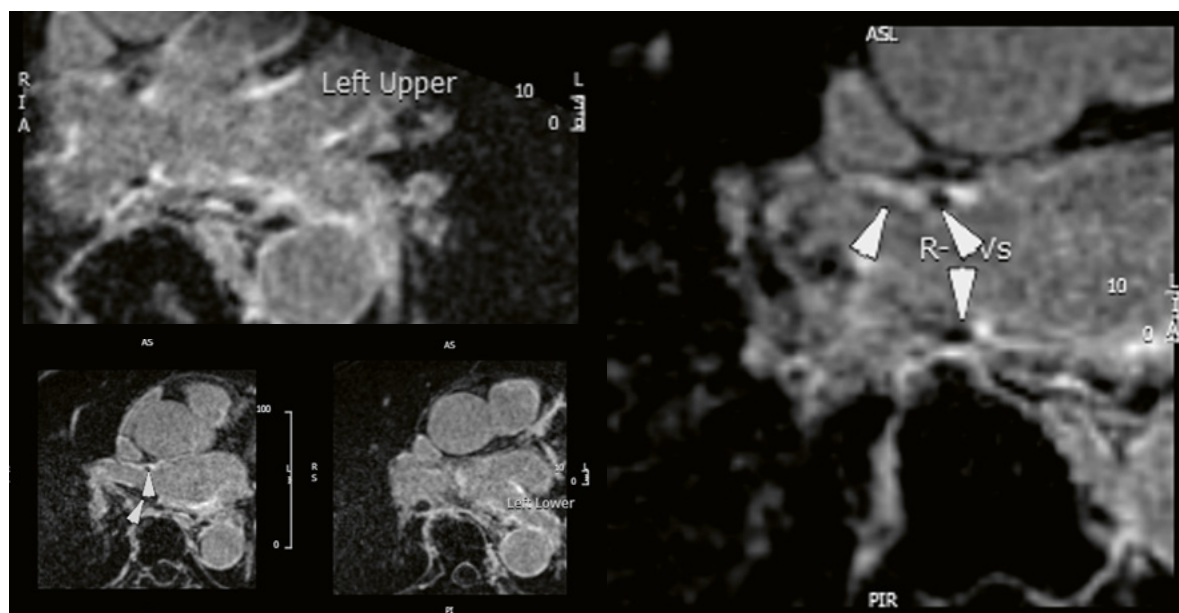
7 24 hours post-cryoablation for atrial fibrillation imaging. 3D LGE whole-heart imaging of the lesions using a novel iNAV Dixon fat-water separation sequence.

For patients with AF, cardioversion is often recommended prior to the study to improve image quality [32].

The time delay between contrast injection and image acquisition is crucial. Despite the lack of official consensus, LGE MRI acquisition is usually performed 15–25 minutes (atrium) or 7–15 minutes (ventricle) after injection of gadolinium contrast agent.

As mentioned earlier, novel motion-corrected whole-heart 3D water/fat LGE imaging has been introduced, showing good agreement with conventional breath-hold 2D LGE imaging. It offers higher spatial resolution and good image quality from a free-breathing acquisition with 100% scan efficiency and a predictable scan time [20].

Finally, a major limitation for arrhythmia patients is the presence of devices (ICDs, CRTs, pacemakers). This is because they can cause hyperintense image artifacts that partially or fully cover the area of interest. To avoid these artifacts, wideband MRI sequences have recently been developed that increase the bandwidth of the inversion and excitation pulse and reduce the incidence of artifacts.

Conclusion

Over the last decade, the technical development of high-resolution 3D whole-heart imaging has provided new insights into congenital heart disease and arrhythmia treatment, increasing diagnostic confidence, patient safety, and procedural success.
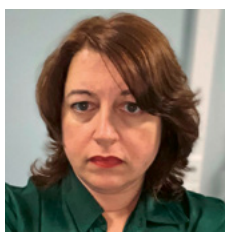
References

1   Sørensen TS, Körperich H, Greil GF, Eichhorn J, Barth P, Meyer H, et al. Operator-independent isotropic three-dimensional magnetic resonance imaging for morphology in congenital heart disease: a validation study. Circulation. 2004;110(2):163-9.
2   Greil G, Tandon AA, Silva Vieira M, Hussain T. 3D Whole Heart Imaging for Congenital Heart Disease. Front Pediatr. 2017;5:36.
3   Toupin S, Pezel T, Bustin A, Cochet H. Whole-Heart High-Resolution Late Gadolinium Enhancement: Techniques and Clinical Applications. J Magn Reson Imaging. 2022;55(4):967-987.
4   Peters AA, Wagner B, Spano G, Haupt F, Ebner L, Kunze KP, et al. Myocardial scar detection in free-breathing Dixon-based fat- and water-separated 3D inversion recovery late-gadolinium enhancement whole heart MRI. Int J Cardiovasc Imaging. 2023;39(1):135-144.
5   Sanchis L, Prat S, Sitges M. Cardiovascular Imaging in the Electrophysiology Laboratory. Rev Esp Cardiol (Engl Ed). 2016;69(6):595-605. English, Spanish.
6   Burchill LJ, Huang J, Tretter JT, Khan AM, Crean AM, Veldtman GR, et al. Noninvasive Imaging in Adult Congenital Heart Disease. Circ Res. 2017;120(6):995-10148.
7   Stout KK, Daniels CJ, Aboulhosn JA, Bozkurt B, Broberg CS, Colman JM, et al. 2018 AHA/ACC Guideline for the Management of Adults With Congenital Heart Disease: Executive Summary: A Report of the American College of Cardiology/American Heart Association Task Force on Clinical Practice Guidelines. J Am Coll Cardiol. 2019;73(12):1494-1563.
8   Nussbaumer C, Bouchardy J, Blanche C, Piccini D, Pavon AG, Monney P, et al. 2D cine vs. 3D self-navigated free-breathing high-resolution whole heart cardiovascular magnetic resonance for aortic root measurements in congenital heart disease. J Cardiovasc Magn Reson. 2021;23(1):65.
9   Kim WY, Stuber M, Kissinger KV, Andersen NT, Manning WJ, Botnar RM. Impact of bulk cardiac motion on right coronary MR angiography and vessel wall imaging. J Magn Reson Imaging. 2001;14(4):383-90.
10 Botnar RM, Stuber M, Danias PG, Kissinger KV, Manning WJ. Improved coronary artery definition with T2-weighted, free-breathing, three-dimensional coronary MRA. Circulation. 1999;99(24):3139-48.
11 Nguyen KL, Ghosh RM, Griffin LM, Yoshida T, Bedayat A, Rigsby CK, et al. Four-dimensional Multiphase Steady-State MRI with Ferumoxytol Enhancement: Early Multicenter Feasibility in Pediatric Congenital Heart Disease. Radiology. 2021;300(1):162-173.
12 Baessato F, Ewert P, Meierhofer C. CMR and Percutaneous Treatment of Pulmonary Regurgitation: Outreach the Search for the Best Candidate. Life (Basel). 2023;13(5):1127.
13 Valverde I, Parish V, Hussain T, Rosenthal E, Beerbaum P, Krasemann T. Planning of catheter interventions for pulmonary artery stenosis: improved measurement agreement with magnetic resonance angiography using identical angulations. Catheter Cardiovasc Interv. 2011;77(3):400-8.
14 Farooqi KM, Nielsen JC, Uppu SC, Srivastava S, Parness IA, Sanz J, et al. Use of 3-dimensional printing to demonstrate complex intracardiac relationships in double-outlet right ventricle for surgical planning. Circ Cardiovasc Imaging. 2015;8(5):e003043.
15 Goo HW, Park SJ, Yoo SJ. Advanced Medical Use of Three-Dimensional Imaging in Congenital Heart Disease: Augmented Reality, Mixed Reality, Virtual Reality, and Three-Dimensional Printing. Korean J Radiol. 2020;21(2):133-145.
16 Khairy P, Silka MJ, Moore JP, DiNardo JA, Vehmeijer JT, Sheppard MN, et al. Sudden cardiac death in congenital heart disease. Eur Heart J. 2022;43(22):2103-2115.
17 Ghonim S, Ernst S, Keegan J, Giannakidis A, Spadotto V, Voges I, et al. Three-Dimensional Late Gadolinium Enhancement Cardiovascular Magnetic Resonance Predicts Inducibility of Ventricular Tachycardia in Adults With Repaired Tetralogy of Fallot. Circ Arrhythm Electrophysiol. 2020;13(11):e008321.
18 Khairy P, Harris L, Landzberg MJ, Fernandes SM, Barlow A, Mercier LA, et al. Sudden death and defibrillators in transposition of the great arteries with intra-atrial baffles: a multicenter study. Circ Arrhythm Electrophysiol. 2008;1(4):250-7.
19 Henningsson M, Smink J, van Ensbergen G, Botnar R. Coronary MR angiography using image-based respiratory motion compensation with inline correction and fixed gating efficiency. Magn Reson Med. 2018;79(1):416-422.
20 Munoz C, Bustin A, Neji R, Kunze KP, Forman C, Schmidt M, et al. Motion-corrected 3D whole-heart water-fat high-resolution late gadolinium enhancement cardiovascular magnetic resonance imaging. J Cardiovasc Magn Reson. 2020;22(1):53.
21 Ginami G, Lòpez K, Mukherjee RK, Neji R, Munoz C, Roujol S, et al. Non-contrast enhanced simultaneous 3D whole-heart bright-blood pulmonary veins visualization and black-blood quantification of atrial wall thickness. Magn Reson Med. 2019;81(2):1066-1079.
22 De Zan G, Calò L, Borrelli A, Guglielmo M, De Ruvo E, Rier S, et al. Cardiac magnetic resonance-guided cardiac ablation: a case series of an early experience. Eur Heart J Suppl. 2023;25(Suppl C):C265-C270.
23 John RM, Tedrow UB, Koplan BA, Albert CM, Epstein LM, Sweeney MO, et al. Ventricular arrhythmias and sudden cardiac death. Lancet. 2012;380(9852):1520-9.

24 Stevenson WG, Khan H, Sager P, Saxon LA, Middlekauff HR, Natterson PD, et al. Identification of reentry circuit sites during catheter mapping and radiofrequency ablation of ventricular tachycardia late after myocardial infarction. Circulation. 1993;88(4 Pt 1):1647-70.

25 Andreu D, Berruezo A, Ortiz-Pérez JT, Silva E, Mont L, Borràs R, et al. Integration of 3D electroanatomic maps and magnetic resonance scar characterization into the navigation system to guide ventricular tachycardia ablation. Circ Arrhythm Electrophysiol. 2011;4(5):674-83.

26 Sanchez-Somonte P, Garre P, Vázquez-Calvo S, Quinto L, Borràs R, Prat S, et al. Scar conducting channel characterization to predict arrhythmogenicity during ventricular tachycardia ablation. Europace. 2023;25(3):989-999.

27 Andreu D, Ortiz-Pérez JT, Boussy T, Fernández-Armenta J, de Caralt TM, Perea RJ, et al. Usefulness of contrast-enhanced cardiac magnetic resonance in identifying the ventricular arrhythmia substrate and the approach needed for ablation. Eur Heart J. 2014;35(20):1316-26.

28 Andreu D, Penela D, Acosta J, Fernández-Armenta J, Perea RJ, Soto-Iglesias D, et al. Cardiac magnetic resonance-aided scar dechanneling: Influence on acute and long-term outcomes. Heart Rhythm. 2017;14(8):1121-1128.

29 Habibi M, Lima JA, Khurram IM, Zimmerman SL, Zipunnikov V, Fukumoto K, et al. Association of left atrial function and left atrial enhancement in patients with atrial fibrillation: cardiac magnetic resonance study. Circ Cardiovasc Imaging. 2015;8(2):e002769.

30 Malcolme-Lawes LC, Juli C, Karim R, Bai W, Quest R, Lim PB, et al. Automated analysis of atrial late gadolinium enhancement imaging that correlates with endocardial voltage and clinical outcomes: a 2-center study. Heart Rhythm. 2013;10:1184–91.

31 Marrouche NF, Wilber D, Hindricks G, Jais P, Akoum N, Marchlinski F, et al. Association of atrial tissue fibrosis identified by delayed enhancement MRI and atrial fibrillation catheter ablation: the DECAAF study. JAMA. 2014;311:498–506.

32 Vijayakumar, S.; Kholmovski, E.; McGann, C.; Marrouche, N.F. Dependence of contrast to noise ratio between ablation scar and other tissues on patient heart rate and flip angle for late gadolinium enhancement imaging of the left atrium. J. Cardiovasc. Magn. Reson. 2012, 14 (Suppl. S1), O107.

Contact

Evangelia Nyktari, M.D.
Cardiovascular MRI Unit
Onassis Cardiac Surgery Center
Leoforos Syngrou 356
17674 Athens
Greece
eyanyktari@yahoo.gr

3D Whole-Heart Applications: Angiography and Delayed Enhancement

Jason Craft[1], Joshua Y. Cheng[1], Nancy Diaz[1], Karl P. Kunze[2], Michaela Schmidt[3]

[1]St. Francis Heart Hospital, DeMatteis Research Center, Greenvale, NY, USA
[2]Siemens Healthcare Limited, Frimley, UK
[3]Siemens Healthineers, Erlangen, Germany

Introduction

It has become more important than ever before to diversify non-invasive imaging methods that involve contrast media administration. Compared to CT imaging, MRI does not involve nephrotoxic iodinated contrast or ionizing radiation. However, ungated first pass magnetic resonance angiography (MRA) cannot effectively freeze cardiac motion; and provides reduced quality of segmentation compared to CT pulmonary vein angiography [1]. Diaphragmatic navigator (dNAV) used for motion correction is associated with unpredictable scan times when respiration is irregular, and imperfect slab tracking ratio [2]. Furthermore, approximately 50–100 Hz off-resonance is frequently observed at the interface of the pulmonary veins and left atrium

due to susceptibility effects and inflow from the lungs [3]. Therefore, the use of balanced steady-state free precession (bSSFP) and fat saturation pulses, particularly at higher field strengths, can be technically unsatisfactory for this application. Thus, the unmet clinical need is to provide robust clinical angiographic methods that can effectively image complex patients with arrhythmias, while minimizing image artifacts.

Instead of tracking the diaphragmatic interface, image navigators (iNAV) track the blood pool contrast of the left ventricle [4]. 2D translational motion in the head-to-foot direction can be extracted and estimated on a per cardiac cycle basis and is used to bin data with

Imaging parameters for whole heart MRA and LGE			
Sequence	Inversion recovery GRE	Saturation recovery GRE	Inversion recovery Dixon GRE
FOV	320 mm (axial)	320 mm (axial)	320 mm (axial)
Spatial resolution	1.3 × 1.3 mm	1.3 × 1.3 mm	1.3 × 1.3 mm
Slice thickness	1.4 mm	1.4 mm	1.4 mm
Slice resolution	90%	90%	90%
Fat Sat	No	Yes	No
Acceleration Factor	2.9	2.9	2.8
Bandwidth	579 Hz/px	579 Hz/px	453 Hz/px
Flip angle	18°	18°	15°
TI/Saturation time	220–260 ms (systolic) 290 ms (diastolic)	150 ms	According to scout
TE/TR	1.42 ms/3.89 ms	1.42 ms/3.89 ms	2.38, 4.76 ms/6.97 ms
Data window duration	62–130 ms	62–130 ms	62–130 ms

Table 1: 3D whole heart sequence parameters.

3D Whole Heart is work in progress. The application is currently under development and is not for sale in the U.S. and in other countries. Its future availability cannot be ensured.

respect to respiration. 3D image volumes are obtained using a non-rigid motion-compensated reconstruction of all binned data [5, 6], leading to 100% scan efficiency and predictable scan time. The sampling pattern consists of spiral-like interleaves acquired alternately based on the golden angle of rotation (variable-density golden-step Cartesian trajectory with spiral profile order sampling, or VD-CASPR)[1] [7].

As a result of scanning more efficiently, the predictable scan time translates into less gadolinium-based contrast agent (GBCA) use. Specifically, compared to dNAV based applications, we can use 33% less contrast [8, 9], and we can do it without the need for higher field strengths. Furthermore, we can acquire angiography and delayed enhancement at higher near isotropic spatial resolution. We acquire all 3D datasets at a true spatial resolution of $1.3 \times 1.3 \times 1.5$ mm^3, with a reconstructed slice thickness of 1.4 mm (Table 1).

Pulmonary vein angiography and arterial delayed enhancement using iNAV

At our institution, we are asked to provide pulmonary vein anatomical imaging for segmentation and importation into the electro-anatomical mapping system. With MRI, not only is anatomical information obtained, but functional information such as atrial and ventricular volumetrics, left atrial delayed enhancement, and quantification of valvular heart disease. Obtaining one MRI examination is simply more logistically efficient than obtaining CT angiography plus echocardiography imaging. Our 3D MRA and late gadolinium enhancement (LGE) imaging is performed on a 1.5T MAGNETOM Sola, but our institution also has experience with the 3D inversion recovery Dixon multi-echo gradient recalled echo (GRE)[1] performed on the 3T MAGNETOM Skyra platform.

Concerning the MRA and LGE exam workflow, the image navigator and saturation band position can be automatically determined using free-breathing 3 plane localizers and the AI cardiac scan companion (AICSC)[1] prototype. The diastolic or systolic rest period of the left atrium can be determined using the included high temporal resolution free breathing 4-chamber (or HLA) cine [10]. The user can manually determine the data window duration, or this can be automatically determined based on the rest period of the right coronary artery by the AICSC. Given the diastolic rest period is longer at slower ventricular rates, we prefer diastolic imaging at regular heart rhythms < 80 BPM. When the ventricular rate is > 80 BPM or significant arrhythmia such as atrial fibrillation is present, systolic imaging is preferential.

In addition to the prototype sequence[1] for *syngo* XA20 featuring 3D inversion recovery Dixon multi-echo GRE,

3D T2 prep bSSFP, and 3D T2 Prep Dixon multi-echo GRE, the user can configure different preparatory pulses to manipulate image contrast. We acquire pulmonary vein angiography using either inversion recovery GRE or saturation recovery GRE. Both methods have respective strengths and weaknesses. Inversion recovery maintains vessel sharpness and is compatible with the 1500 Hz wideband pulse which mitigates device artifacts. Furthermore, inversion recovery can be used without fat saturation, which makes this option especially attractive at higher field strengths. The inversion time parameter at 1.5T represents a balance between SNR and background suppression-values range from 220 ms to 300 ms at 1.5T [11–14]. Similar to previous literature [15], we have observed that image contrast is quite consistent even with irregular rhythms; iNAV tracking similarly remains quite robust despite the dependence of the beat-to-beat image contrast on the RR interval. Figure 1 depicts excellent image quality despite underlying atrial fibrillation, using inversion recovery GRE. Saturation recovery images have overall higher signal-to-noise, and can be used without manipulation of the inversion time parameter.

Simplifying the contrast injection scheme is important to reduce human error and to optimize workflow. Our contrast injection scheme does not involve the use of look-up tables, saline dilution, or manipulation of extra tubing and/or stop cocks. To provide adequate signal for iNAV tracking, 0.05 mmol/kg of 1 molar contrast agent is injected at 2 ml/sec, followed by 20 ml of saline at the same rate. Immediately after, the remaining 0.10 mmol/kg contrast is administered as a slow infusion, followed by saline at the same rate (0.2 ml/sec). The contrast is injected after starting the first 3D scan, and after observing satisfactory cardiac gating and appropriate iNAV placement prescription. This scan is solely run for the iNAV functionality in order to visualize contrast passage and arrival. The first, second pass, and continuous infusion dose is observed passing through the heart (Fig. 2). The first 3D scan is stopped as soon as the contrast peaks in the pulmonary artery. The exact same protocol is restarted by using STOP/CONTINUE on the inline display (which was linked by the copy reference "copy everything"). We target a maximum scan duration of 4 minutes given the length of the contrast administration and need to perform other imaging prior to delayed enhancement. 15 minutes after the initial injection of GBCA, we perform delayed enhancement of the left atrium using the inversion recovery Dixon multi-echo GRE whole heart sequence at identical spatial resolution. If desired, residual fat can be subtracted from the 3D MRA using the inversion recovery Dixon multi-echo.

---

[1] *Work in progress. The application is currently under development and is not for sale in the U.S. and in other countries. Its future availability cannot be ensured.*
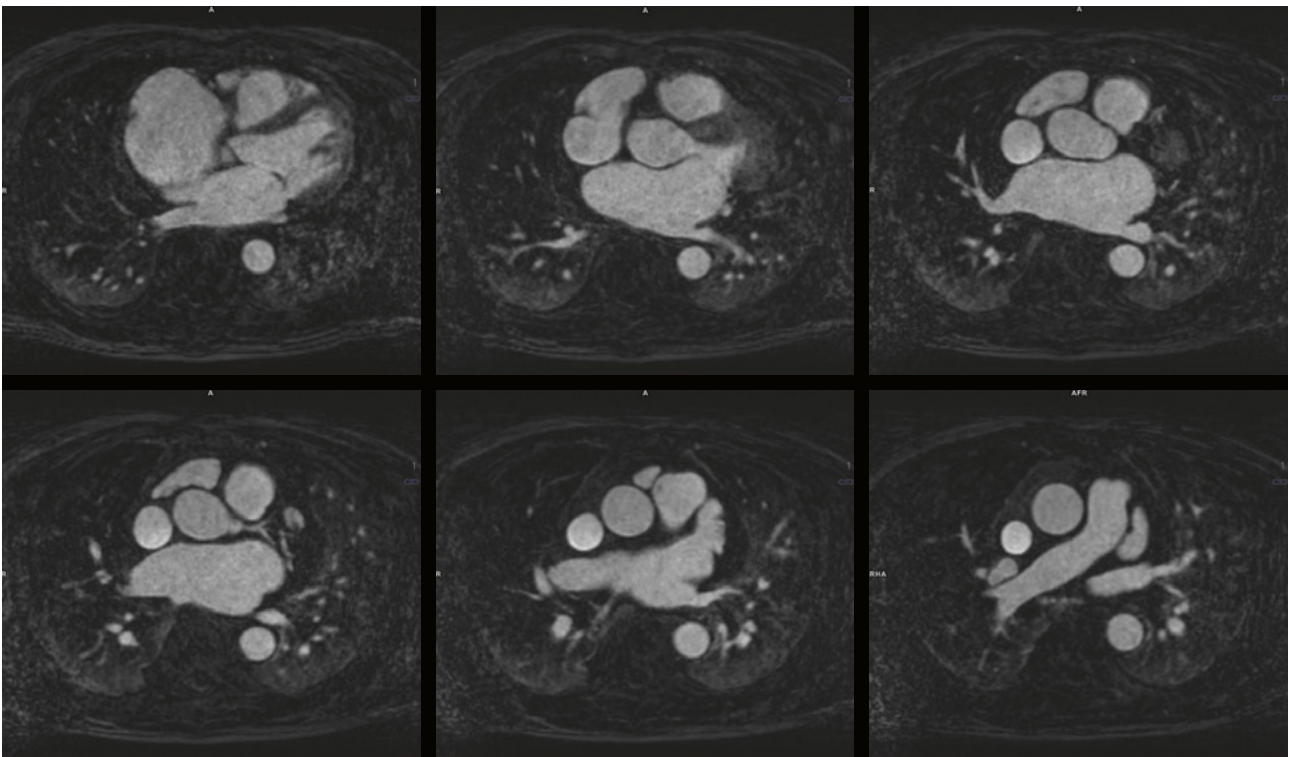
**1** 3D whole heart MRA inversion recovery subtracted images from a patient in atrial fibrillation.
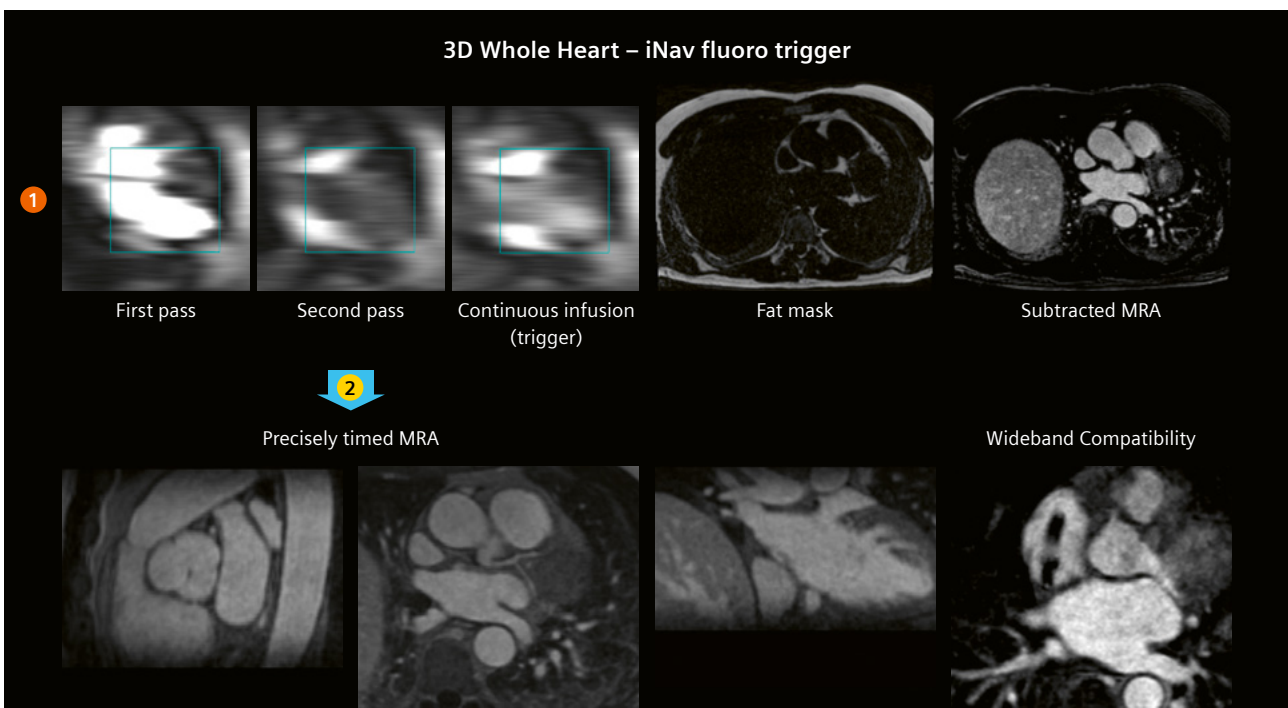
2 The iNAV fluoro trigger method for MR angiography. Two identical 3D whole heart program steps are created in the workflow. The first step (1) is used only for monitoring the passage of contrast with the iNAV. The second step (2), which will run to completion, is triggered at the peak of the continuous infusion in the pulmonary artery.

GRE fat image as a mask. As mentioned, because of the scan efficiency of the iNAV and precision timing of the contrast infusion, we are able to reduce contrast from 0.20 mmol/kg to 0.15 mmol/kg while still providing robust image quality whether patient is in sinus rhythm or has atrial fibrillation.

Case 1

A 59-year-old male was referred for evaluation of COVID-19 myocarditis and to evaluate the left atrial appendage. The patient contracted COVID-19 three weeks prior; one week prior to cardiac MRI imaging, the patient had new onset atrial fibrillation and dyspnea on exertion. Ventricular function with bSSFP cine demonstrated enlargement of the right ventricle with mildly reduced systolic function. Revised Lake Louise criteria was not met for acute myocarditis; however the patient had bilateral pulmonary emboli involving the right middle, right upper, right lower, and left lower segmental branches, with thrombus extending into the right main pulmonary artery. There was no evidence of left atrial appendage thrombus. Figure 3 illustrates the findings on 3D whole heart saturation recovery angiography and inversion recovery Dixon multi-echo GRE. Subsequent CT pulmonary angiogram agreed with MRI findings, and ultrasound Doppler was positive for acute right popliteal deep venous thrombosis. It is important to understand that CT pulmonary venography is timed

| SR-MRA | LGE | CTPA |
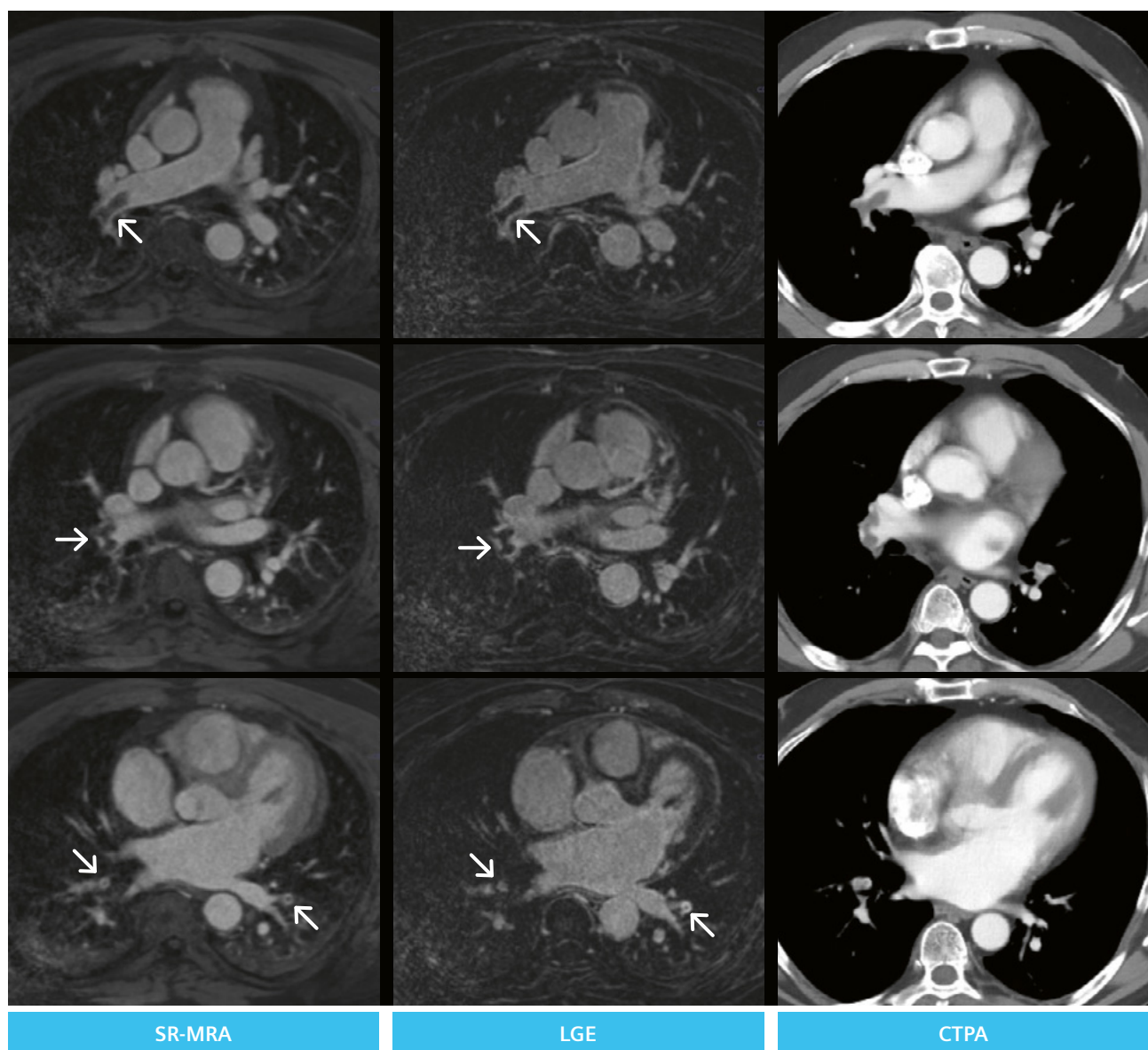
3 Incidentally discovered bilateral pulmonary emboli (arrowheads). From left to right column: saturation recovery MRA, inversion recovery Dixon multi-echo GRE, and CT pulmonary angiography.

to opacification of the left atrium; therefore abnormalities involving the pulmonary arteries may be incompletely characterized. Imaging with 3D whole heart, however, does not suffer from this limitation.

3D left ventricular delayed enhancement

In most cases, 2D PSIR LGE can provide sufficient detail and quantification of left ventricular scar burden. However there are clinical scenarios where providing a 3D dataset is beneficial, such as pre-planning for electrophysiology procedures, or for improved visualization of the right ventricle [16]. Specifically, 3D high resolution LGE can identify substrate features that may be subtle or absent on 2D imaging. By acquiring these 3D datasets in high resolution and reduced partition thickness we can minimize partial volume effects, allow for visualization of heterogeneity within regions of enhancement, scar channels, and the presence of epicardial components. Here, the user has flexible options: the 3D inversion recovery Dixon multi-echo GRE which provides more robust fat separation and is most beneficial at 3T; whereas fat saturated inversion recovery GRE can be used for scan efficiency at 1.5T. Both methods are compatible with the 1500 Hz wideband pulse which suppresses metallic artifacts caused by implanted devices such as ICDs or pacemakers.[2]

Case 2

A 67-year-old male referred for evaluation of non-sustained ventricular tachycardia (NSVT). The patient has frequent ventricular arrhythmia throughout the study, and ventricular function was only possible by using compressed sensing real time cine. Whole heart inversion recovery with fat sat LGE demonstrates heterogenous inferolateral scar with clear borders, scar channels, and epicardial component. A transmural segment of enhancement is also demonstrated in the mid anterolateral wall. 3D LGE with a restrictive temporal window is able to capture small and relevant details missing in the traditional 2D approach. This is only possible due to the 100% efficiency of the iNAV since we can trade acquisition efficiency for a smaller data acquisition window. In contrast, 2D PSIR LGE effectively freezes cardia motion, but incompletely characterizes respective areas of enhancement (Fig. 4).

[2]The MRI restrictions (if any) of the metal implant must be considered prior to patient undergoing MRI exam. MR imaging of patients with metallic implants brings specific risks. However, certain implants are approved by the governing regulatory bodies to be MR conditionally safe. For such implants, the previously mentioned warning may not be applicable. Please contact the implant manufacturer for the specific conditional information. The conditions for MR safety are the responsibility of the implant manufacturer, not of Siemens Healthineers.

3D LGE | **2D LGE**
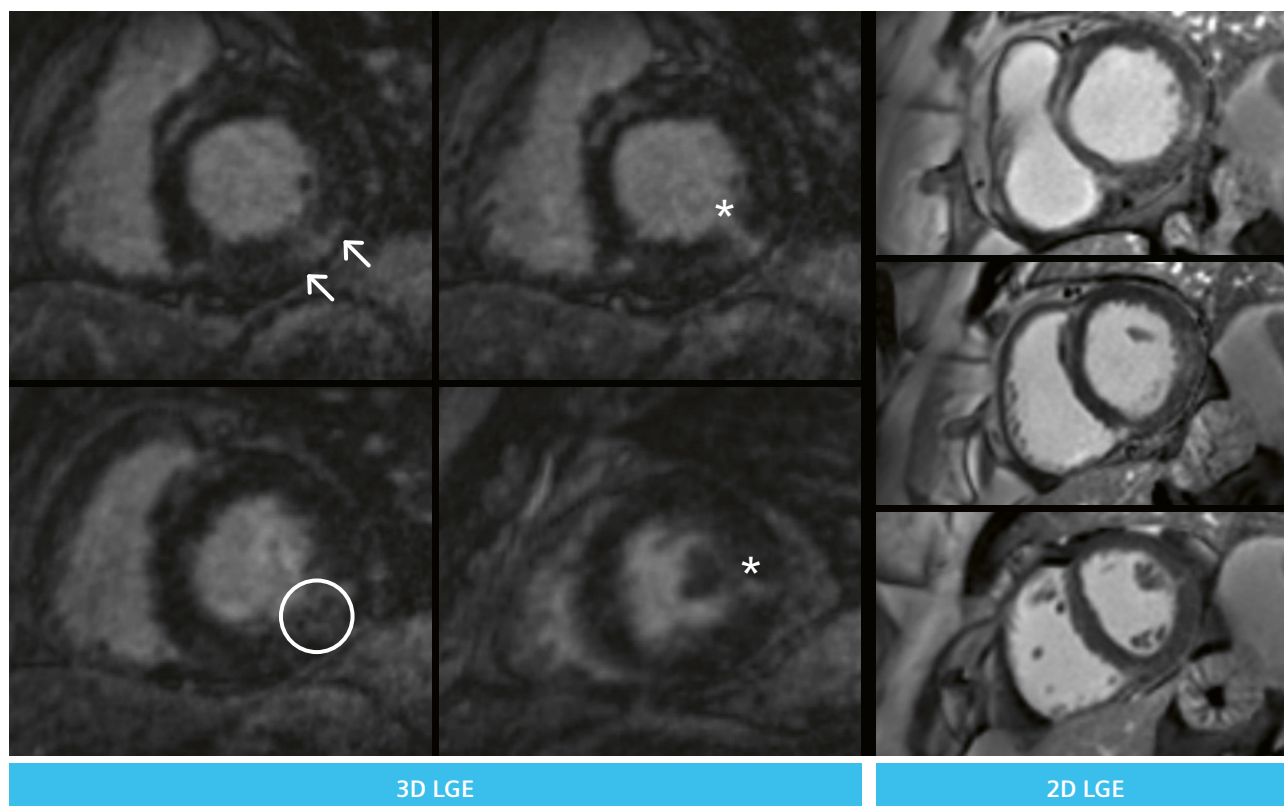
4 Comparison of 3D LGE vs 2D LGE. 3D LGE clearly demonstrates a heterogenous rim-like area of enhancement (circle), scar channels (asterisks), and epicardial component to scar (arrows). Features are ill-descript on 2D LGE.

Summary

In addition to what has already been described in this article, the potential for 3D whole heart to similarly accelerate coronary MRA has also been explored [17]. Submillimeter isotropic spatial resolution, with faithful representation of detail compared with the fully sampled reference can be obtained in a fraction of the time. Likewise, whole chest non-contrast MRA can be acquired more efficiently with 3D T2 prep fat saturated bSSFP at 1.5T [18] or using 3D T2 prep Dixon GRE at 3T. In conclusion, 3D whole heart is a versatile and robust package that overcomes the limitations of traditional dNAV methods for motion correction, combining VD-CASPR and iNAVs for acquisition and SNR efficiency as well as predictable scan time. Furthermore, AI based automatic positioning features and rest period scout facilitate ease of use for new and experienced users alike.

References

1 Dong J, Dickfeld T, Dalal D, Cheema A, Vasamreddy CR, Henrikson CA, Marine JE, Halperin HR, Berger RD, Lima JA, Bluemke DA, Calkins H. Initial experience in the use of integrated electroanatomic mapping with three-dimensional MR/CT images to guide catheter ablation of atrial fibrillation. J Cardiovasc Electrophysiol. 2006;17: 459-66.

2 Moghari MH, Hu P, Kissinger KV, Goddu B, Goepfert L, Ngo L, Manning WJ, Nezafat R. Subject-specific estimation of respiratory navigator tracking factor for free-breathing cardiovascular MR. Magn Reson Med. 2012;67(6):1665-72.

3 Hu P, Peters DC, Stoeck C, Kissinger KV, Goddu B, Goepfert L, Manning WJ, Nezafat R. Off-resonant pulmonary vein imaging. J Cardiovasc Magn Reson. 2009;11(Suppl 1):P185.

4 Henningsson M, Koken P, Stehning C, Razavi R, Prieto C, Botnar RM. Whole-heart coronary MR angiography with 2D self-navigated image reconstruction. Magn Reson Med. 2012;67(2):437-45.

5 Cruz G, Atkinson D, Henningsson M, Botnar RM, Prieto C. Highly efficient nonrigid motion-corrected 3D whole-heart coronary vessel wall imaging. Magn Reson Med. 2017;77(5):1894-1908.

6 Zeilinger MG, Kunze KP, Munoz C, Neji R, Schmidt M, Croisille P, Heiss R, Wuest W, Uder M, Botnar RM, Treutlein C, Prieto C. Non-rigid motion-corrected free-breathing 3D myocardial Dixon LGE imaging in a clinical setting. Eur Radiol. 2022;32(7):4340-4351.

7 Munoz C, Bustin A, Neji R, Kunze KP, Forman C, Schmidt M, Hajhosseiny R, Masci PG, Zeilinger M, Wuest W, Botnar RM, Prieto C. Motion-corrected 3D whole-heart water-fat high-resolution late gadolinium enhancement cardiovascular magnetic resonance imaging. J Cardiovasc Magn Reson. 2020;22(1):53.

8 Bustin A, Sridi S, Gravinay P, Legghe B, Gosse P, Ouattara A, Rozé H, Coste P, Gerbaud E, Desclaux A, Boyer A, Prevel R, Gruson D, Bonnet F, Issa N, Montaudon M, Laurent F, Stuber M, Camou F, Cochet H. High-resolution Free-breathing late gadolinium enhancement Cardiovascular magnetic resonance to diagnose myocardial injuries following COVID-19 infection. Eur J Radiol. 2021;144:109960.

9 Tandon A, James L, Henningsson M, Botnar RM, Potersnak A, Greil GF, Hussain T. A clinical combined gadobutrol bolus and slow infusion protocol enabling angiography, inversion recovery whole heart, and late gadolinium enhancement imaging in a single study. J Cardiovasc Magn Reson. 2016;18(1):66.

10 Yoon SS, Hoppe E, Schmidt M, Forman C, Chitiboi T, Sharma P, Tillmanns C, Maier A, Wetzl JA. Robust Deep-Learning-based Automated Cardiac Resting Phase Detection: Validation in a Prospective Study. Proc Intl Soc Mag Reson Med. 2020;28:2210.

11 Dabir D, Naehle CP, Clauberg R, Gieseke J, Schild HH, Thomas D. High-resolution motion compensated MRA in patients with congenital heart disease using extracellular contrast agent at 3 Tesla. J Cardiovasc Magn Reson. 2012;14:75.

12 Lam CZ, Pagano JJ, Gill N, Vidarsson L, de la Mora R, Seed M, Grosse-Wortmann L, Yoo SJ. Dual phase infusion with bolus tracking: technical innovation for cardiac and respiratory navigated magnetic resonance angiography using extracellular contrast. Pediatr Radiol. 2019;49(3):399-406.

13 Febbo JA, Galizia MS, Murphy IG, Popescu A, Bi X, Turin A, Collins J, Markl M, Edelman RR, Carr JC. Congenital heart disease in adults: Quantitative and qualitative evaluation of IR FLASH and IR SSFP MRA techniques using a blood pool contrast agent in the steady state and comparison to first pass MRA. Eur J Radiol. 2015;84(10):1921-1929.

14 Zheng J, Bae KT, Woodard PK, Haacke EM, Li D. Efficacy of slow infusion of gadolinium contrast agent in three-dimensional MR coronary artery imaging. J Magn Reson Imaging. 1999;10(5):800-805.

15 Groarke JD, Waller AH, Vita TS, Michaud GF, Di Carli MF, Blankstein R, Kwong RY, Steigner M. Feasibility study of electrocardiographic and respiratory gated, gadolinium enhanced magnetic resonance angiography of pulmonary veins and the impact of heart rate and rhythm on study quality. J Cardiovasc Magn Reson. 2014 ;16(1):43.

16 Ghonim S, Ernst S, Keegan J, Giannakidis A, Spadotto V, Voges I, Smith GC, Boutsikou M, Montanaro C, Wong T, Ho SY, McCarthy KP, Shore DF, Dimopoulos K, Uebing A, Swan L, Li W, Pennell DJ, Gatzoulis MA, Babu-Narayan SV. Three-Dimensional Late Gadolinium Enhancement Cardiovascular Magnetic Resonance Predicts Inducibility of Ventricular Tachycardia in Adults With Repaired Tetralogy of Fallot. Circ Arrhythm Electrophysiol. 2020;13(11):e008321.

17 Bustin A, Ginami G, Cruz G, Correia T, Ismail TF, Rashid I, Neji R, Botnar RM, Prieto C. Five-minute whole-heart coronary MRA with sub-millimeter isotropic resolution, 100% respiratory scan efficiency, and 3D-PROST reconstruction. Magn Reson Med. 2019;81(1):102-115.

18 Hajhosseiny R, Rashid I, Bustin A, Munoz C, Cruz G, Nazir MS, Grigoryan K, Ismail TF, Preston R, Neji R, Kunze K, Razavi R, Chiribiri A, Masci PG, Rajani R, Prieto C, Botnar RM. Clinical comparison of sub-mm high-resolution non-contrast coronary CMR angiography against coronary CT angiography in patients with low-intermediate risk of coronary artery disease: a single center trial. J Cardiovasc Magn Reson. 2021;23(1):57.

Contact

Jason Craft, M.D.
Department of Cardiovascular Imaging
St. Francis Heart Hospital
DeMatteis Research Center
101 Northern Blvd
Greenvale NY, 11548
USA
Jason.craft@chsli.org

Non-Contrast Breath-Hold 3D Renal Artery MR Imaging

Hui Liu, Ph.D.

Siemens Healthineers, Zhengzhou, China

Background

Non-contrast free-breathing 3D renal artery MR imaging (Native_Trufi3d_tra_resp_trig) has become one of the preferred methods for detecting nephrogenic hypertension. This is because of its safety and simplicity, with no need for contrast agent injections. Rising living standards are leading to an increase in the number of patients with hypertension, which in turn is causing a gradual rise in the clinical demand for renal artery imaging. However, free-breathing renal artery imaging places high demands on patients, and irregular breathing can easily lead to imaging failure. In addition, the scan time is related to the patient's breathing rate, so if the patient is breathing relatively slowly, the scan will take longer. This paper will show how modifying sequence parameters and optimizing scan time can enable breath-hold 3D renal artery MR imaging (Native_Trufi3d_tra_bh), resulting in a new method for non-contrast 3D renal artery MR imaging.

Introduction

The acquisition time of a conventional non-contrast free-breathing 3D renal artery imaging sequence is about 4 minutes and 50 seconds. By modifying sequence parameters, we were able to reduce the time to 18 seconds, thereby enabling breath-hold imaging. Going from 4 minutes and 50 seconds to 18 seconds doesn't just mean faster imaging: It also makes imaging easier because there is no need to place the respiratory belt, cushion, and the Physiologic ECG & Respiratory Unit (PERU) – if you are not using the BioMatrix Respiratory Sensor. The success rate of breath-hold renal artery imaging is also better than that of conventional free-breathing renal artery imaging.

Materials and methods

The images shown in Case 1 were acquired on a 3T MAGNETOM Lumina system using *syngo* MR XA20 software and a combination of the 18-channel body and the integrated spine coil. We used the system's BioMatrix Respiratory Sensor as the respiratory trigger.

The images shown in Case 2 were acquired on a 3T MAGNETOM Vida system using *syngo* MR XA10 software and a combination of the 18-channel body and the integrated spine coil. We used the BioMatrix Respiratory Sensor as the respiratory trigger.

	TA	Slices	Slice thickness [mm]	Base resolution × phase resolution × slice resolution	Trigger	Slice partial Fourier	Phase partial Fourier	TI [ms]
Free-breathing	4:50 min	64	1.1	256 × 100% × 81%	Respiratory	off	off	1500
Breath-hold	18–19 sec	36–40	1.5	256 × 70% × 50%	None (breath-hold)	6/8	5/8	1100–1200

Table 1: Parameter changes.

The images shown in Case 3 were acquired on a 1.5T MAGNETOM Sempra system using *syngo* MR XA12 software and a combination of the 6-channel body and the integrated spine coil. We used the respiratory belt, cushion, and PERU.
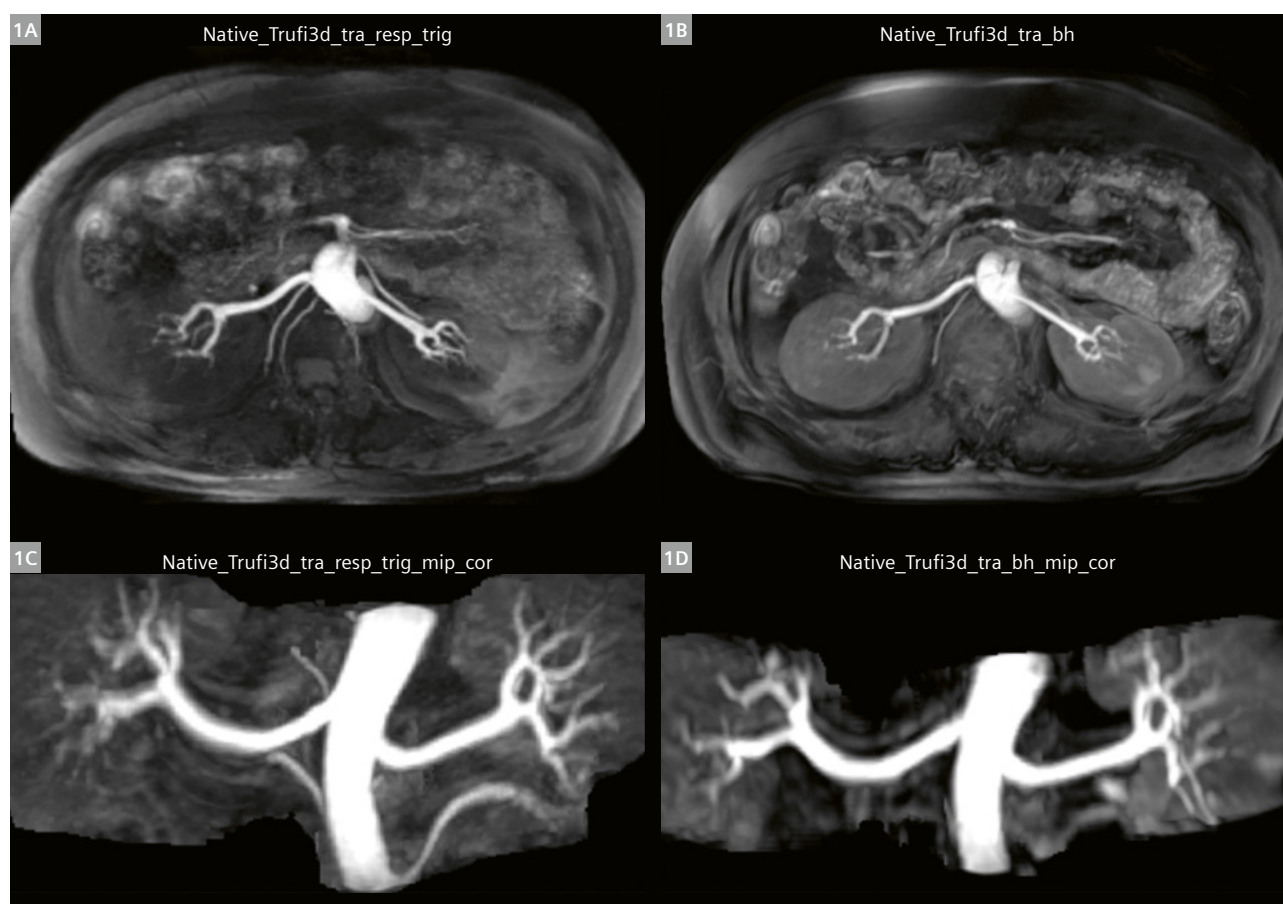
For the free-breathing renal artery imaging, we used the default sequence from Siemens Healthineers, without any parameter changes. For the breath-hold renal artery imaging, we adapted the parameters to patient needs. All the main parameter changes are shown in Table 1.

For the breath-hold acquisition, the resolution must be reduced in order to reduce the sequence time. Therefore, the resolution of breath-hold renal artery imaging is not as good as that of free-breathing renal artery imaging. However, the low resolution does not affect the display of renal artery branches and will not hamper clinical diagnosis.
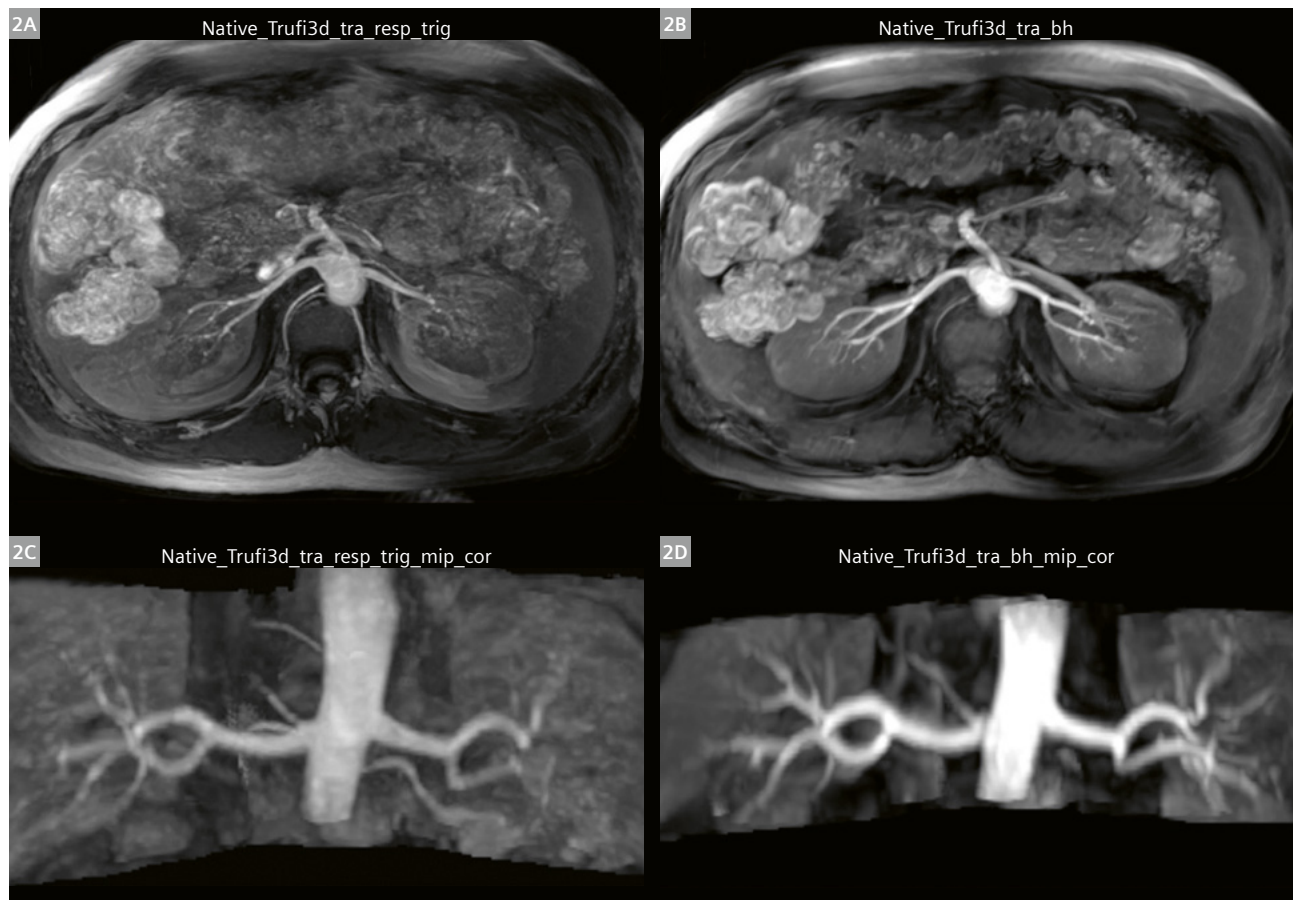
Case 1

Healthy 47-year-old female volunteer.

1 (1A) Non-contrast free-breathing 3D renal artery imaging. (1B) Non-contrast breath-hold 3D renal artery imaging. (1C) Coronal MIP image of non-contrast free-breathing 3D renal artery. (1D) Coronal MIP image of non-contrast breath-hold 3D renal artery.

Both imaging methods were successful. The image-quality comparison found that the free-breathing imaging showed the branch of the renal artery more clearly, but the difference was not significant. The free-breathing method took longer: While the sequence time is 3 minutes and 41 seconds, the patient's slow respiratory rate meant that the actual acquisition time was more than 5 minutes. The sequence time of the breath-hold renal artery imaging was 18 seconds, and the actual acquisition time was 18 seconds. Breath-hold renal artery imaging therefore has a better balance between time and image quality.
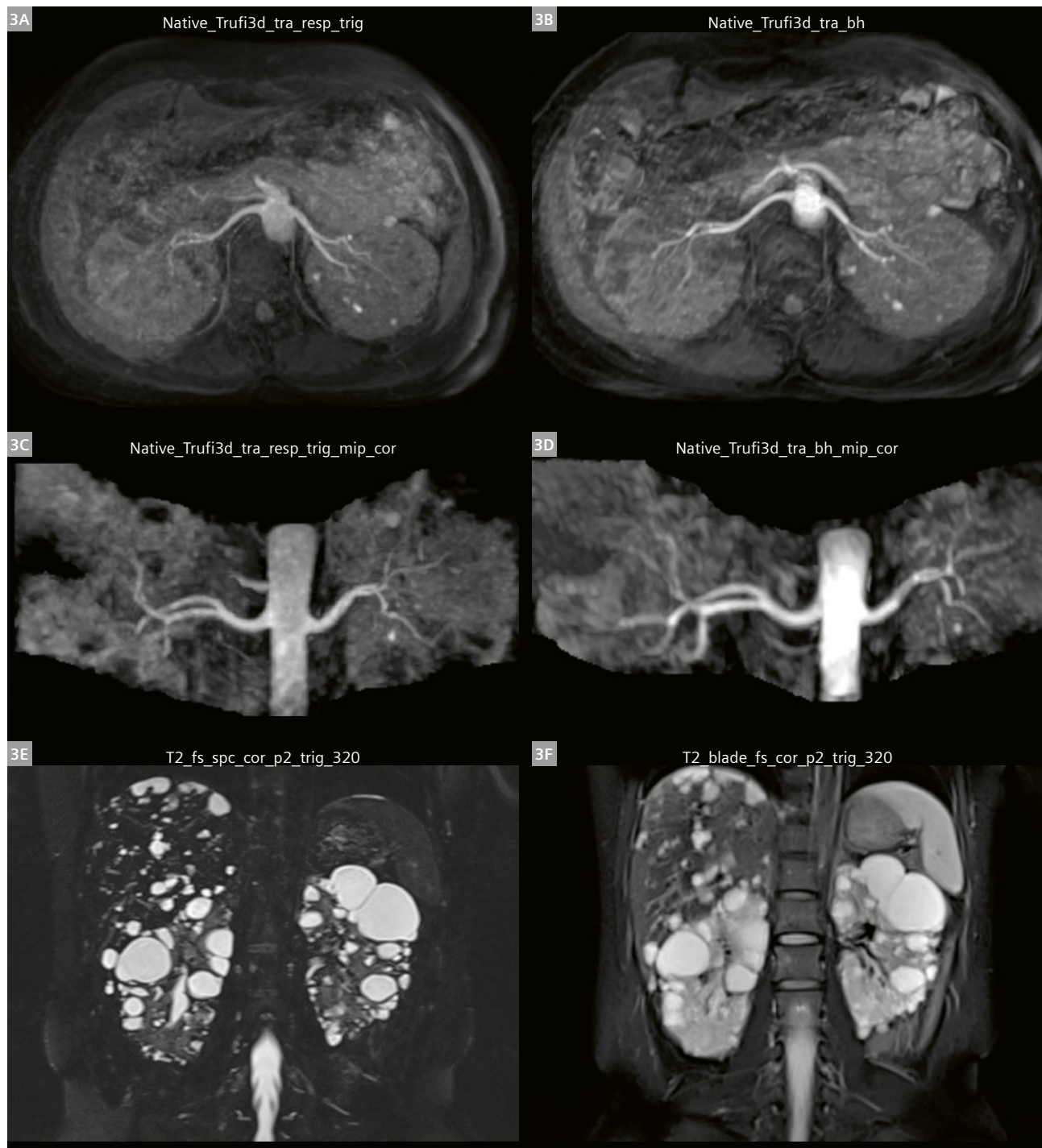
Case 2

Healthy 33-year-old male volunteer.

2 **(2A)** Non-contrast free-breathing 3D renal artery imaging. **(2B)** Non-contrast breath-hold 3D renal artery imaging. **(2C)** Coronal MIP image of non-contrast free-breathing 3D renal artery. **(2D)** Coronal MIP image of non-contrast breath-hold 3D renal artery.

The free-breathing method hardly shows the distant segmental branches of the renal artery, and imaging fails. The breath-hold method clearly shows the more distant segmental branches of the renal artery. A series of tests comparing the two imaging methods found that the success rate of breath-hold renal artery imaging is much higher than with free-breathing imaging. Both methods only failed in one case – a patient with malignant hypertension (blood pressure of 220 mmHg).

Because non-contrast renal artery imaging relies on blood-flow imaging, and because blood flows very slowly in patients with malignant hypertension, the renal artery begins to appear when the inversion time (TI) is set for more than two seconds, and the display effect of both methods is not good. Breath-hold renal artery imaging has a higher success rate.

Case 3

A 36-year-old female patient with polycystic liver and kidney disease.

3 **(3A)** Non-contrast free-breathing 3D renal artery imaging. **(3B)** Non-contrast breath-hold 3D renal artery imaging. **(3C)** Coronal MIP image of non-contrast free-breathing 3D renal artery. **(3D)** Coronal MIP image of non-contrast breath-hold 3D renal artery. **(3E and 3F)** Conventional T2 fat-suppression coronal imaging of the abdomen.

The breath-hold method showed the branch of the renal artery more clearly than with free-breathing. Faster imaging leads to smaller breathing motion artifacts and a clearer view of the renal artery.

Conclusion

Breath-hold 3D renal artery imaging is faster, has a higher success rate, and achieves better imaging quality than the free-breathing method. We also tested non-contrast breath-hold renal artery imaging on other MR systems with different field strengths, such as a 1.5T MAGNETOM Area, a 3T MAGNETOM Skyra, and a 3T MAGNETOM Prisma, and used the respiratory belt, cushion, and PERU. All were successful, and parameter modifications were similar.

Discussion

In patients with good breath-hold ability, non-contrast breath-hold 3D renal artery imaging can be used as a good alternative to the conventional free-breathing method. For patients whose breath-hold abilities are not good, we conducted a series of tests with free-breathing renal artery imaging and found a feasible method to improve the success rate of this type of imaging. The method will be presented in the next article.

References

1 Maki JH, Wilson GJ, Eubank WB, Glickerman DJ, Pipavath S, Hoogeveen RM. Steady-state free precession MRA of the renal arteries: breath-hold and navigator-gated techniques vs. CE-MRA. J Magn Reson Imaging. 2007;26(4):966–973.

2 Zhang Y, Xing Z, Liu Y, She D, Zeng Z, Cao D. Nonenhanced renal MR angiography using steady-state free precession (SSFP) and time-spatial labeling inversion pulse (Time-SLIP): repeatability and comparison of different tagging location. Abdom Imaging. 2014;39(5):1000–1008.

3 Lanzman RS, Kröpil P, Schmitt P, Freitag SM, Ringelstein A, Wittsack HJ, et al. Nonenhanced free-breathing ECG-gated steady-state free precession 3D MR angiography of the renal arteries: comparison between 1.5 T and 3 T. AJR Am J Roentgenol. 2010;194(3):794–798.

4 Glockner JF, Takahashi N, Kawashima A, Woodrum DA, Stanley DW, Takei N, et al. Non-contrast renal artery MRA using an inflow inversion recovery steady state free precession technique (Inhance): comparison with 3D contrast-enhanced MRA. J Magn Reson Imaging. 2010;31(6):1411–1418.

5 Zhang W, Lin J, Wang S, Lv P, Wang L, Liu H, et al. Unenhanced respiratory-gated magnetic resonance angiography (MRA) of renal artery in hypertensive patients using true fast imaging with steady-state precession technique compared with contrast-enhanced MRA. J Comput Assist Tomogr. 2014;38(5):700–704.

6 Katoh M, Buecker A, Stuber M, Günther RW, Spuentrup E. Free-breathing renal MR angiography with steady-state free-precession (SSFP) and slab-selective spin inversion: initial results. Kidney Int. 2004;66(3):1272–1278.

Contact

Hui Liu, Ph.D.
Siemens Healthineers, Zhengzhou, China
SHS CHN CS-CRM APP MR NS
76, Kangning Street
Zhengzhou, HA
Zhengzhou 450000
China

Clinical Impact of Combining Novel Non-Contrast-Enhanced MR Angiography with Multivenc 4D Flow MRI for Cardiovascular Diseases

Satoshi Higuchi[1], Yoshiaki Komori[2], Michaela Schmidt[3], Daniel Giese[3], Hideki Ota[1]

[1]Department of Diagnostic Radiology, Tohoku University Hospital, Miyagi, Japan
[2]Siemens Healthcare K.K., Tokyo, Japan
[3]Siemens Healthcare GmbH, Erlangen, Germany

Introduction

Non-contrast-enhanced magnetic resonance angiography (non-CE MRA) is a non-invasive examination which allows to visualize the vascular morphology and its vascularity without the ionizing radiation or administration of contrast agents required in CT angiography. Four-dimensional flow MRI (4D Flow MRI), which allows hemodynamic assessment in blood vessels, provides additional information for predicting cardiovascular events and understanding their pathology in patients with cardiovascular diseases.

However, these imaging techniques have the drawback of long scan times, due to the need for an electrocardiogram (ECG) and respiratory gating. Therefore, novel Compressed Sensing (CS) techniques and their application to non-CE MRA and 4D Flow MRI are emerging [1]. This paper reviews the clinical usefulness of highly accelerated non-CE MRA and highly accelerated 4D Flow MRI acquisition with multivenc (MV). These techniques will be termed *Advanced MRA* and *MV CS 4D Flow* in the following.

Non-contrast conventional MRA

Non-contrast Advanced MRA
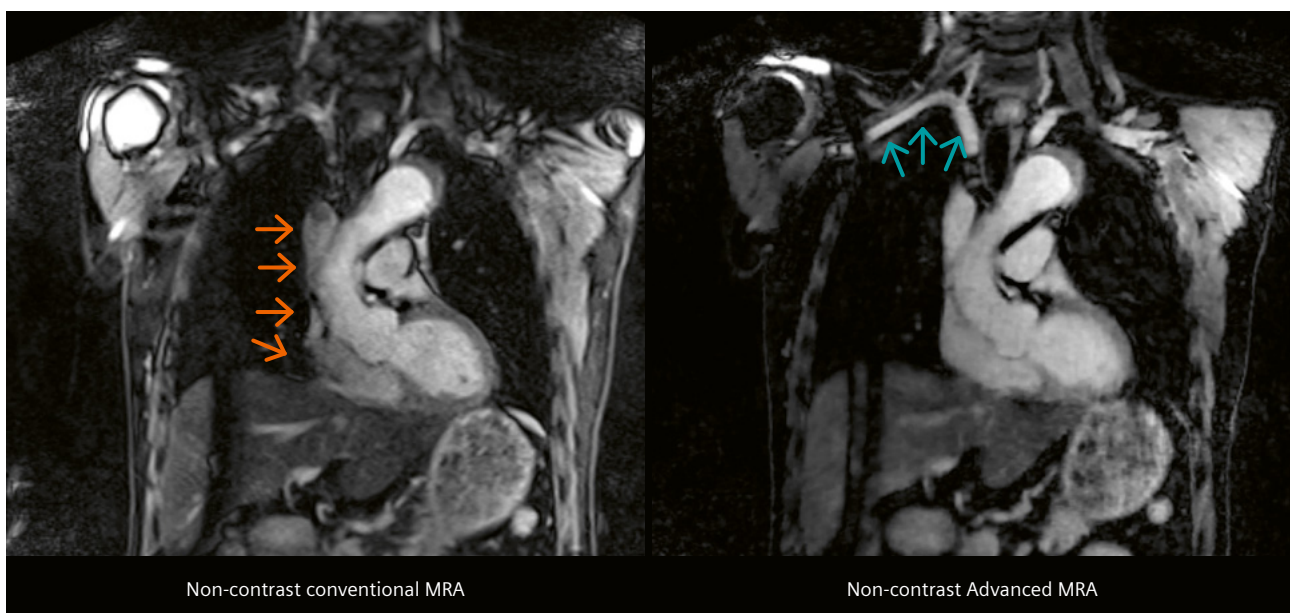
1 Comparison between conventional non-contrast MR angiography (MRA) and non-contrast Advanced MRA in a healthy volunteer.
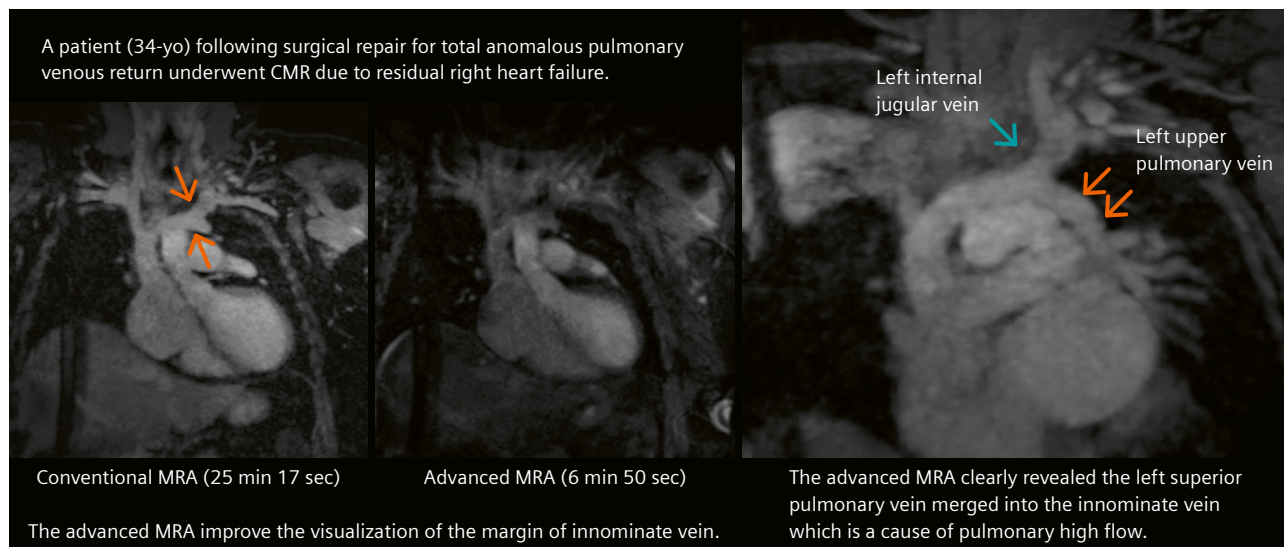
Advanced MRA

Non-contrast MRA can be applicable to many patients with cardiovascular disease, but it is especially useful for imaging patients with congenital heart disease, patients with contraindications for contrast agent injection, and patients who need repeated follow-up imaging. However, the clinical use of free-breathing and ECG-gated native MRA acquisitions is often hampered by the long scan times needed to achieve high-resolution image quality. Siemens Healthineers recently introduced a novel non-CE MRA research sequence that uses Compressed Sensing (CS) and accurately reconstructs high-quality images from sparsely sampled *k*-space data with a significant reduction in scan time. The shorter scan time is expected to reduce motion artifacts, resulting in better image quality.

Furthermore, conventional MRA methods often use a spectral adiabatic inversion recovery (SPAIR) technique for fat suppression. This can cause non-uniform signal reduction in blood vessels due to the sensitivity to main magnetic field (B_0) inhomogeneities, especially at the boundaries of the lung and at locations with complex body morphology, such as the shoulders and neck [2]. Advanced MRA therefore uses a 2-point Dixon technique, which offers a robust fat-water separation technique that is less sensitive to B_0 inhomogeneity and therefore results in less signal inhomogeneity in the blood vessels and potentially improved diagnostic performance. Results from a volunteer show that the heterogeneous signal distribution in the right subclavian artery, superior vena cava, and ascending aorta in conventional MRA is improved using Advanced MRA (Fig. 1). Figure 2 shows the MRA results from a patient with partial anomalous pulmonary venous return (PAPVR) of the left upper pulmonary vein. The scan time

for Advanced MRA was reduced to 7 minutes, compared to 26 minutes for conventional MRA. In Advanced MRA, the PAPVR is clearly visualized without the signal inhomogeneities seen around the apex of the left lung in the conventional MRA image. Thus, Advanced MRA is a promising and emerging imaging technique that is expected to be clinically useful for patients with cardiovascular disease. It clearly depicts vascular morphological and vascular course abnormalities in arteries and veins while reducing both scan time and any artifacts caused by motion and B_0 inhomogeneities.

MV CS 4D Flow

4D Flow MRI is an imaging technique that enables the visualization and quantification of physiological hemodynamics within the vasculature. While the assessment of vascular morphology using CTA has traditionally played a central role in diagnosis and treatment planning for vascular diseases, recent research efforts have focused on studying hemodynamics for further risk stratification and optimizing treatment strategies. Stanford type B aortic dissection is one of the diseases for which there is growing interest in developing hemodynamic biomarkers to predict prognosis. This is because evidence increasingly suggests that conservative management results in a favorable outcome in the acute phase, but a poor prognosis in the chronic phase [3–6]. We also retrospectively analyzed conventional 4D Flow MRI in patients with chronic Stanford type B aortic dissection and investigated the relationship between hemodynamic parameters at entry, true lumen, and false lumen and aortic growth rate derived from a CTA series (Fig. 3). This study revealed that patients with a


A patient (34-yo) following surgical repair for total anomalous pulmonary venous return underwent CMR due to residual right heart failure.

Left internal jugular vein

Left upper pulmonary vein

Conventional MRA (25 min 17 sec)   Advanced MRA (6 min 50 sec)

The advanced MRA improve the visualization of the margin of innominate vein.

The advanced MRA clearly revealed the left superior pulmonary vein merged into the innominate vein which is a cause of pulmonary high flow.

2 Partial anomalous pulmonary venous return (PAPVR), in which the left upper pulmonary vein drains into the left innominate vein.
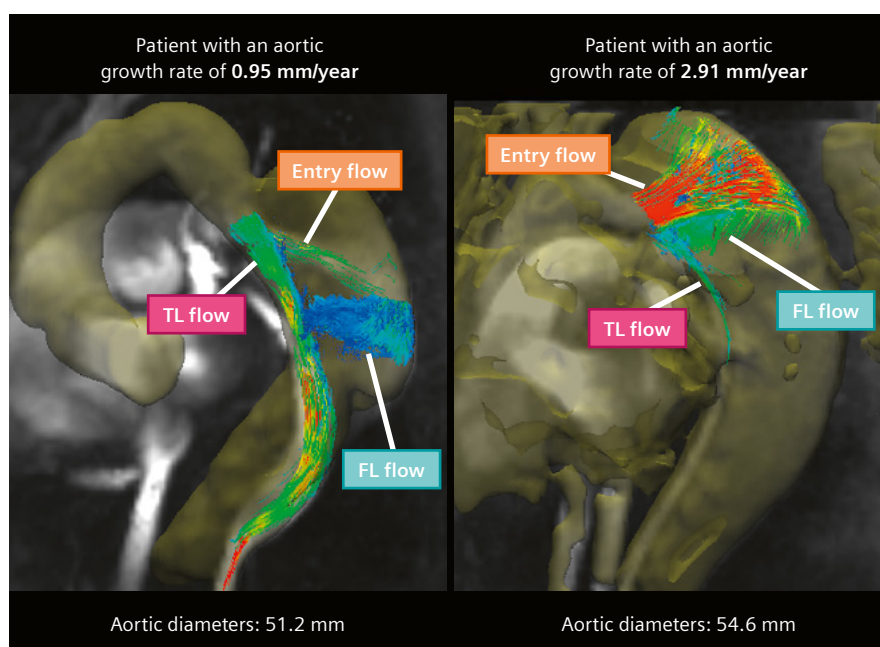
higher rate of flow velocity or volume in the entry and false lumen compared to the true lumen were associated with fast aortic growth rate (Fig. 4) [7]. These hemodynamic parameters could be a new predictor of cardiovascular diseases. However, widespread clinical implementation of 4D Flow MRI is hindered by the long acquisition time and limited sensitivity to a large spectrum of velocities. These shortcomings can be addressed by applying CS in combination with a multivenc acquisition, which was recently included in the MV CS 4D Flow research sequence developed by Siemens Healthineers. Regularization is performed both in space and time. The shorter acquisition time makes it possible to perform the previously challenging multivenc scans, which acquire phase-contrast datasets with different velocity encoding (VENC) values within a single acquisition [8]. Figure 5 shows phase-contrast images for three different VENC values. Fast flow in the true lumen and entry, which cannot be depicted by the lower VENC due to aliasing, is clearly depicted by the

higher VENC. Meanwhile, slow flow in the false lumen, which is not well depicted by the higher VENC due to a limited velocity-to-noise ratio (VNR), is clearly depicted by the lower VENC. The merged images are calculated using a Bayesian unfolding approach utilizing all phase-contrast images as well as their corresponding magnitude images to extract an optimal phase-contrast image. This image corresponds to the VNR-optimal combination of all single-VENC acquisitions and thereby accurately depicts a wide range of blood-flow velocities in a single series of images, complementing the limitation of each VENC setting (Figs. 6, 7).

Besides the long acquisition time, another reason for the limited clinical use of 4D Flow MRI is the post-processing with vessel segmentation. In conventional 4D Flow MRI, areas of slow blood flow are not recognized as intravascular regions, making it difficult to obtain accurate vessel segmentation easily (Fig. 8). By using the flow-independent vessel contrast of Advanced MRA and
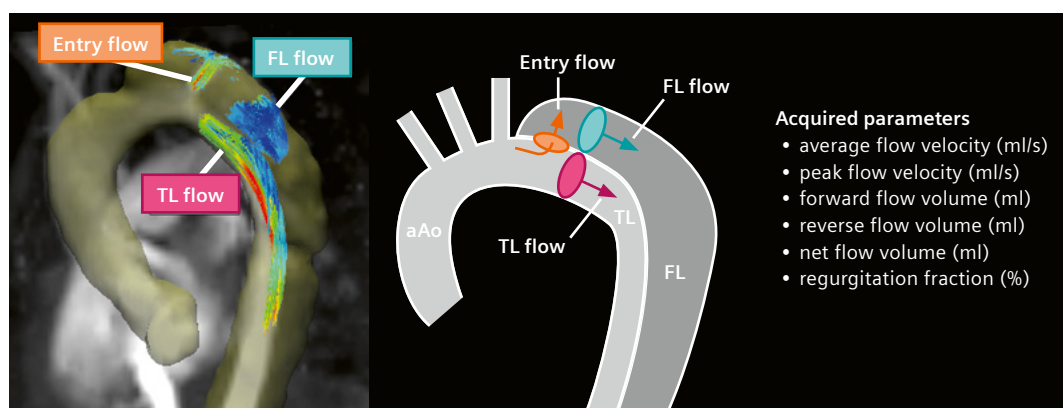
3 Evaluation of flow parameters in 4D Flow MRI in our study of patients with uncomplicated Stanford type B aortic dissection.
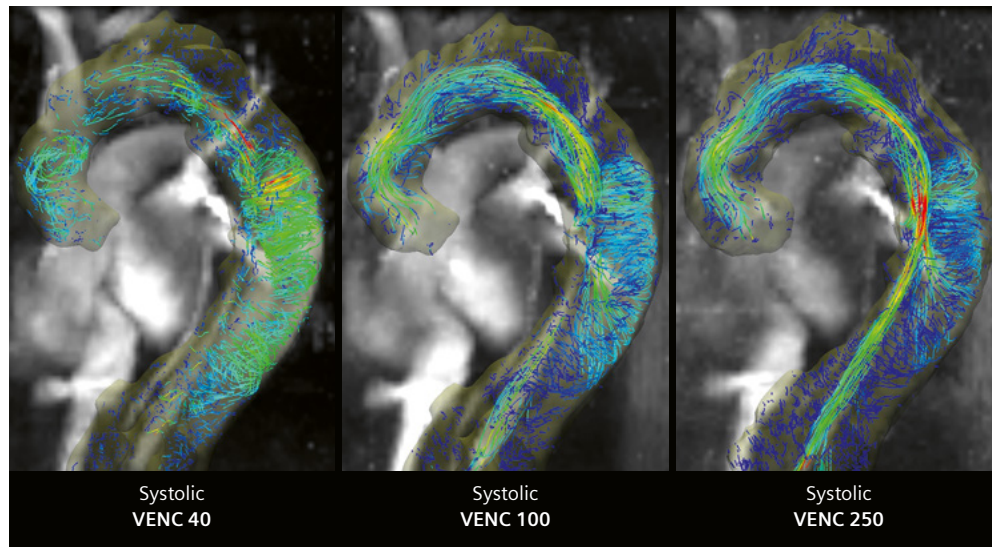TL: True lumen
FL: False lumen

Acquired parameters
- average flow velocity (ml/s)
- peak flow velocity (ml/s)
- forward flow volume (ml)
- reverse flow volume (ml)
- net flow volume (ml)
- regurgitation fraction (%)

Patient with an aortic growth rate of **0.95 mm/year**

Patient with an aortic growth rate of **2.91 mm/year**

Aortic diameters: 51.2 mm

Aortic diameters: 54.6 mm

4 Patient with a low aortic growth rate demonstrates higher flow velocity and volume in true lumen (TL) than that in entry and false lumen (FL) (peak flow = 111, 23, and 83 mL/sec and net forward volume = 32, 5, and 16 mL in TL, entry, and FL, respectively). A patient with higher aortic growth rate shows lower flow in TL (peak flow = 45, 168, and 219 mL/sec and net forward volume = 16, 34, and 59 mL in TL, entry, and FL, respectively).

its higher resolution for segmentation, the 4D Flow analysis time can be reduced and vessels with low flow are optimally included in the segmentation for particle tracing.

Conclusion

The introduction of Advanced MRA and MV CS 4D Flow MRI is a groundbreaking advancement in cardiovascular

imaging. In addition, as 4D Flow MRI becomes more widely available, more facilities will be able to perform it in clinical practice, and the accumulation of data from multiple facilities will accelerate the development of hemodynamic assessment methods. These non-invasive imaging techniques provide accurate diagnoses and hemodynamic information in vascular diseases in a shorter time and thus have the potential to transform trends in clinical
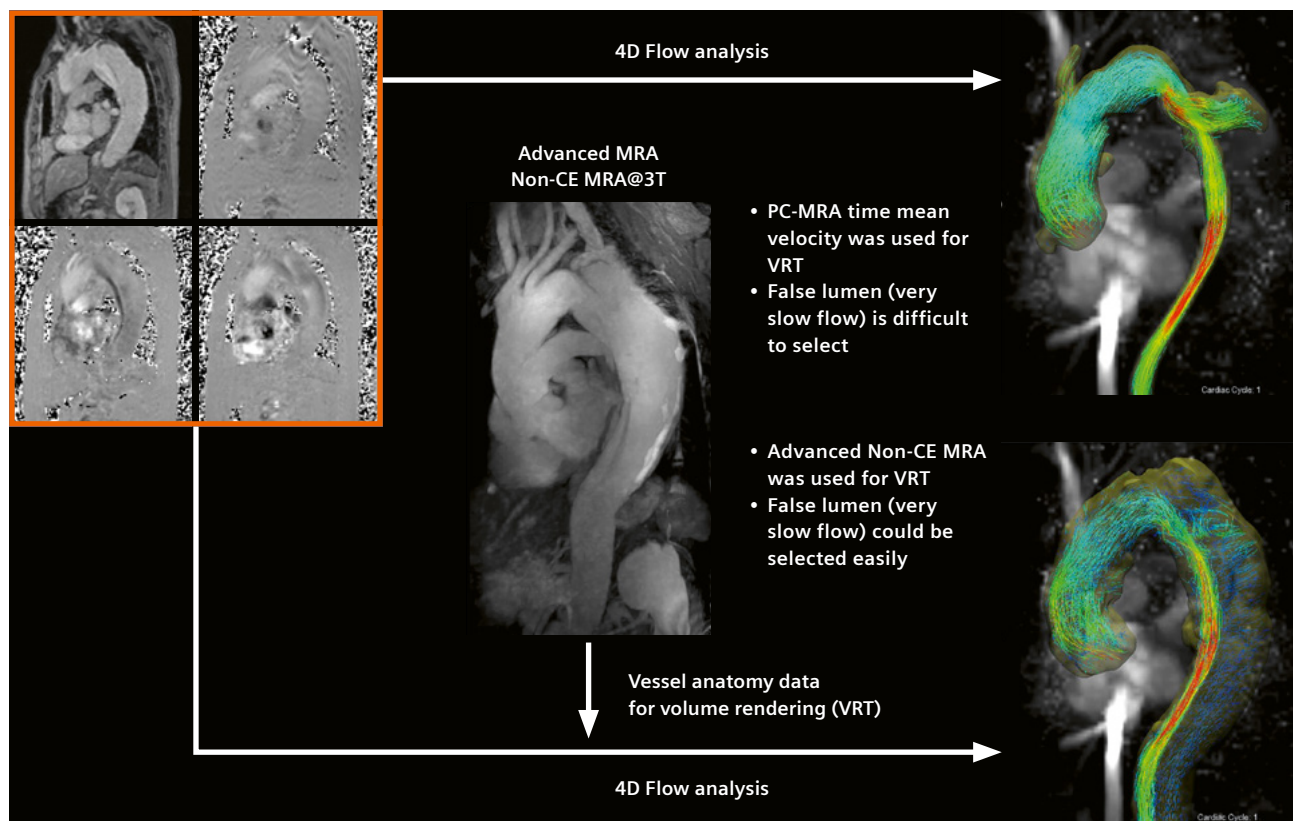

5 Differences in flow visualization in true lumen (fast flow) and false lumen (slow flow) due to differences in VENC settings.
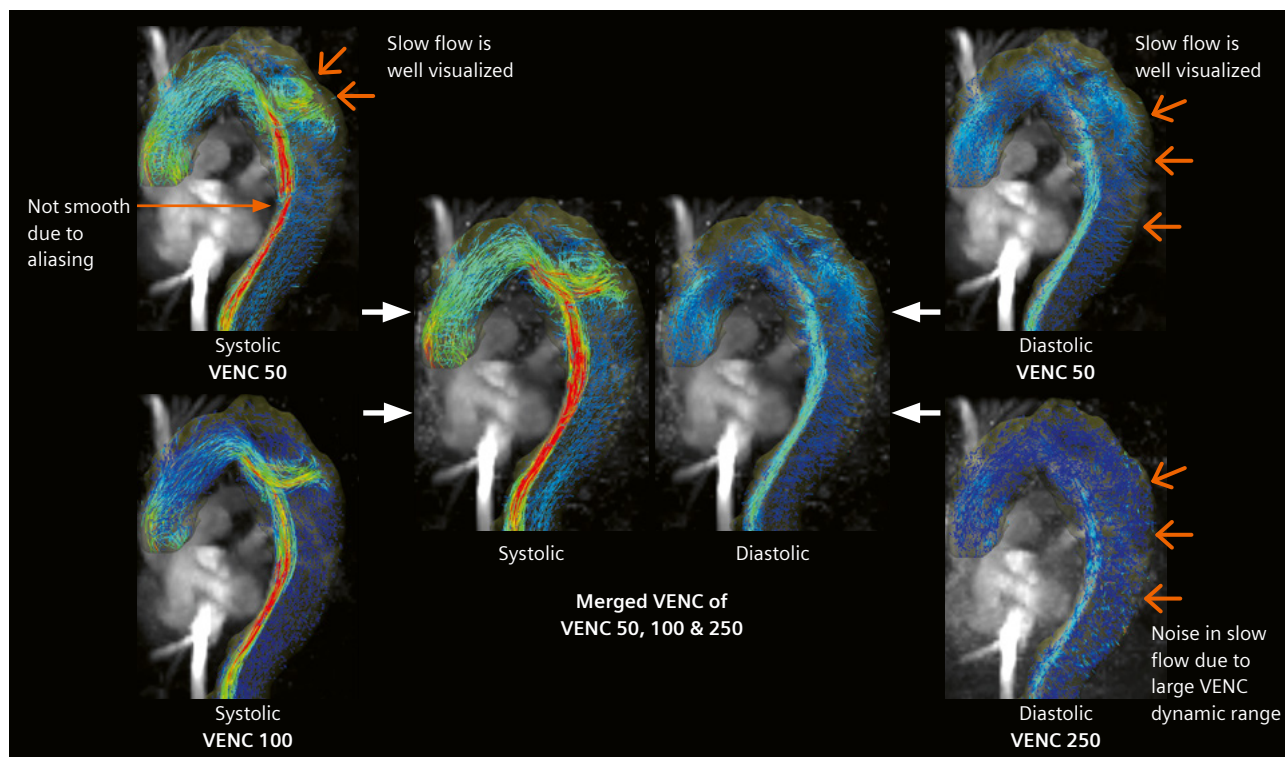
6 Merged VENC images are generated by synthesizing only the best signal from each dynamic range of the VENC images.
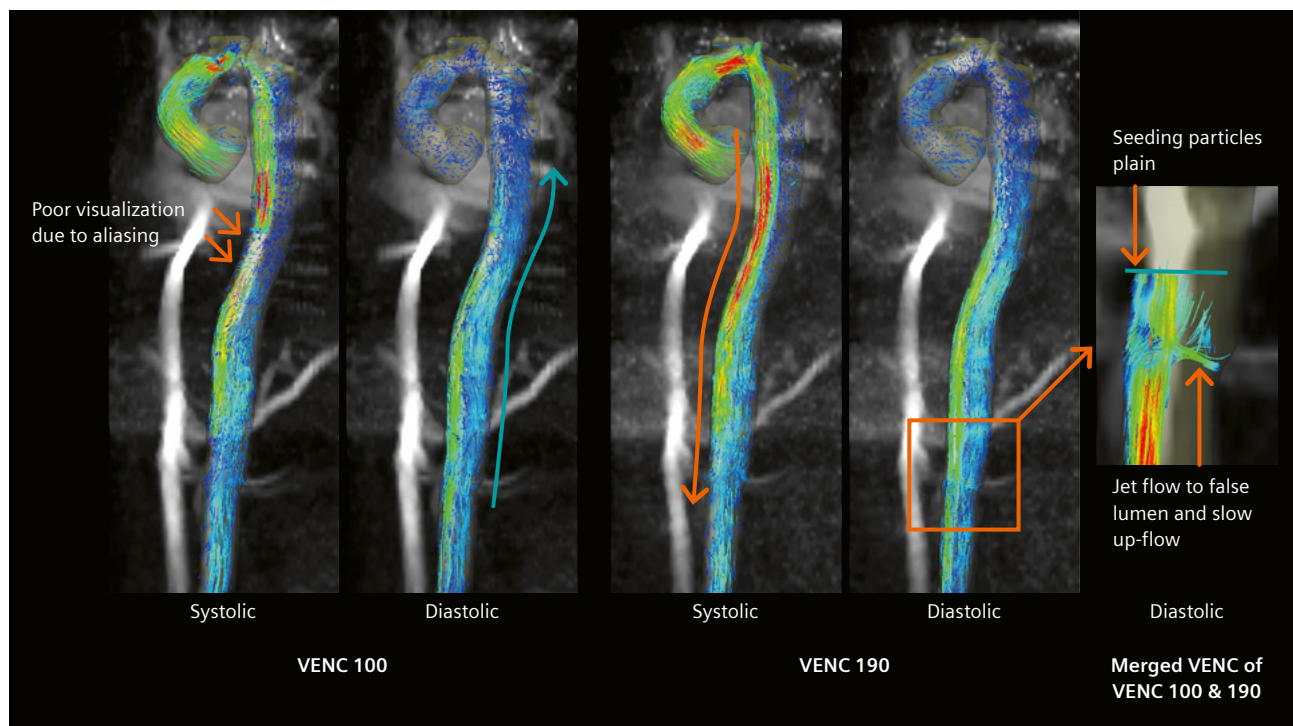
7 A merged VENC image visualizes the complex flow in both the true and false lumens.

8 Improvement of 4D Flow postprocessing analysis using anatomical data with non-CE Advanced MRA.

	Advanced MRA	**CS 4D Flow**
Sequence type	T2-preped 3D FLASH	3D phase contrast cine
Acceleration technique	CS	CS
TE/TR (ms)	TE1 1.34, TE2 2.87/7.8	3.42/57.5
FOV (mm)	450 × 450	400 × 320
Image matrix	192 × 125	160 × 128
Reconstructed spatial resolution (mm)	1.2 × 1.2	2.5 × 2.5
Slice thickness (mm)	1.2	2.5
Slices per Slab	128	35
Orientation	Coronal	Sagittal
Flip angle (degrees)	12	7
Bandwidth (Hz/pixel)	799	558
Segments	25	1
Fat sat.	DIXON	–
Respiratory Gating	1D PACE, ± 6.5 mm	1D PACE, ± 8 mm, ReCAR
Acceleration factor	11	7.7
Iterative reconstruction (n)	20	30
VENC	–	dual or triple

Table 1: Imaging Parameters of Advanced MRA and CS 4D Flow
CS: compressed sensing, TE: echo time, TR: repetition time, FOV: field of view, VENC: velocity encoding,
ReCAR: Respiratory Controlled Adaptive *k*-space Reordering.

practice by helping alleviate the patient burden and enhance overall workflow efficiency. Thus, these technologies hold great promise for improving patient management and advancing the field of cardiovascular medicine.

References

1   Feng L, Benkert T, Block KT, Sodickson DK, Otazo R, Chandarana H. Compressed sensing for body MRI.
J Magn Reson Imaging. 2017;45(4):966-987.
2   Bley TA, Wieben O, François CJ, Brittain JH, Reeder SB. Fat and water magnetic resonance imaging.
J Magn Reson Imaging. 2010;31(1):4-18.
3   Fleischmann D, Afifi RO, Casanegra AI, Elefteriades JA, Gleason TG, Hanneman K, et al. Imaging and Surveillance of Chronic Aortic Dissection: A Scientific Statement From the American Heart Association. Circ Cardiovasc Imaging. 2022;15(3):e000075.
4   Burris NS, Nordsletten DA, Sotelo JA, Grogan-Kaylor R, Houben IB, Figueroa CA, et al. False lumen ejection fraction predicts growth in type B aortic dissection: preliminary results.
Eur J Cardiothorac Surg. 2020;57(5):896-903.
5   Evangelista A, Pineda V, Guala A, Bijnens B, Cuellar H, Rudenick P, et al. False Lumen Flow Assessment by Magnetic Resonance Imaging and Long-Term Outcomes in Uncomplicated Aortic Dissection. J Am Coll Cardiol. 2022;79(24):2415-2427.
6   Ruiz-Muñoz A, Guala A, Dux-Santoy L, Teixidó-Turà G, Servato ML, Valente F, et al. False lumen rotational flow and aortic stiffness are associated with aortic growth rate in patients with chronic aortic dissection of the descending aorta: a 4D flow cardiovascular magnetic resonance study.
J Cardiovasc Magn Reson. 2022;24(1):20.
7   Satoshi H, Hideki O, Ryuichi M, Yuki I, Hiroki K, Kei T. Evaluation of hemodynamic parameters for prediction of aortic growth in patients with chronic Stanford type B aortic dissection using 4D flow MRI. In: Proceedings of the 31st Annual Meeting of ISMRM, Toronto, 2023. (abstract 1088).
8   Callaghan FM, Kozor R, Sherrah AG, Vallely M, Celermajer D, Figtree GA, et al. Use of multi-velocity encoding 4D flow MRI to improve quantification of flow patterns in the aorta.
J Magn Reson Imaging. 2016;43(2):352-363.

Contact

Satoshi Higuchi, M.D., Ph.D.
Tohoku University Hospital
Department of Diagnostic Radiology
1-1 Seiryomachi, Aoba, Sendai, Miyagi
Japan
Tel: +81-22-717-7312
satoshi.higuchi.b4@tohoku.ac.jp

Ferumoxytol-Enhanced 4-Dimensional MR Imaging in Pediatric and Adult Congenital Heart Disease

J. Paul Finn, M.D.[1,2]; Takegawa Yoshida, M.D.[1]; Arash Bedayat, M.D.[1]; Ashley Prosper, M.D.[1]; Chang Gao[1]; Xiaodong Zhong, Ph.D.[1]; Ning Jin, Ph.D.[3]; Xiaoming Bi, Ph.D.[4]; Kim-Lien Nguyen, M.D.[1,2,5]

[1]Diagnostic Cardiovascular Imaging Laboratory, Department of Radiological Sciences, David Geffen School of Medicine at UCLA, Los Angeles, CA, USA

[2]Physics and Biology in Medicine Graduate Program, University of California, Los Angeles, CA, USA

[3]MR R&D Collaborations, Siemens Medical Solutions USA, Inc., Cleveland, OH, USA

[4]MR R&D Collaborations, Siemens Medical Solutions USA, Inc., Los Angeles, CA, USA

[5]Division of Cardiology, David Geffen School of Medicine at UCLA and VA Greater Los Angeles Healthcare System, Los Angeles, CA, USA

Introduction

MRI has unique strengths for cardiac imaging and is particularly useful in patients with congenital heart diseases. In recent years, multidimensional cardiac imaging has shown spectacular results by combining advanced techniques with ferumoxytol[1] enhancement of the blood pool. In this short report, we will show how 4-dimensional imaging can be applied successfully to children[2] and adults with congenital heart disease (CHD), with one illustrative example in each respective category.

Children with congenital heart disease

In children, our goal is high-resolution, artifact-free images over the full cardiac cycle in patients who may weigh less than 2 kg, whose heart rate may exceed 180 beats per minute, who breathe up to 40 times per minute, and who may move spontaneously at any time. What could possibly go wrong!

The holy grail is to perform these studies without sedation while the patient breathes spontaneously. Intensive research is underway in many laboratories (including our own) to make this a reality [1–7], but significant technical challenges remain. Meanwhile, with certain constraints,

detailed and comprehensive 4-dimensional MR imaging of children with CHD is possible today, using a well-established methodology. The approach we have adopted is simple and consistent for all children who require sedation, independent of patient size, age, or disease complexity. The key components include:

1. Enhancement of the blood pool in the steady state distribution of ferumoxytol
2. A controlled and regular respiratory pattern, ensured by positive pressure ventilation and muscle relaxants
3. Cardiac-triggered and respiratory-gated volumetric acquisitions over all desired anatomy with 4D MUSIC[3] [8] and 4D flow[4] (non-product) sequences, during uninterrupted ventilation

With the sequences we use, image reconstruction is inline and immediate, although the 4D flow images require advanced processing with commercial software. We use Arterys (Tempus, Chicago, IL, USA) for 4D flow processing, but other commercial options are available. The MUSIC images are immediately available as DICOM input to any platform with a 4D viewing option, where 2D cines can be reconstructed in any plane and saved to an archival (PACS) system. We use OsiriX (Pixmeo SARL, Bernex, Switzerland) on a Mac workstation.

---

[1] Ferumoxytol is not approved for diagnostic applications and its use for MRI is off-label.

[2] MR scanning has not been established as safe for imaging fetuses and infants less than two years of age. The responsible physician must evaluate the benefits of the MR examination compared to those of other imaging procedures. Note: This disclaimer does not represent the opinion of the author.

[3] MUSIC is a prototype sequence developed at UCLA.

[4] The authors are using a non-product sequence, but 4D Flow has been available as a product since software version syngo MR XA30.

In our practice, the typical imaging time from the first scout sequences to completion of the last series is less than 30 minutes, without any requirement for breath-holding and irrespective of how complex the disease is. The covered anatomy includes the heart and the blood vessels of the neck, chest, and abdomen. For context, conventional imaging with 2D cine, 3D contrast-enhanced MRA, and targeted 2D flow requires repeated breath-holding and interactive scanning prescription that may take 60 to 90 minutes. Moreover, in the end, it may be that certain image planes that in hindsight were relevant had not been acquired and cannot be retrospectively reconstructed. With the 4D approach, this is never the situation.

Case 1

A 22-month-old[1] male patient with heterotaxia and double outflow right ventricle (DORV) had undergone bilateral Glenn shunt procedures and was being assessed for possible bi-ventricular repair. MRI was requested to define cardiac chamber anatomy and size, vascular anatomy, and the integrity of the Glenn shunts. The patient underwent general anesthesia, intubation, and controlled ventilation, and received ferumoxytol, 4 mg/kg, by slow intravenous infusion before being advanced into the bore of a 3T MAGNETOM Trio scanner (Siemens Healthcare, Erlangen, Germany). A small flex coil was positioned over the heart, and continuous monitoring of ECG, pulse oximetry, airway pressure, and non-invasive blood pressure was performed. Following initial scout images, a real-time cine series in the coronal plane was acquired over 20 seconds to confirm satisfactory ventilatory movement of both hemi-diaphragms. A 4D MUSIC acquisition [8] was then performed encompassing the neck, chest, and abdomen. Non-interpolated spatial resolution was 1 mm isotropic, and 11 cardiac phases were acquired, gated to end-expiration. Following the MUSIC acquisition, a 4D flow sequence was run with 1.7 × 1.7 × 1.9 mm (non-interpolated) voxels and 45 ms temporal resolution, also during uninterrupted ventilation and gated to end-expiration. The respiratory gating efficiency for both 4D sequences was 60% and the total acquisition time was 20 minutes (8 minutes for MUSIC and 12 minutes for 4D flow). The MUSIC DICOM images were pushed to OsiriX, Vitrea (Rishon LeZion, Israel), and Mimics (Materialise, Leuven, Belgium) workstations for multi-planar cine recon (OsiriX), volume rendering (Vitrea), and quantitative segmentation of chamber sizes (Mimics). The 4D flow DICOM images were uploaded to the Arterys cloud for processing.

Results

The MUSIC images confirmed heterotaxia with a left-sided inferior vena cava (IVC), right-sided aortic arch, and distended hepatic veins draining to the right atrium (Fig. 1).
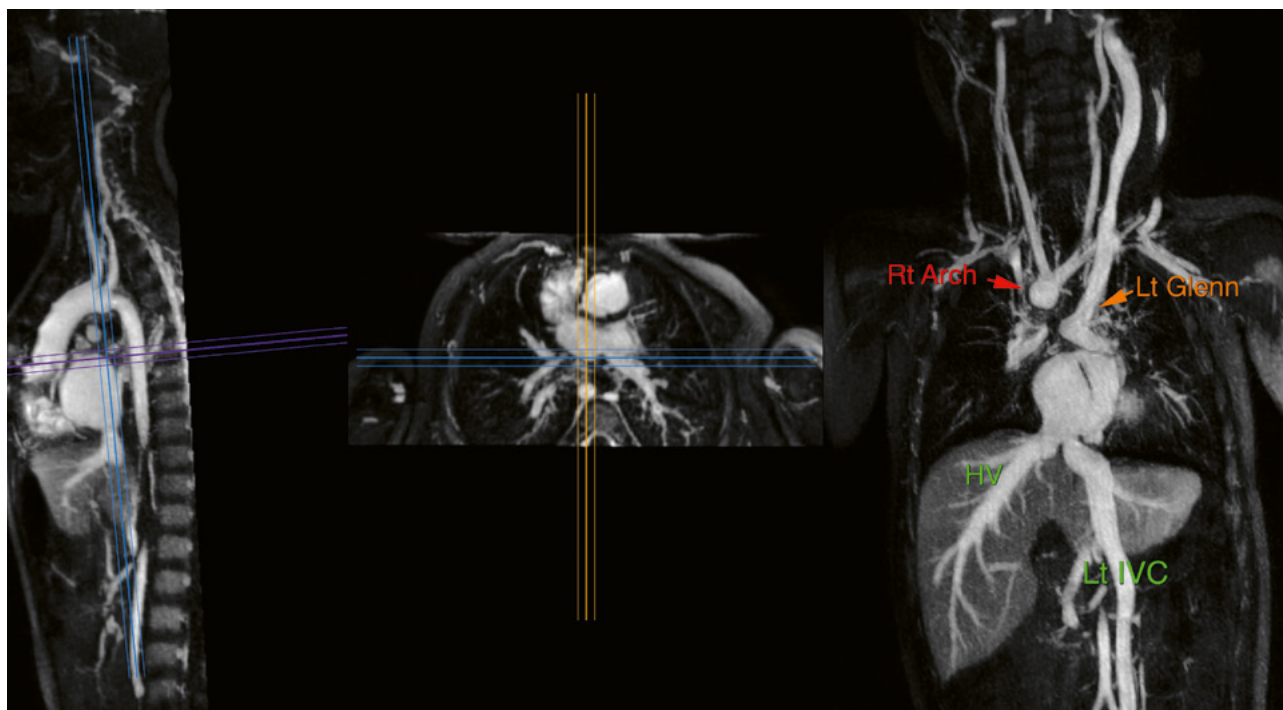

1 Thin MIP reconstructions from the 4D MUSIC acquisition in OsiriX showing the venous anatomy and the right-sided aortic arch (HV: hepatic vein; Lt IVC: left inferior vena cava; MIP: maximum intensity projection).

Dynamic cardiac chamber anatomy was clearly shown, and chamber volumes were confidently measured (Fig. 2). 4D flow confirmed normal hemodynamics in the aorta and branches, and documented the outflow pattern from the left ventricle to the aorta (Fig. 3). The origins and courses of the coronary arteries were conventional (Fig. 4). The left Glenn shunt was widely patent with appropriate flow (Fig. 5). The right Glenn was small, stenosed, and non-functional with minimal flow (Fig. 6). 3D frames from the MUSIC data were printed to help in surgical
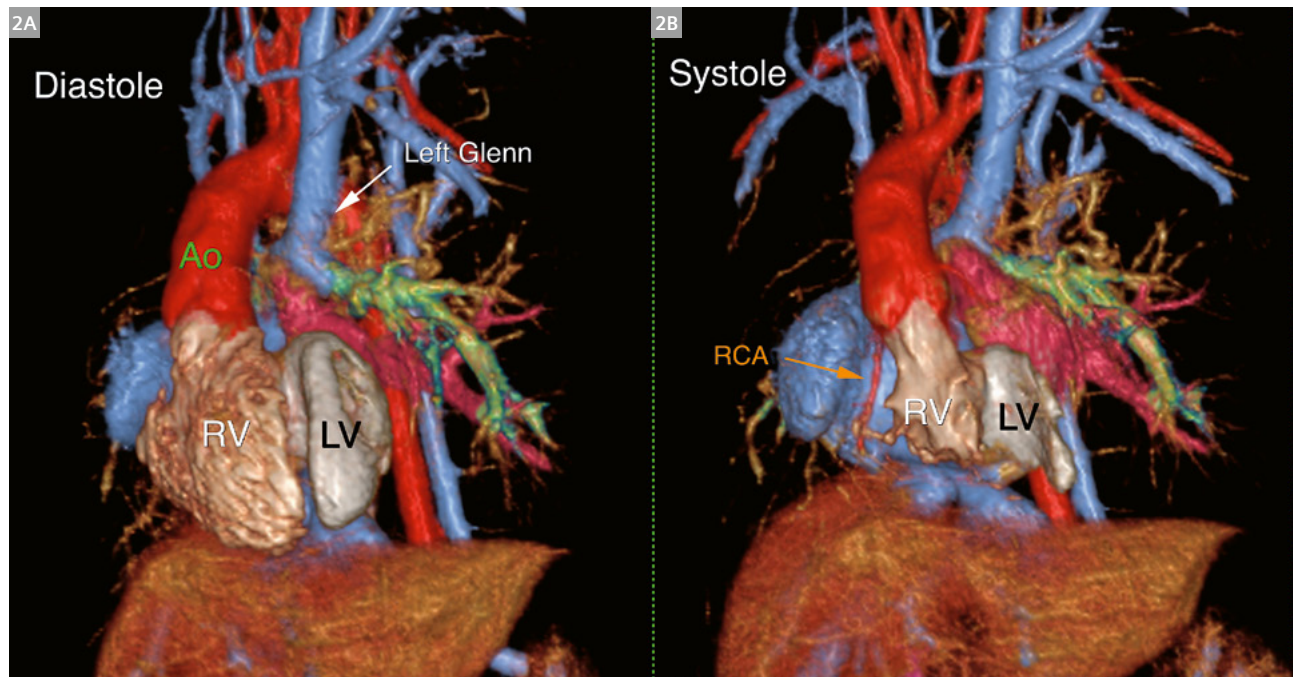
2 Color volume-rendered reconstructions (Vitrea) of the heart and great vessels in diastole **(2A)** and systole **(2B)** show the left Glenn shunt, aorta (Ao), left ventricle (LV), right ventricle (RV), and right coronary artery (RCA).
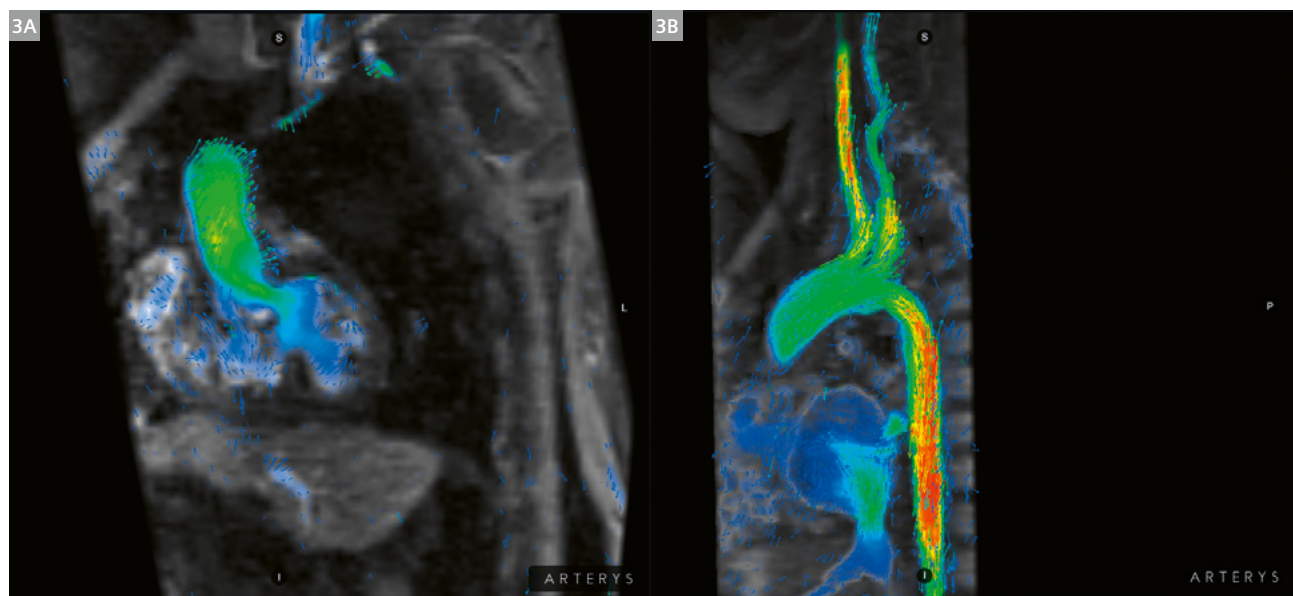

3 Frames reconstructed from the 4D flow data (Arterys) show the outflow pathway from the left ventricle to the Aorta (**3A**, oblique coronal) and normal flow patterns in the aortic arch and great vessels (**3B**, oblique sagittal).

planning and procedure simulation. Movie files for all figures are available as an online supplement at https://www.magnetomworld.siemens-healthineers.com/clinical-corner/case-studies/ferumoxytol.

It is important to note that, in addition to the specific findings noted above in this patient, the steady state of ferumoxytol makes every vessel in the chest, neck, abdomen, and pelvis clearly assessable.
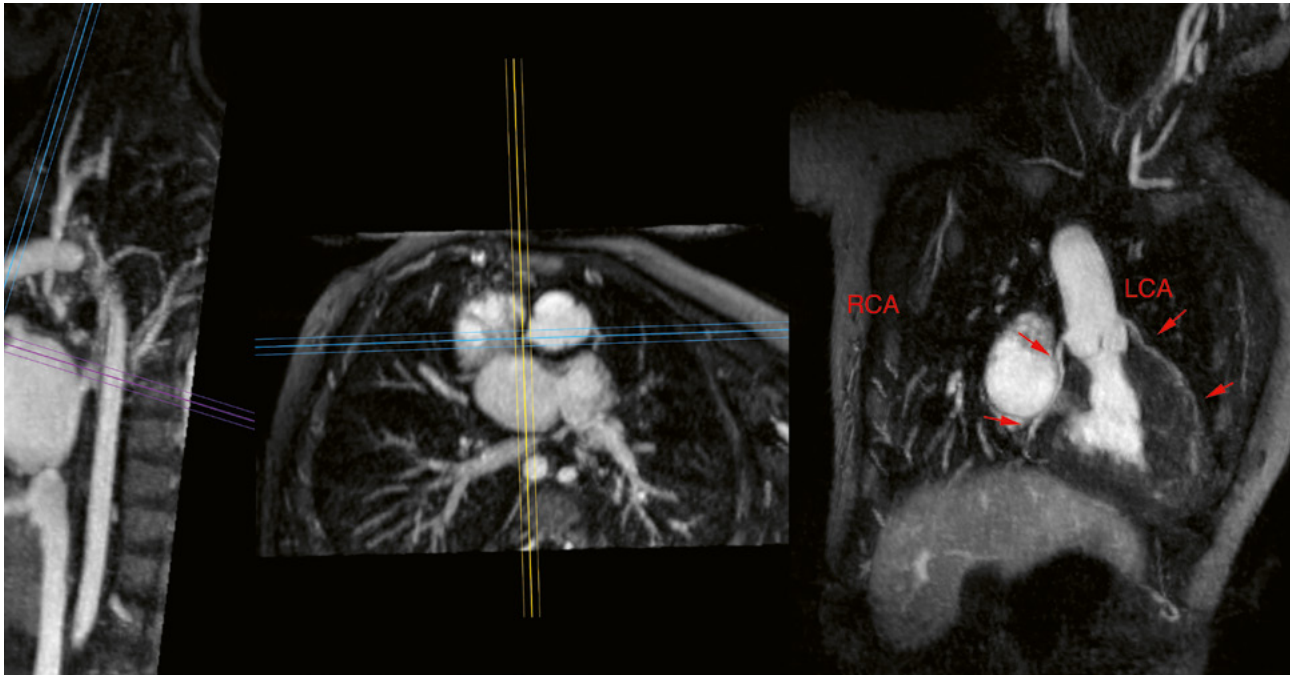
4 Thin MIP reconstructions from the 4D MUSIC acquisition in OsiriX showing the right coronary artery (RCA) and left coronary artery (LCA).
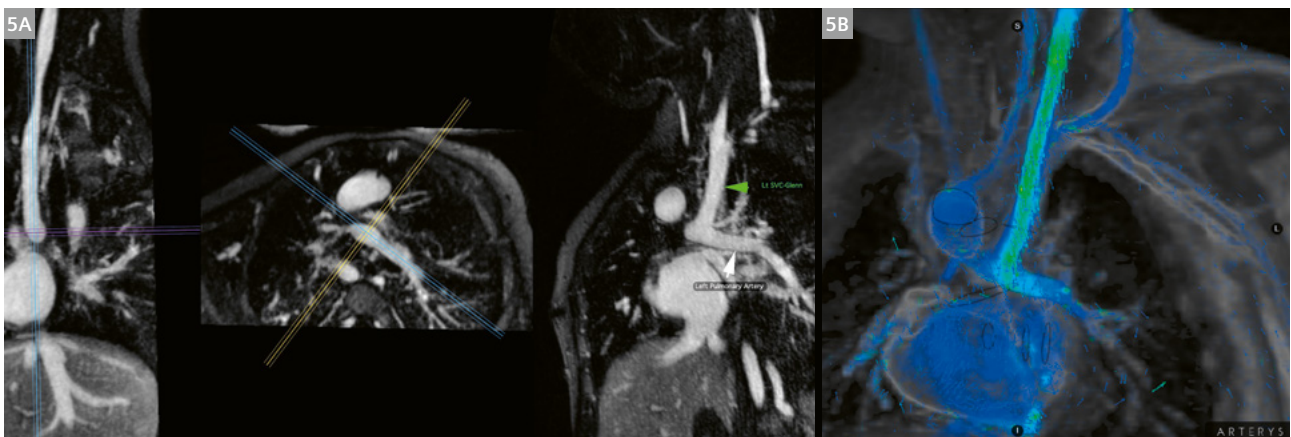
5 Thin MIP reconstructions from the 4D MUSIC acquisition in OsiriX show anatomy of the intact left Glenn shunt **(5A)**, and a frame from the 4D flow shows appropriate flow in the left Glenn (Arterys).
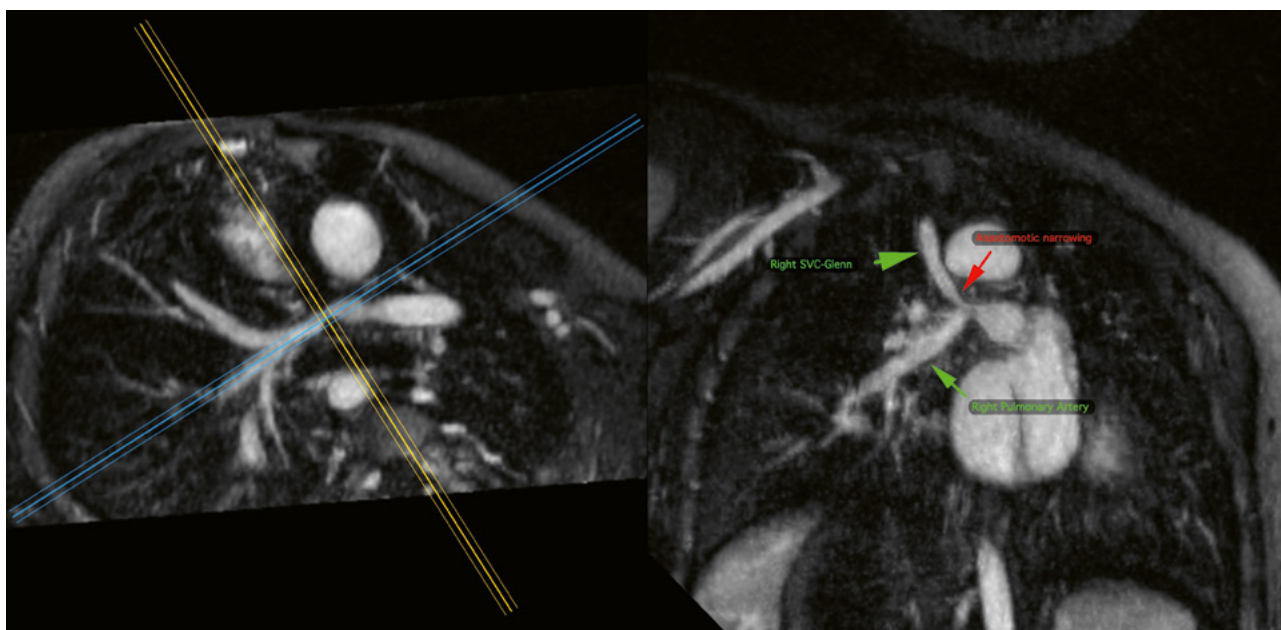
6 Thin MIP reconstructions from the 4D MUSIC acquisition in OsiriX show anatomy of the stenosed right Glenn shunt and the stenosed origin of the right pulmonary artery.

Adults with congenital heart disease

Whereas anesthesia and controlled ventilation solve the motion artifact problem in small children, we must use different tools in adults. Breath holding is generally very effective for 2D or 3D imaging, but for 4D flow imaging, some form of respiratory gating or compensation is needed. Recent advances in compressed sensing (CS) show great promise for highly accelerated 4D flow imaging and ferumoxytol enhancement can mitigate much of the SNR penalty that aggressive undersampling imposes. In the example below, we illustrate how CS 4D flow and ferumoxytol combine to generate high quality data in a practical acquisition time.

Case 2

A 30-year-old male patient with congenital bicuspid aortic valve had undergone valve-sparing surgery for an ascending aortic aneurysm. Follow-up echocardiography showed aortic valve incompetence, and the patient was referred to MR for a more detailed evaluation. The study was performed on a 1.5T MAGNETOM Sola (Siemens Healthcare, Erlangen, Germany). Following infusion of 4 mg/kg of ferumoxytol, the patient was advanced into the scanner bore, with two body array coils in place. The routine clinical acquisition protocol included multiplanar cine with breath-hold SGE (FLASH), 3D MRA, 2D flow imaging through the aortic valve, and non-breath-hold HASTE imaging. 4D flow imaging was then performed using a research sequence that incorporates compressed sensing (CS) acceleration

and a diaphragmatic navigator for respiratory gating. A CS acceleration factor of 12.8 was used in the current study. Spatial resolution was 2 mm isotropic (non-interpolated) and temporal resolution was 48 ms. ECG retro-gating was employed, and 20 cardiac phases were calculated.

Results

Cine confirmed the bicuspid aortic valve (Fig. 7A) and MRA showed satisfactory appearances of the surgical aortic graft (Fig. 7B). Respiratory gating efficiency for the 4D flow acquisition was 65% and the total acquisition time was 5 minutes 40 seconds. The image quality for the 4D flow acquisition was excellent, with high SNR for all vascular structures (Fig. 8). The aortic regurgitation fraction for both the 2D and 4D flow measurements was in full agreement at 43%. The 4D flow additionally showed the 3D geometry of the regurgitation jet, and provided a graphic depiction of the volumetric flow fields in the aorta, pulmonary artery, and included cardiac chambers. MRA confirmed the integrity of the surgical aortic graft repair, and cine imaging confirmed the congenitally bicuspid nature of the aortic valve. Additionally, cine and HASTE showed left ventricular non-compaction, not appreciated on echo.

In children with CHD, ferumoxytol has ushered in a paradigm shift for MRI. Because of its long half-life in the blood, ferumoxytol supports high-resolution 4D imaging and has been used successfully in several centers at both 3T and 1.5T [9, 10]. When implemented with cardiac and respiratory gating, high-dimensional techniques such

as MUSIC and Free-Running Framework [5] can produce images with uniformly high contrast throughout the cardiac chambers and blood vessels.

Ferumoxytol enhancement lays the groundwork for uniformly high vascular signal without concerns for saturation of the blood. This effect gives a new lease of life to the entire family of T1-weighted spoiled gradient echo (SGE, FLASH) sequences that are tolerant of magnetic field non-uniformities and artifacts from devices. Moreover, the benefits apply to all field strengths. The high blood SNR

also supports more aggressive under-sampling schemes for parallel imaging and, as shown in our adult case above, for compressive sensing in 4D flow. In the adult patient illustrated above, the 4D flow acquisition used an acceleration factor of 12.8, while maintaining high signal on the bright blood magnitude images. The same mechanism that supports high signal on the magnitude images supports more reliable estimation of flow-induced phase shifts, since the phase is less noisy if the magnitude signal is high [11]. It should be noted that ferumoxytol
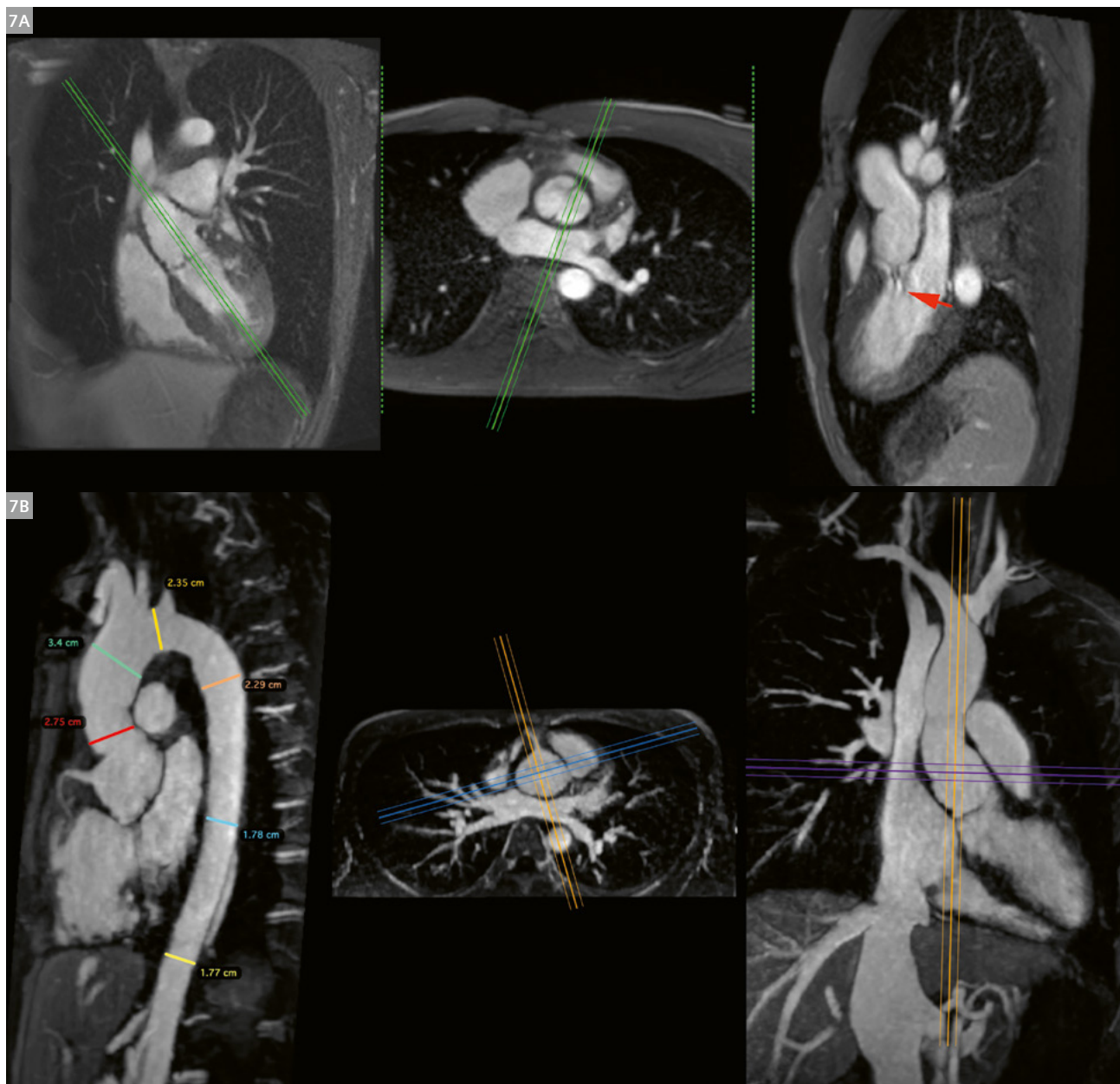
7 **(7A)** 30-year-old male patient with bicuspid aortic valve. Diastolic frames from 2D FLASH cine show the bicuspid aortic valve (middle panel) and aortic regurgitant jet (right panel). **(7B)** 30-year-old male patient with bicuspid aortic valve. Thin MIP reconstructions from gated MRA (OsiriX) post-ferumoxytol show the dimensions of the ascending aortic surgical graft and thoracic aorta (left panel).
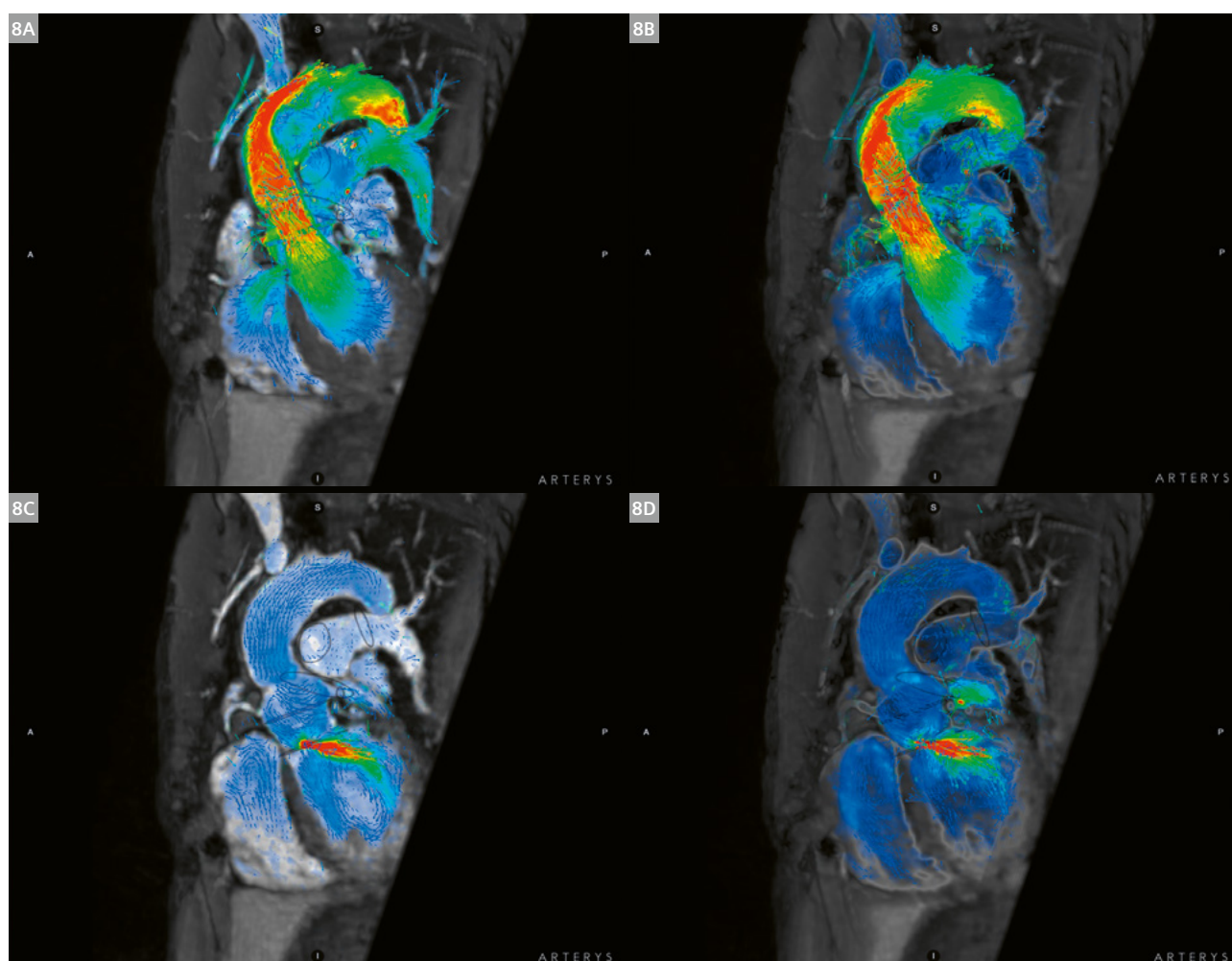
8 30-year-old male patient with bicuspid aortic valve. Systolic (upper row) and diastolic (lower row) frames from CS 4D flow reconstruction (Arterys). The left column is displayed on a bright blood background (note the high vascular signal due to the ferumoxytol) and the right column on a filtered black blood background. The posteriorly orientated, large aortic regurgitant jet is well-appreciated, as are the flow vectors throughout the arch and cardiac chambers. The regurgitation fraction was estimated at 43% both on 4D flow and 2D flow. (The exactness of the correspondence was surprising!)

is a therapeutic agent that is approved by the U.S. Food and Drug Administration for treatment of iron deficiency anemia in patients at all levels of renal function [12]. It is not approved for diagnostic applications and its use for MRI is off-label. Moreover, ferumoxytol has carried a boxed warning since March 2015. This concerns the risk of anaphylactic reactions, apparently linked to rapid administration during therapeutic use [13]. When used for MRI, ferumoxytol is normally infused slowly and in diluted form with close monitoring, and preliminary safety data on diagnostic use suggest an adverse event rate similar to the macrocyclic gadolinium agents [14]. Further data and analysis on the safety and diagnostic performance of ferumoxytol are needed, but the potential of the agent is clear when used appropriately.

Conclusion

In summary, we discussed the applications of 4D imaging in children and adult patients with congenital heart disease, illustrated with one example from each cohort. The combination of ferumoxytol and multi-dimensional MR imaging represents a powerful blend of MR technology and pharmacological contrast enhancement. The hope for the future is that, with more widespread availability of advanced multi-dimensional techniques and ferumoxytol enhancement, the true clinical potential of this approach will be realized in the broader community.

References

1   Han F, Zhou Z, Han E, Gao Y, Nguyen KL, Finn JP, et al.
    Self-gated 4D multiphase, steady-state imaging with contrast
    enhancement (MUSIC) using rotating cartesian K-space (ROCK):
    Validation in children with congenital heart disease.
    Magn Reson Med. 2017;78(2):472–483.

2   Zhou Z, Han F, Rapacchi S, Nguyen KL, Brunengraber DZ, Kim GJ,
    et al. Accelerated ferumoxytol-enhanced 4D multiphase, steady-
    state imaging with contrast enhancement (MUSIC) cardiovascular
    MRI: validation in pediatric congenital heart disease.
    NMR Biomed. 2017;30(1):10.1002/nbm.3663.

3   Han F, Zhou Z, Han E, Gao Y, Nguyen KL, Finn JP, et al. Self-gated
    4D multiphase, steady-state imaging with contrast enhancement
    (MUSIC) using rotating cartesian K-space (ROCK): Validation in
    children with congenital heart disease.
    Magn Reson Med. 2017;78(2):472–483.

4   Di Sopra L, Piccini D, Coppo S, Stuber M, Yerly J. An automated
    approach to fully self-gated free-running cardiac and respiratory
    motion-resolved 5D whole-heart MRI.
    Magn Reson Med. 2019;82(6):2118–2132.

5   Roy CW, Di Sopra L, Whitehead KK, Piccini D, Yerly J, Heerfordt J,
    et al. Free-running cardiac and respiratory motion-resolved 5D
    whole-heart coronary cardiovascular magnetic resonance
    angiography in pediatric cardiac patients using ferumoxytol.
    J Cardiovasc Magn Reson. 2022;24(1):39.

6   Munoz C, Fotaki A, Botnar RM, Prieto C. Latest Advances in Image
    Acceleration: All Dimensions are Fair Game.
    J Magn Reson Imaging. 2023;57(2):387–402.

7   Falcão MBL, Di Sopra L, Ma L, Bacher M, Yerly J, Speier P, et al.
    Pilot tone navigation for respiratory and cardiac motion-resolved
    free-running 5D flow MRI. Magn Reson Med. 2022;87(2):718–732.

8   Han F, Rapacchi S, Khan S, Ayad I, Salusky I, Gabriel S, et al.
    Four-dimensional, multiphase, steady-state imaging with contrast
    enhancement (MUSIC) in the heart: a feasibility study in children.
    Magn Reson Med. 2015;74(4):1042–1049.

9   Nguyen KL, Han F, Zhou Z, Brunengraber DZ, Ayad I, Levi DS, et al.
    4D MUSIC CMR: value-based imaging of neonates and infants with
    congenital heart disease. J Cardiovasc Magn Reson. 2017;19(1):40.

10 Nguyen KL, Ghosh RM, Griffin LM, Yoshida T, Bedayat A, Rigsby CK,
    et al. Four-dimensional Multiphase Steady-State MRI with
    Ferumoxytol Enhancement: Early Multicenter Feasibility in Pediatric
    Congenital Heart Disease. Radiology. 2021;300(1):162–173.

11 Mukai K, Burris NS, Mahadevan VS, Foster ED, Ordovas KG,
    Hope MD. 4D flow image quality with blood pool contrast:
    a comparison of gadofosveset trisodium and ferumoxytol.
    Int J Cardiovasc Imaging. 2018;34(2):273–279.

12 U.S. Food and Drug Administration. Feraheme Label.
    [cited February 5, 2018]; Available from: https://www.accessdata.
    fda.gov/drugsatfda_docs/label/2018/022180s009lbl.pdf

13 U.S. Food and Drug Administration. FDA Drug Safety
    Communication: FDA strengthens warnings and changes
    prescribing instructions to decrease the risk of serious allergic
    reactions with anemia drug Feraheme (ferumoxytol). 2015.
    [cited September 18, 2023]. Available from:
    http://www.fda.gov/Drugs/DrugSafety/ucm440138.htm

14 Nguyen KL, Yoshida T, Kathuria-Prakash N, Zaki IH, Varallyay CG,
    Semple SI, et al. Multicenter Safety and Practice for Off-Label
    Diagnostic Use of Ferumoxytol in MRI.
   Radiology. 2019;293(3):554–564.
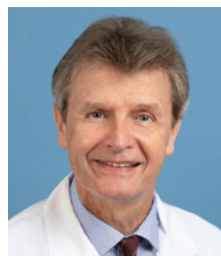
Contact

J. Paul Finn, M.D.
Department of Radiological Sciences
University of California Los Angeles
Peter V. Ueberroth Building, Suite 3371
10945 Le Conte Ave
Los Angeles, CA 90095-7206
USA
PFinn@mednet.ucla.edu

Check out the movie files for all figures at
**magnetomworld.siemens-healthineers.com/
clinical-corner/case-studies/ferumoxytol**
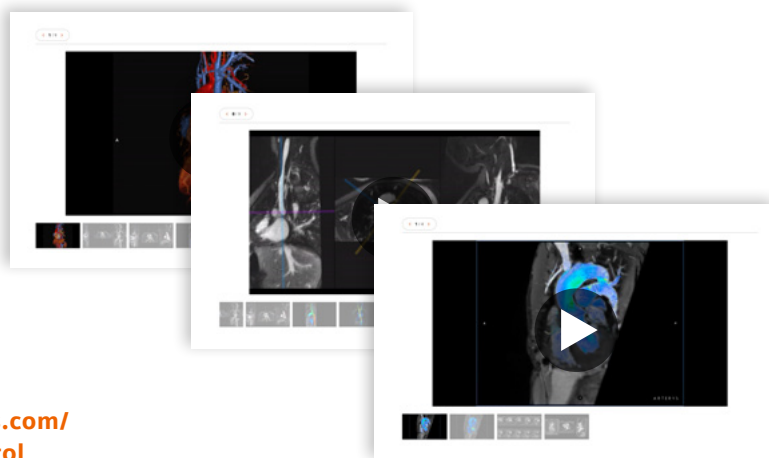
How to Perform a Non-Contrast and Sedation-Free Neonatal Feed and Wrap Cardiac MRI at 3 Tesla

David A Broadbent[1]*, Rawan Abuzinadah[2]*, Malenka M Bissell[2,3]

[1]Department of Medical Physics, Leeds Teaching Hospitals Trust, Leeds, United Kingdom
[2]Leeds Institute of Cardiovascular and Metabolic Medicine, University of Leeds, United Kingdom
[3]Department of Paediatric Cardiology, Leeds Teaching Hospitals Trust, Leeds, United Kingdom
*Both authors contributed equally to the manuscript

Neonatal feed and wrap cardiac MRI

Non-contrast, sedation-free neonatal feed and wrap uses natural sleep after feeding and swaddling. Centers also refer to it as feed and sleep, feed and bundle, or feed and swaddle. This technique can be used to scan babies up to the age of 3 to 5 months[1] using a free-breathing protocol. Traditionally, neonatal cardiac MRI scanning often required the administration of contrast agent to improve signal-to-noise ratio (SNR) and thereby image quality. Further limitations of cardiac MRI scanning in this group of patients include the need for general anesthesia or medical sedation due to the long scan times. However, with the advances in acceleration techniques, feed and wrap cardiac MRI can be acquired in a feasible scan time lasting 20–35 minutes. Using dedicated small body coils and a 3-Tesla MAGNETOM Prisma MRI scanner can improve SNR sufficiently so that no contrast administration is needed.

Pre-appointment preparation

Parents play an important role in the successful imaging of babies. Cardiac imaging can be stressful for parents of babies with congenital heart disease, and therefore a calm environment is important. Sending clear information out to the parents helps them prepare for the MRI scan. Our patient information leaflet tells parents how to dress the baby (metal-free clothing without poppers), to bring a feed along, and to try not to let the baby nap just prior to the scan. It also describes how the scan will be performed (including pictures of the equipment with a doll) and answers common MRI safety questions and concerns. On the day of the scan, enough time should be allowed prior to the scan to fully explain to the parents how the scan is performed and to discuss any concerns or questions they might still have. Calm parents increase the likelihood of the baby going to sleep quickly.

Baby transfer preparation

Successful implementation of the neonatal cardiac MRI requires good preparation. A variety of options are available to perform a neonatal feed and wrap MRI scan:
1) Transfer the sleeping baby directly onto the scanner table from the parents' arms.
2) Transfer the baby in an open-top basinet or immobilizer cushion.
3) Transfer the baby in a closed incubator.

In our experience, option 3 has the highest success rate [1]. This could be due to the extra noise attenuation provided by the incubator housing (in addition to the hearing protection worn by the baby), as well as the option to warm the incubator.

When using an MRI-safe incubator, it is important to make sure that the incubator is fully charged prior to the scan. A feed and wrap MRI checklist can be useful for making sure that the incubator is fully prepared. This includes baby sheets, positioning devices, blankets, electrode stickers, a skin cleaning solution, spare baby leggings (metal-free clothing), MRI-compatible monitoring equipment, dedicated coils, and MRI-compatible headphones. Additional equipment needed for inpatient MRI scanning might include MRI-safe infusion pumps.

---

[1]Siemens Healthineers disclaimer: MR scanning has not been established as safe for imaging fetuses and infants less than two years of age. The responsible physician must evaluate the benefits of the MR examination compared to those of other imaging procedures. Note: This disclaimer does not represent the opinion of the authors.

Baby preparation

Prior to feeding, the baby's length and weight should be measured. It is advisable to place the electrode stickers on the baby's chest and ask parents to prophylactically change the diaper prior to feeding the baby. At this point, it is also important to check that the baby is wearing metal-free clothes.

After the baby has been fed, the MRI cardiac monitoring box and any additional monitoring (such as a saturation monitor) are attached. The baby is then swaddled in a blanket and transferred to the MRI-safe incubator. If the baby is upset, an additional cuddle from the parents to calm the baby after swaddling is helpful before transferring to the incubator. The dedicated MRI coils are secured. Then the MRI-compatible baby headphones that provide additional noise cancellation are placed over the baby's ears. Some babies really dislike the headphones and get upset. In this instance, it is

1 Placement of electrode stickers.

advisable to wait to place the headphones until the baby is asleep. To keep the baby calm and cozy, the incubator can be warmed to variable temperatures and humidity. After the baby has been transferred and prepared, the feed and wrap MRI safety checklist is completed to ensure the baby is metal-free and the incubator is free of any equipment, before entering the MRI control room. Some babies benefit from being wheeled up and down the corridor in the incubator to aid sleep, while others fall asleep with gentle rocking of the incubator in a darkened room. Playing sleep music or white noise may also be helpful, and the parents can often advise how the baby normally best falls asleep.

Preparing the MRI scanner room

A dark and calm environment should be prepared. This includes dimming the lights in the MRI control room and scanner room. We also advise playing loud sleep music in the MRI scanner room – with the volume matching the scanner volume. This provides a constant noise. We have found that babies often stir and awaken from the start/stop of MRI sequences. This is greatly reduced by playing loud, calming, and continuous music.

Transferring the baby into the scanner room

In the MRI control room, another safety checklist should be completed by the assigned member of staff, and safety guidelines to be followed in the event of an emergency should be read out to make sure that everyone is aware of the MRI safety considerations. At least two team members trained in MRI safety are required to transfer the incubator onto and off the scanner table.

2 Neonatal incubator setup. The baby is swaddled and placed in the incubator with dedicated coils, monitoring, and noise protection.

Challenges during the MRI scan

Even though our feed and wrap MRI scan technique has a > 95% success rate, performing MRI scans in babies aiming to achieve high-quality diagnostic images can be challenging (especially in babies > 2 months) and individualized protocol adaptation is often necessary. Babies sometimes awaken or stir briefly, often because they have lost their pacifier. It helps to stop the scan and offer the baby the pacifier while the incubator stays in position, as often the baby settles and the scan can be continued. If frequent startling is observed, continuous scanning is important, with some pictures requiring repeated acquisition for optimal image quality.

General sequence and safety considerations

When scanning neonatal patients, care must be taken to avoid excessive radiofrequency (RF) or acoustic noise exposure. For the former, the patient's height and weight must be entered during registration to allow accurate specific absorption rate (SAR) modelling. For the latter, hearing protection suitable for babies' heads with appropriate noise attenuation must be used. Restricting gradient modes can help reduce acoustic noise generation. We therefore use Whisper gradient modes where possible, although we will use higher gradient modes for sequences where Whisper mode is either not available or is not consistent with other desired parameters, as long as this does not result in excessively noisy sequences.

When scanning sleeping babies, both the type and level of acoustic noise can influence the likelihood of the baby stirring and moving excessively. In our experience, sequences generating intermittent noises are more likely to wake and disturb the baby than continuous noise. We therefore consider this aspect when performing our protocols and try to keep sequences with intermittent noise generation to later in the protocol, after key sequences have been acquired. The Compressed Sensing 4D Flow MRI[2] research sequence is in our experience the best sequence to keep babies asleep, and we almost always manage to acquire at least these sequences.

---

[2]*Work in progress. The application is currently under development and not for sale in the U.S. and in other countries. Its future availability cannot be ensured.*

Scanner table movement may also disturb the baby's sleep, and we avoid this during scanning. Given the small size of the patient, there is not much need for repeated table movement as the entire thoracic anatomy will be close to isocenter once positioned. We therefore acquire one localizer at the initial table position prescribed by the lasers (FIX table positioning mode with 0 mm head/foot offset), a second with a small table move (if required) to move the heart to isocenter (ISO table positioning mode), and then for all subsequent sequences, we reference all table positions to the second localizers to avoid further movement.

Due to the very small body size of these patients (and their cardiac anatomy) it is necessary to acquire images with greater spatial resolution than in adult cardiac MRI. Small fields of view can easily be used without risk of wrap due to the small patient size, and therefore the necessary resolutions can be achieved within an acceptable timeframe. However, achieving this while maintaining adequate SNR can be challenging. To aid this, we use a 3T MRI scanner with dedicated small coils which cover the baby's torso with a high density of coil elements.

Signal scaling around neonatal hearts does not suffer from the same issues as described in our previous fetal cardiac MRI article [2], whereby signals can be dominated by those from maternal tissue or amniotic fluid closer to the coil. However, for some sequences we found that some fine-tuning of receiver gain and/or Image Scaling Correction can result in better contrast resolution for the neonatal heart. Trial and improvement may be needed to find optimal values for each center's individual sequence setup. In our experience, increasing scaling values up to around 5 works well for some sequences (note that this is 2 to 3 times less than we use for some fetal sequences). This setting can be edited in retrospective reconstructions, which can allow fine-tuning without the need to repeat image acquisition.

As long as the baby remains asleep and well wrapped, large-scale motion is generally not an issue. Furthermore, as it is not possible to instruct breath-holds, imaging of each sequence (or slice) must be performed quickly to minimize respiratory motion artifacts, or averaged over longer periods of time. For many of our sequences, TE and TR are set to be automatically minimized and fast RF pulse shapes are used to minimize scan duration and (in the case of TE) maximize SNR.

Sequences

Vasculature-triggered TurboFLASH
(approx. 1 minute for 50 overlapping slices)

After acquiring standard three-plane localizers we acquire a transverse stack using 2D TurboFLASH imaging, which generates high signal from the vasculature due to inflow enhancement effects. These are acquired as 4.5 mm thick contiguous slices, but with -50% distance to provide overlapping slices with the higher SNR associated with the thicker slices.

Single-shot (per slice) triggered imaging is performed, which provides resilience to motion and allows stacks of 50 slices to be acquired in approximately 1 minute using GRAPPA acceleration factor 2. A high flip angle (for a FLASH sequence) of 30° is used to maximize saturation of stationary tissue, which yields high contrast of the flowing blood. We find that a single acquisition (no averaging) and no phase partial Fourier yields sufficient SNR with this sequence. A base resolution of 256 yields in-plane resolution of approximately 0.8×0.8 mm^2 for a typical field of view.

Acquisition is triggered (single-phase) to acquire data every other heartbeat with a minimal trigger delay of 1 ms for systolic imaging, and repeated with a trigger delay for diastolic imaging.

This sequence may also be repeated with fewer slices to provide targeted views of specific vascular anatomy, for example aligned to show the aortic arch.

As this sequence generates a high contrast-to-noise ratio within an acceptable acquisition time, we find that use of a high receiver bandwidth (1149 Hz/pixel) maximizes image quality, and we allow use of performance gradient mode to achieve this for this sequence.

3 Planning of the transverse stack using triggered TurboFLASH.

CS 4D Flow MRI
(approx. 2 minutes for 20 slices / 5 minutes for 60 slices)
To assess blood hemodynamics over extended volumes, we use the Compressed Sensing 4D Flow MRI[2] research sequence, which allows volume coverage of the heart and proximal vasculature in an acceptable time for neonatal imaging. This approach allows a 3D volume to be acquired with velocity encoding in all three dimensions. It can therefore be significantly simpler and more robust than planning multiple 2D flow acquisitions, particularly in this application, as in the 2D approach, where it is critical for each view to be accurately prescribed, it is common for repeat scanning to be required when the patient moves during the time needed to accurately plan each acquisition.

Furthermore, making use of inflow enhancement, the magnitude data can also be used for anatomical assessment in 3D (as a substitute for a separate 3D whole-heart acquisition).

We acquire data with approximately 1.0 mm³ isotropic resolution, retrospectively gated into 25 cardiac phases using electrocardiographic (ECG) gating. Strong asymmetric echoes are used to allow TE and TR to be minimized, and a constant 7° is used. Different venc values are applied depending on the anatomy of interest, e.g., 150 cm/s for the aorta (oblique sagittal planning), 100 cm/s for a whole-heart acquisition (sagittal planning), and 350 cm/s for pulmonary arteries (transverse planning). Likewise, the coverage will vary from approximately 20 slices for targeted vessels (aorta/pulmonary arteries) to approximately 60 slices for whole-heart coverage. We standardized these 3 anatomical acquisitions to account for different venc requirements but also to make use of inflow enhancement for 3D assessment of the branch pulmonary arteries and aorta in the magnitude images.

It should be noted that image reconstruction can take significantly longer than acquisition for this sequence (up to around 15 minutes), and other sequences acquired subsequently will not be reconstructed until the 4D Flow MRI reconstruction completes. We reconstruct during the scan while cine stacks are running to allow for visual quality assurance of the reconstructed 4D Flow MRI acquisition.

---

[2]Work in progress. The application is currently under development and not for sale in the U.S. and in other countries. Its future availability cannot be ensured.

4 Planning of the aortic 4D Flow MRI sequence using oblique sagittal placement of the slab.
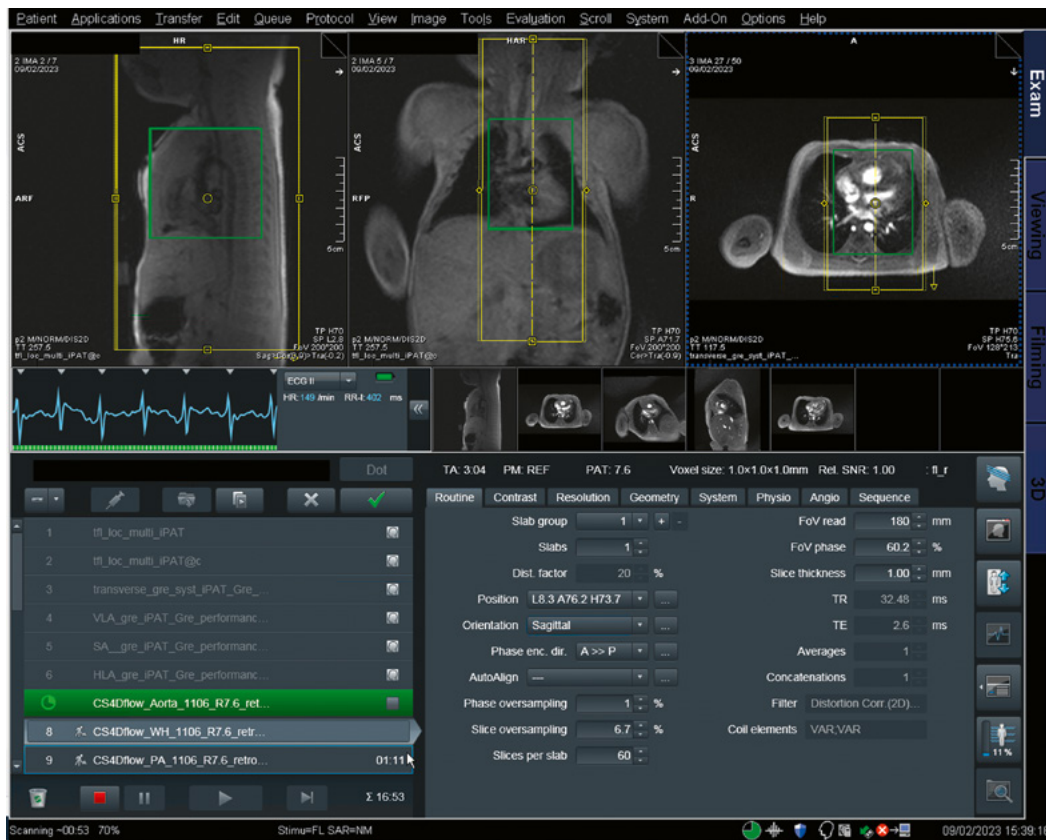
5 Planning of the whole-heart 4D Flow MRI sequence using sagittal placement of the slab.

6 Planning of the branch pulmonary arteries 4D Flow MRI sequence using transverse placement of the slab.

Cine imaging
(approx. 30 seconds per slice)

For cine imaging, we also use a 2D TurboFLASH acquisition with 4 mm slice thickness and approximately 0.7×0.7 mm^2 in-plane resolution. TE and TR are minimized, and we use a 12° flip angle. GRAPPA (acceleration factor 2) averaging (NSA = 3) gives an acceptable balance of SNR and scan time, and weak asymmetric echoes are allowed to minimize TE. Short-term averaging mode is used to minimize motion artifacts.

Our sequence is retrospectively gated into 25 cardiac phases using ECG. Where multiple slices are required (e.g., short-axis stack), they are acquired contiguously in sequential mode. Unlike the single-phase imaging above, we limit gradients to Whisper mode for this cine, and scan with a lower receiver bandwidth of 400 Hz/pixel.

2D flow
(approx. 30 seconds per slice)

To assess hemodynamics over targeted locations, a similar 2D TurboFLASH cine sequence is used, but with velocity encoding and reduced spatial resolution. A venc (through-plane) of typically 150 cm/s is used for the aorta and 450 cm/s for the pulmonary arteries. Single slices with 4 mm thickness and in-plane resolution of 1.0×1.0 mm^2 are acquired using 3 averages, GRAPPA (acceleration factor 3), 6/8 phase partial Fourier, and strong asymmetric echoes to minimize TE (and TR). A flip angle of 20° is used. Images are retrospectively gated into 30 phases using ECG. As for the cine imaging, Whisper mode gradients are used, with a receiver bandwidth of 454 Hz/pixel.

7 Planning of the aortic arch cine.
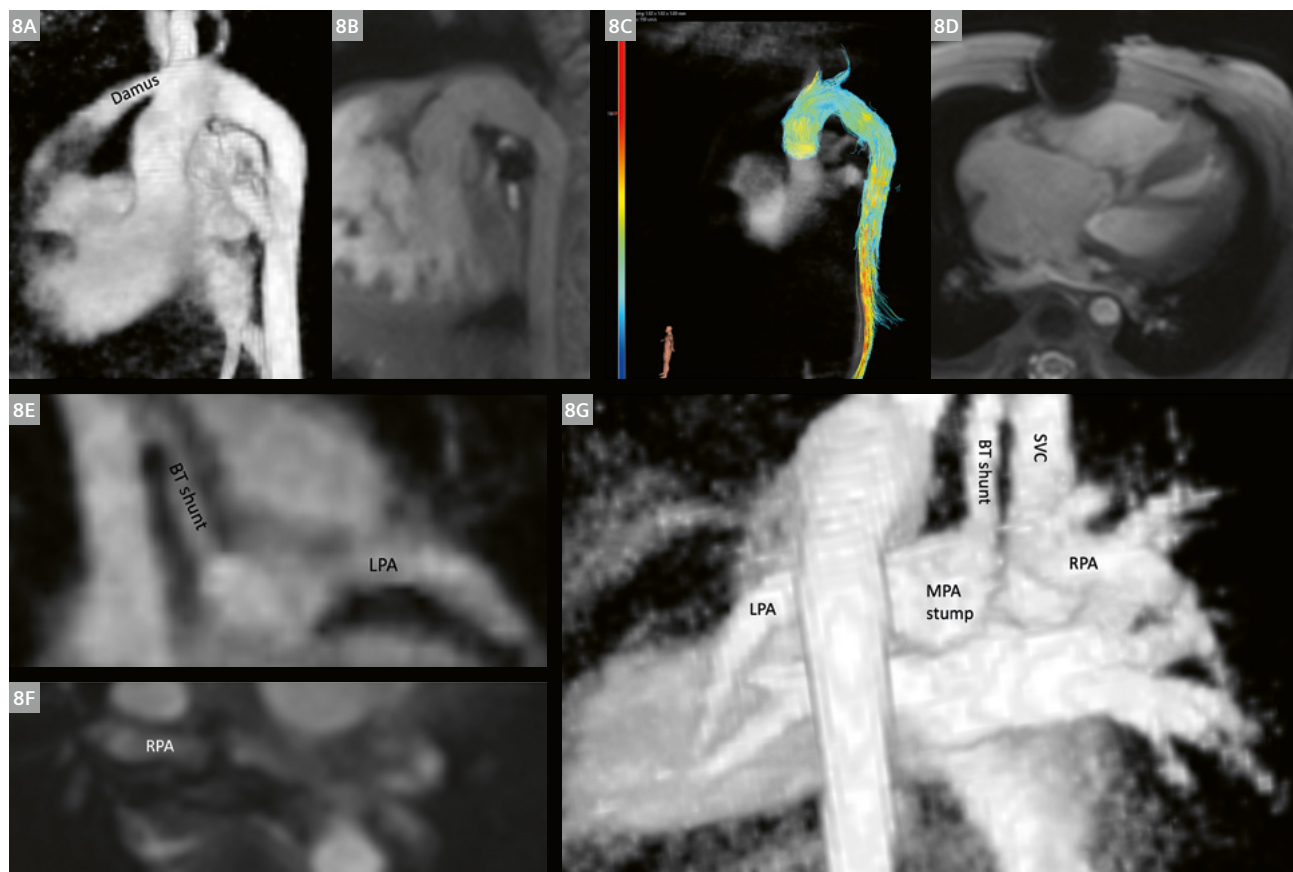
8 Summary of the imaging in a baby with mitral atresia, large ventricular septal defect (VSD), and transposed great arteries after Norwood operation with a Blalock-Taussig (BT) shunt. Images **(8A)**, **(8E)**, and **(8G)** are based on magnitude images from CS 4D Flow MRI images; images **(8B)**, **(8D)**, and **(8F)** are GRE cine images; image **(8C)** is CS 4D Flow MRI data.

Other sequences

For single ventricle assessment, we often also include a standard T2 SPACE sequence (for lymphatic assessment). For babies who are waking easily/frequently, we also some-times use real-time imaging instead of the cine imaging described above.

References

1   Panayiotou HR, Mills LK, Broadbent DA, Shelley D, Scheffczik J, Olaru AM, et al. Comprehensive Neonatal Cardiac, Feed and Wrap, Non-contrast, Non-sedated, Free-breathing Compressed Sensing 4D Flow MRI Assessment.
    J Magn Reson Imaging. 2023;57(3):789–799.
2   Abuzinadah R, Broadbent DA, Jin N, Bissell MM. How To Do Fetal Cardiac MRI at 3T. MAGNETOM Flash. 2023;83(1):49–57.
    Available at https://marketing.webassets.siemens-healthineers.com/793ca03bffa786b6/22a9f818db92/siemens-healthineers_clinical-corner_bissell_fetal_cmr_SCMR_2023.pdf

Contact

Dr. Malenka M Bissell, DPhil, MD, BM, MRCPCH, FSCMR
Clinical Lecturer in Paediatric Cardiology
Department of Biomedical Imaging Science
Leeds Institute of Cardiovascular and Metabolic Medicine
Worsley Building, Room 8.49f
Clarendon Way
University of Leeds
Leeds
LS2 9NL
United Kingdom
M.M.Bissell@leeds.ac.uk

Clinical Experience with the BioMatrix Beat Sensor: Cardiac MRI Exams Without ECG Leads

Naokazu Mizuno[1]; Yuka Otaki[1]; Akihiro Manabe[2]; Nobuo Iguchi[3]

[1]Department of Radiology, Sakakibara Heart Institute, Tokyo, Japan
[2]Siemens Healthcare K.K, Tokyo, Japan
[3]Department of Cardiology, Sakakibara Heart Institute, Tokyo, Japan

Introduction

ECG gating is essential for performing cardiac MRI examinations. However, the accuracy of cardiac synchronization with ECG gating is significantly influenced by the patient's condition and characteristics, such as their body size, chest hair, cardiac location, motion, and arrhythmia. ECG gating aims to detect the variations in the electric potential of the heart, but it is often difficult to obtain the original ECG waveform due to radio frequency (RF) pulses or magnetic field interference. The BioMatrix Beat Sensor, which was recently launched by Siemens Healthineers, is an innovative technology that can acquire biological information including cardiac activity and diaphragmatic motion without placing ECG leads or respiratory belts. Therefore, this technique is expected to simplify patient preparation and reduce examination time in cardiac MRI examinations and improve the patient experience during the scan.

In this article, we introduce our experience with clinical patients and healthy volunteers who underwent cardiac MRI with the BioMatrix Beat Sensor on a 1.5T MAGNETOM Sola with BioMatrix Body 12-channel and Spine 32-channel coils.
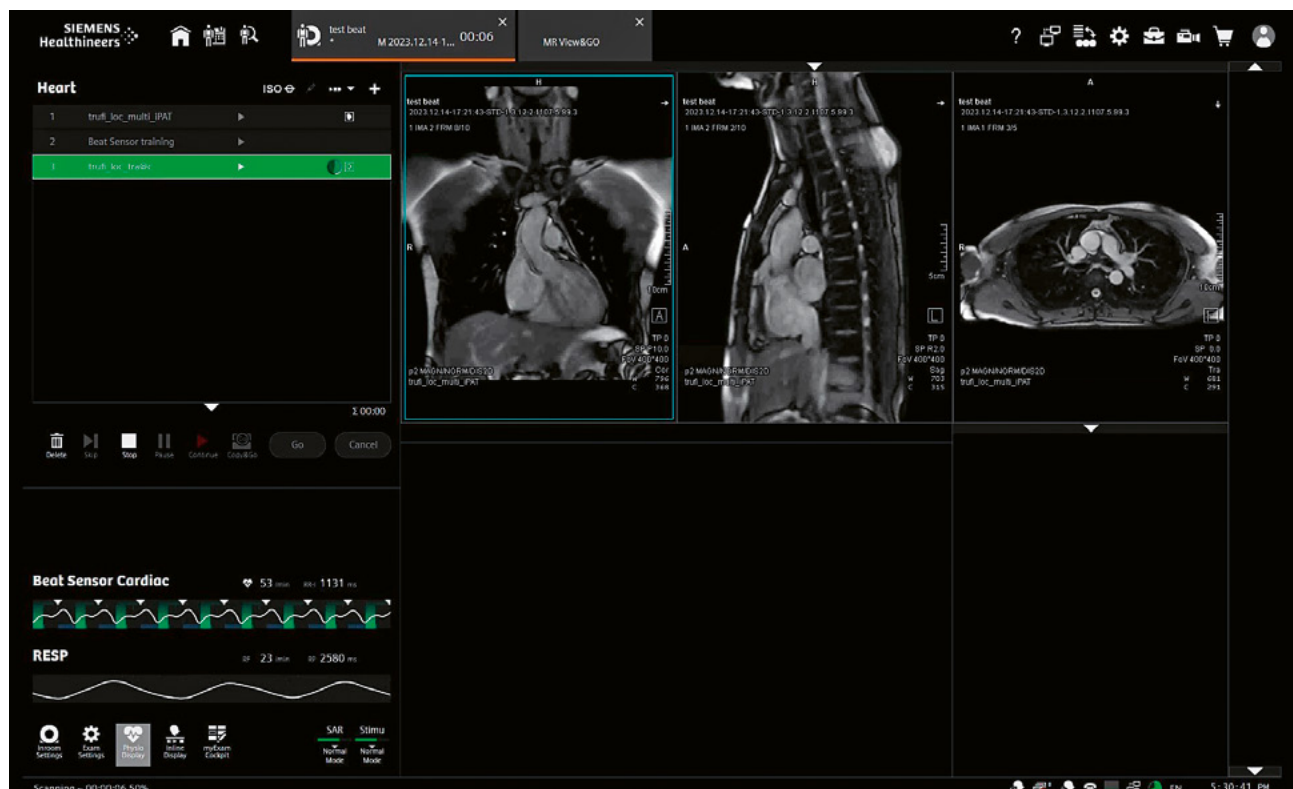
1 BioMatrix Beat Sensor interface for a cardiac MRI scan.

BioMatrix Beat Sensor

Pilot Tone (PT), which was developed based on the principle that a constant RF signal can be modulated by physiological, especially cardiac motion, enables the detection of cardiac motion when the BioMatrix Body coil (Fig. 1) is used. As mentioned earlier, since the Beat Sensor does not require ECG leads placed on chest walls, or respiratory belts, it is expected to improve the clinical workflow of MRI examinations by avoiding preparations involving direct skin contact. This is especially helpful for patients with chest hair. Before imaging with the BioMatrix Beat Sensor, a training scan ("learning") has to be performed to confirm the position of the heart, the appropriate type of coil, and to perform training of the signal processing

for isolation of the cardiac signal component und suppression of RF artifacts. After the training scan, the trigger source Beat Sensor can be applied to all imaging protocols including cine, T2-weighted, myocardial mapping, and late gadolinium enhancement (Fig. 2). For comparison, in general, a vectorcardiography-based QRS detection algorithm is used for ECG gating, which aims to detect the R-wave at its peak by recognizing the R-wave's rising edge. However, the timing of cardiac triggers detected by the Beat Sensor is about 200 milliseconds delayed with respect to the R-wave, which is detected by ECG triggering. Triggering with the Beat Sensor in the acceleration phase of the cardiac contraction and subsequent low pass filter processing both contribute to this delay [1] (Fig. 3).
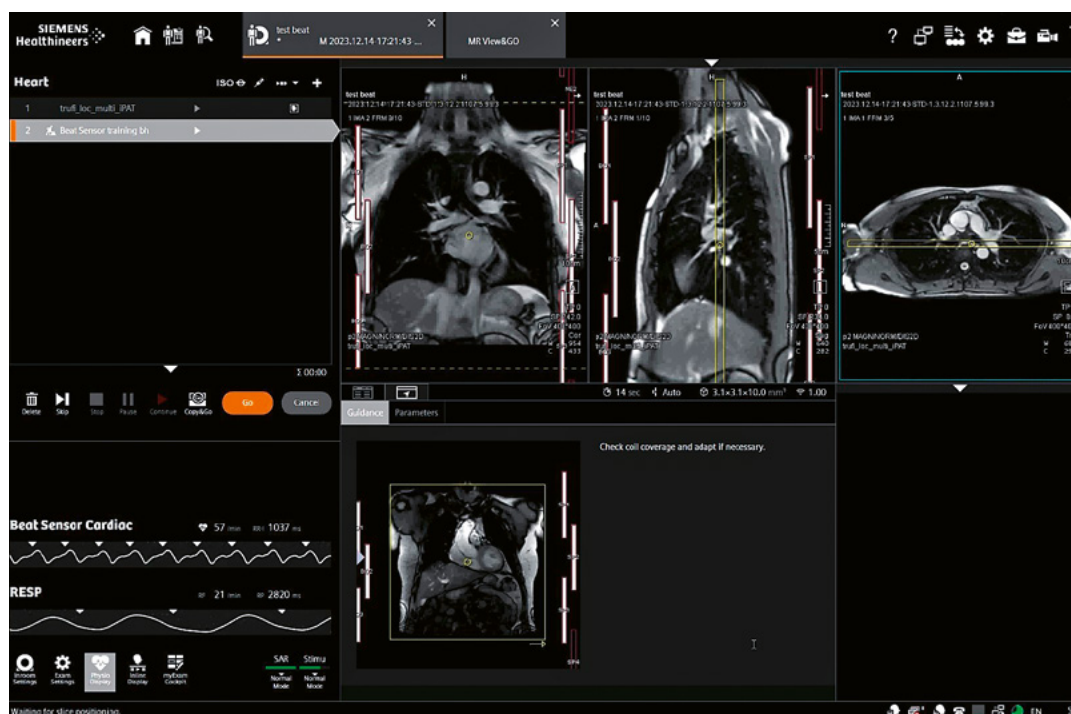
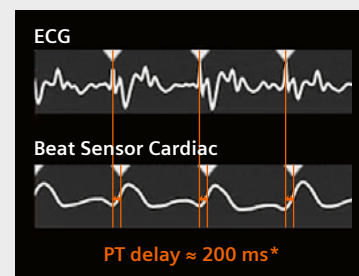**2** BioMatrix Beat Sensor interface for a training scan.
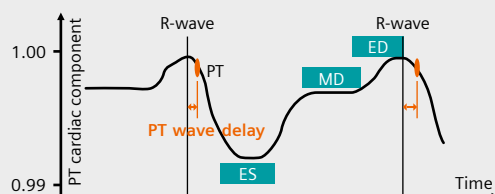
**3** PT signal characteristics and trigger time point [1].

Left ventricular functional analysis in healthy volunteers

In 8 healthy volunteers, we compared left ventricular (LV) volumes derived by the Beat Sensor to those derived by ECG gating. We found that there were no significant differences in end-diastolic (EDV) and end-systolic volumes (ESV) between the two groups (not shown). The beginning of the LV volume filling curves recorded by the Beat Sensor was delayed by approx. 200 milliseconds as previously estimated [1] (Fig. 4). These characteristics of the Beat
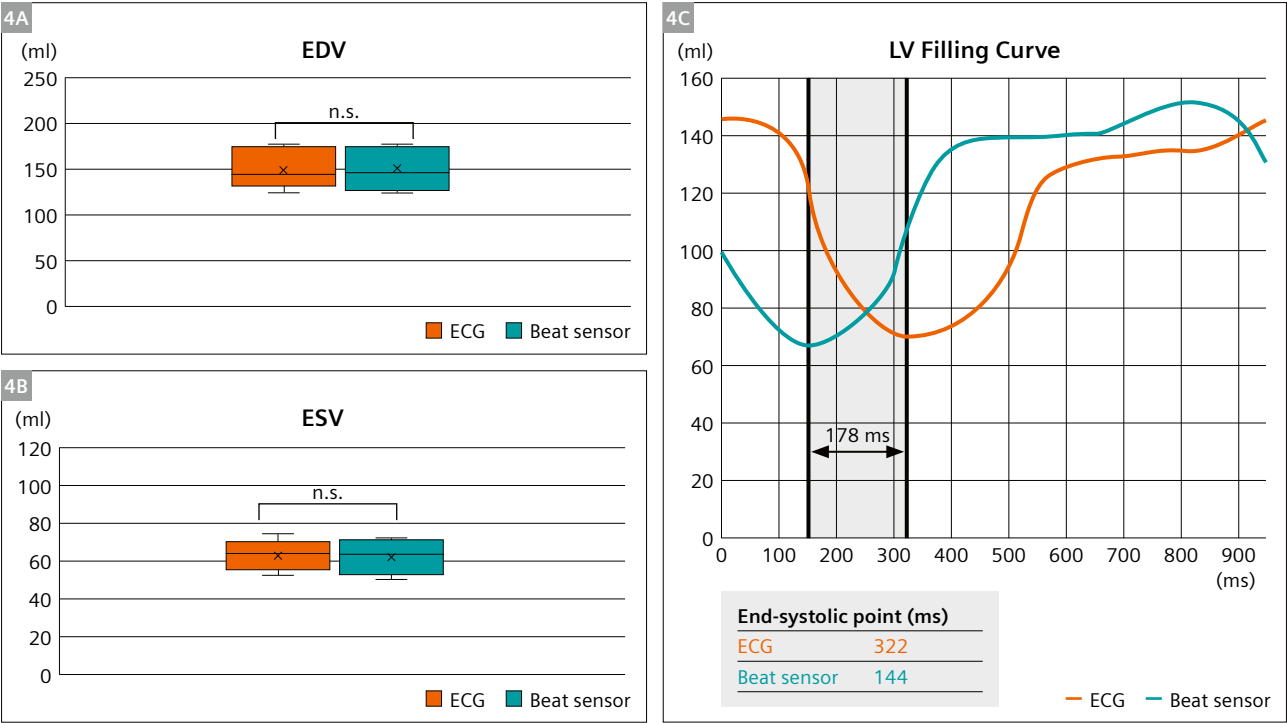
4 LV volume and filling curves in healthy volunteers undergoing cine cardiac MRI with Beat-Sensor and ECG gating. **(4A)** EDV, **(4B)** ESV, and **(4C)** example of LV filling curves. EDV = end-diastolic volume, ESV = end-systolic volume.
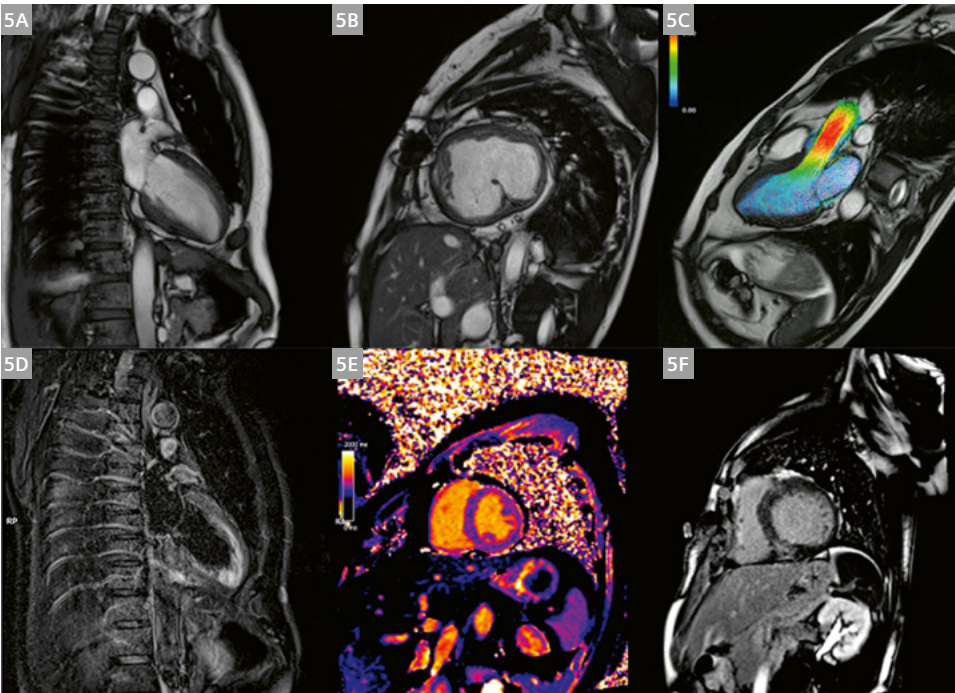
5 Example images of cardiac MRI with the BioMatrix Beat Sensor. Cine imaging, 4D-flow imaging, and T1 mapping using the Beat Sensor in a healthy volunteer are shown in Figures **5A**, **5C**, and **5D**, respectively. Figure **5B** shows cine imaging in a case with a single ventricle, and **5F** shows MOCO PSIR for the hypertrophic cardiomyopathy patient.

Sensor should be kept in mind, especially when scanning still-imaging protocols such as T2-weighted and myocardial mapping, and late-gadolinium enhancement with manual positioning of the scan window, which are often scanned in diastole.

Clinical patients

In our experience, reading physicians could adeptly evaluate cardiac motion through cine imaging and could conduct tissue characterization via myocardial mapping and late gadolinium enhancement, thereby effectively addressing the majority of clinical cases. Notably, the Beat Sensor has reliably achieved cardiac synchronization in a wide spectrum of cases, including patients with hyper-

trophic cardiomyopathy, complex congenital heart disease, and reduced ejection fraction (Fig. 5). Our observations extend published results of successful cardiac synchronization [2, 3] also to patients with arrhythmias, high heart rates, and pacing rhythms (Fig. 6). In an overweight patient [4] the Beat Sensor signal was more easily disturbed by other contributions, e.g., patient motion, but trigger time points corresponded very well to ECG (Fig. 7C).

In a newborn[1] the Beat Sensor training failed, resulting in unreliable triggering (Fig. 7A), likely due to the high heart rate and large size of coil elements of the BioMatrix Body 12. Figure 7 also shows results in patients with Wolff-Parkinson-White syndrome, bigeminy, and complete atrioventricular (AV) block.

[1]Siemens Healthineers disclaimer: MR scanning has not been established as safe for imaging fetuses and infants less than two years of age. The responsible physician must evaluate the benefits of the MR examination compared to those of other imaging procedures. Note: This disclaimer does not represent the opinion of the author.
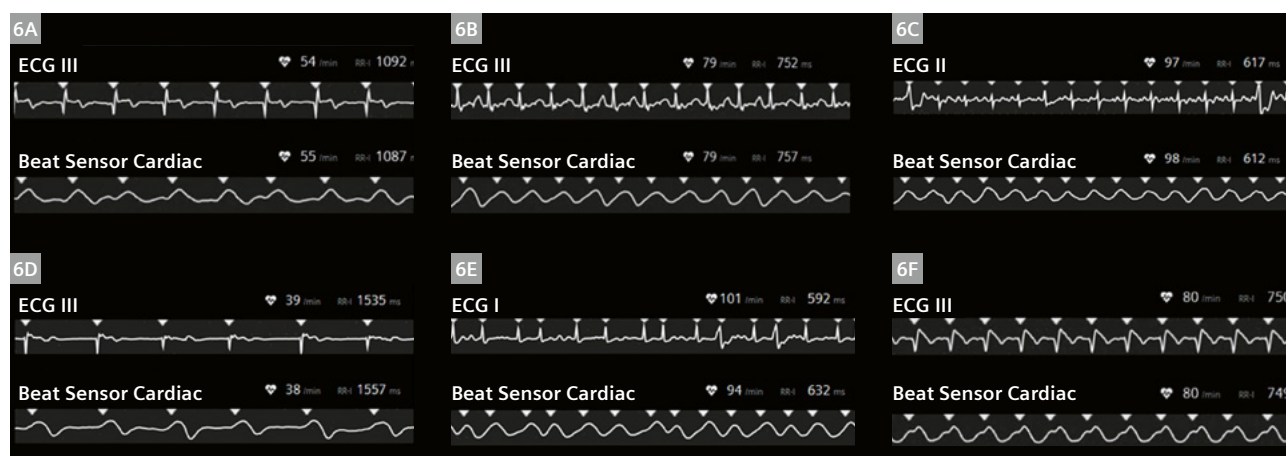
6 ECG waveform during cardiac MRI with ECG gating and the BioMatrix Beat Sensor. ECG waveform in patients with hypertrophic cardiomyopathy **(6A)**, a single ventricle **(6B)**, a reduced LV ejection fraction **(6C)**, atrial fibrillation with low heart rates **(6D)**, atrial fibrillation with high heart rates **(6E)**, and pacing rhythm (DDD implantation) **(6F)**.
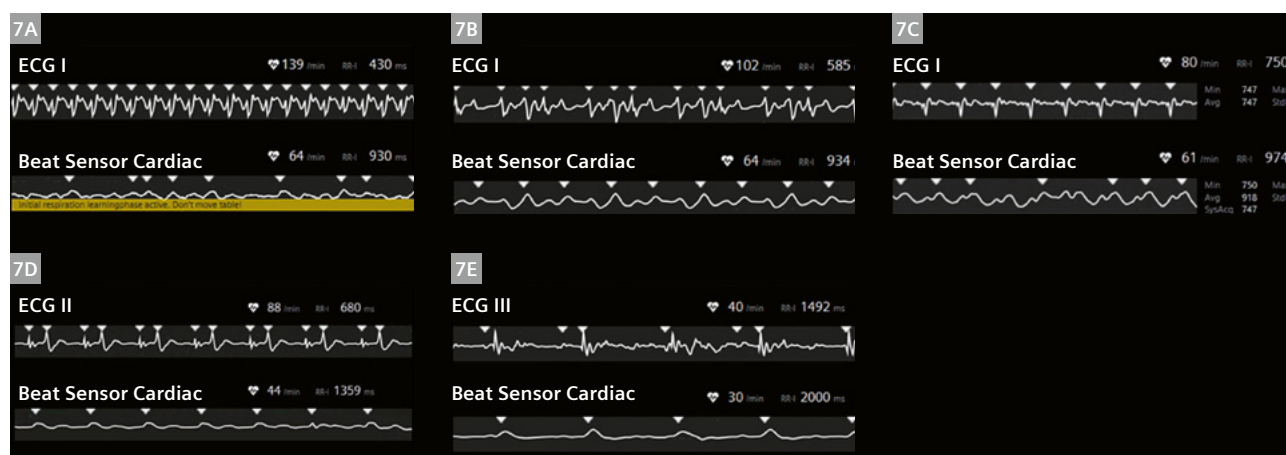
7 ECG waveform during cardiac MRI with ECG gating and the BioMatrix Beat Sensor. ECG waveform during cardiac MRI with ECG gating and the Beat Sensor in a newborn[1] with high heart rate **(7A)**, and in patients with Wolff-Parkinson-White syndrome **(7B)**, overweight **(7C)**, bigeminy **(7D)**, and complete AV block **(7E)** are shown.

The advantages of the BioMatrix Beat Sensor

Using the BioMatrix Beat Sensor provides a crucial advantage, in that it enables cardiac MRI scans even in challenging scenarios, such as with arrhythmias or difficulties in breath-holding, which are difficult conditions for ECG gating. Further, by conducting a preparatory training scan, the Beat Sensor facilitates imaging with both breath-holding and free breathing. Additionally, after the training, the operator can simply switch between ECG and Beat Sensor gating, eliminating the need for extra settings or preparation.

Cardiac MRI examinations do not aim to detect waveforms that detect the electrical potential difference of the heart. Rather, they aim to assess cardiac motion and perform tissue characterization. In our experience cardiac synchronization with the Beat Sensor is sufficient for these exams. ECG gating may not only acquire cardiac signals from heart motion, but also subtle electrical signals generated by muscles or arrhythmias, which can often cause reduced imaging quality. Since the Beat Sensor directly detects the heartbeat, it enables scanning at the cardiac phase without cardiac motion, especially for still cardiac imaging.

In the following section, we present clinical cases with bigeminy and complete atrioventricular block, for which the Beat Sensor provided efficient cardiac MRI scanning.
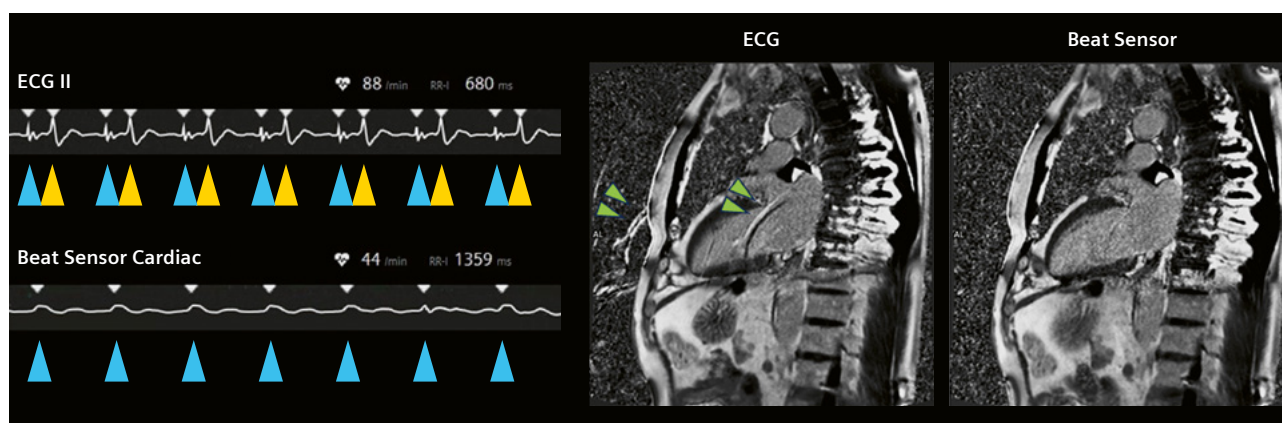
1. Bigeminy

Bigeminy is a cardiac arrhythmia that repeats ventricular premature contraction (VPC) every other beat. When patients with bigeminy are scanned with ECG triggering, all R-waves including VPCs are triggered, which results in motion artifacts. Motion artifacts can influence image quality and the values of the resulting quantitative parameters in cine imaging, T1, T2 mapping, and late gadolinium enhancement. Like the Beat Sensor, ECG gating includes retrospective and prospective gating. When scanning arrhythmic patients with ECG gating, a cardiac arrhythmia detection function with retrospective gating can be performed to remove the arrhythmia dataset during the preset R-R interval. However, the arrhythmia detection function involves determining the appropriate phase manually, especially in the case of bigeminy. Although prospective ECG gating is useful for severe cardiac arrhythmia, it is impossible to capture cardiac information during the entire cardiac cycle. When using the Beat Sensor, it is possible to accurately trigger the timing of the diastolic phase without detecting small contractions related to VPC (Fig. 8). Beat Sensor skipped every second trigger, thus the cine contained one bigeminy period (2 heart beats) and resolved both the short and long cardiac cycle. Interestingly, an LV filling curve could be generated for the case with bigeminy, which can be distorted with ECG gating. The resulting LV filling curve can be seen in Figure 9.

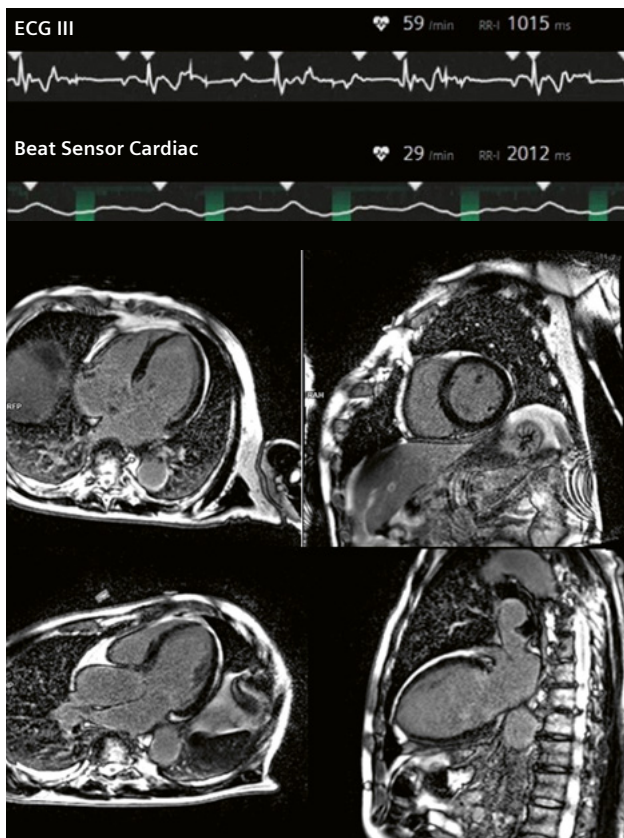### 2. Complete atrioventricular block

Complete atrioventricular (AV) block is a type of arrhythmia characterized by an incomplete electrical AV dissociation, with independent atrial and ventricular rates, which are often seen in patients with coronary artery disease or cardiac sarcoidosis undergoing cardiac MRI. As atria and ventricles function independently of each other during imaging with a complete AV block, all R-waves, including irregular R-waves, generate ECG triggers, thus diastolic imaging is impossible. Since the Beat Sensor is sensitive to the contractile motion of the heart, and generates triggers only after irregular R-waves. Therefore the Beat Sensor allows to synchronize acquisition to the diastole for still imaging. In the example with complete AV block in Figure 10, Beat-Sensor triggering was successful in acquiring interpretable images from a motion-corrected phase-sensitive inversion recovery (MOCO PSIR) acquisition and acts as an automatic arrhythmia detection function.

8 Comparison of late gadolinium enhancement images in a patient with bigeminy with ECG gating and the BioMatrix Beat Sensor. There is a motion artifact (green arrow) in late gadolinium imaging of the VPC patient using ECG gating, but no motion artifact with the Beat Sensor.
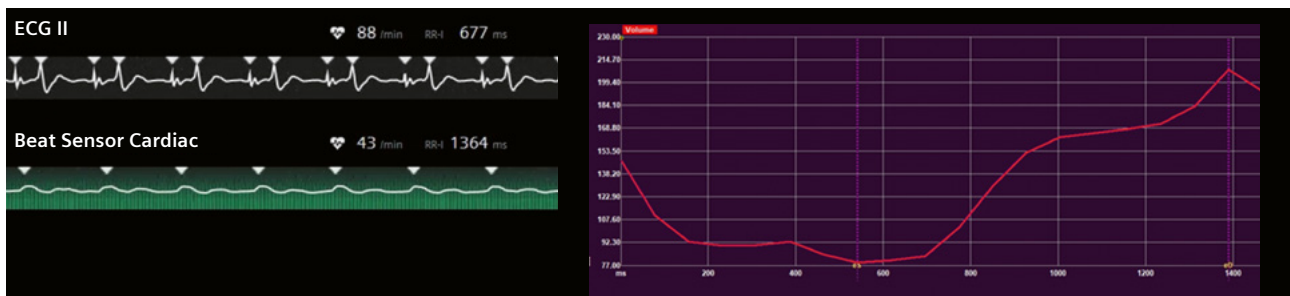
9 LV filling curve in a patient with bigeminy.

10 BioMatrix Beat Sensor with MOCO PSIR (free breathing). The Beat Sensor enabled capturing diastole with MOCO PSIR for the patient with complete atrioventricular block.

were unattainable with ECG gating. Its efficacy warrants validation across multiple facilities to enhance clinical workflows by offering substantial support in advanced cardiac MR imaging.

References

1 Speier P, Bacher M. Skip the Electrodes, But Not A Beat: The Engineering Behind the Beat Sensor. MAGNETOM Flash. 2023;83(2):106–117. Available at https://www.magnetomworld.siemens-healthineers.com/clinical-corner/case-studies/biomatrix-beat-sensor

2 Lin K, Sarnari R, Speier P, Hayes C, Davids R, Carr JC, Markl M. Pilot Tone-Triggered MRI for Quantitative Assessment of Cardiac Function, Motion, and Structure. Invest Radiol. 2023;58(3):239-243.

3 Pan Y, Varghese J, Tong MS, Yildiz VO, Azzu A, Gatehouse P, et al. Two-center validation of Pilot Tone Based Cardiac Triggering of a Comprehensive Cardiovascular Magnetic Resonance Examination. Res Sq [Preprint]. 2023:rs.3.rs-3121723. doi: 10.21203/rs.3.rs-3121723/v1.

4 Karamarkou C, Thielmann C. Clinical Approach of BioMatrix Beat Sensor Cardiac Triggering. MAGNETOM Flash. 2023;83(1):7–10.

5 Axel L, Bhatla P, Halpern D, Magnani S, Stojanovska J, Barbhaiya C. Correlation of MRI premature ventricular contraction activation pattern in bigeminy with electrophysiology study-confirmed site of origin. Int J Cardiovasc Imaging.2023. 39:145–152. doi.org/10.1007/s10554-022-02707-8.

6 Chen C, Liu Y, Simonetti OP, Tong M, Jin N, Bacher M, et al. Cardiac and respiratory motion extraction for MRI using Pilot Tone – a patient study. Accepted at The International Journal of Cardiovascular Imaging. Eprint at arXiv:2202.00055.

7 Falcão MBL, Di Sopra L, Ma L, Bacher M, Yerly J, Speier P, et al. Pilot tone navigation for respiratory and cardiac motion-resolved free-running 5D flow MRI. Magn Reson Med. 2022;87(2):718-732.

Conclusion

BioMatrix Beat Sensor is a new technology that enables cardiac MRI examinations without the need for ECG leads. Not only does it eliminate the need for electrodes and the discomfort of tape irritation and direct skin contact, but it also frees up technologists by streamlining the clinical workflow. By directly detecting cardiac motion, the Beat Sensor introduces novel cardiac synchronization with advantages in handling arrhythmic patient that

Contact

Naokazu Mizuno, RT
Sakakibara Heart Institute
Department of Radiology
Asahi-cho 3-16-1, Fuchu-shi
Tokyo, 183-0003
Japan
Tel: +81 24-314-3111
Fax: +81 24-314-3199
nmizuno@shi.heart.or.jp

Expert Insights: Hidden Gems from Application Specialists at Siemens Healthineers
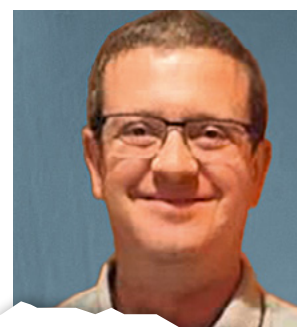
Alberto Cruces on the Echo Spacing parameter

Alberto Cruces

Alberto is a member of the application specialists team in Madrid, Spain. After training as a lab technician and radiographer, he started his journey in MRI almost by chance, more than 20 years ago. He remembers the day he was assigned to operate an MRI system for the first time and how he had to learn about this new world and its many possibilities. Perhaps this is why he is now so passionate about teaching. Before joining Siemens Healthineers in 2012, he worked as a radiographer and educator in the fields of MRI, CT, PET-CT, and mammography.

Alberto is committed to helping new users learn the nuts and bolts of MRI, and there is no better reward for him than seeing customers get the most out of equipment from Siemens Healthineers to arrive at an accurate patient diagnosis. In addition to his role as an applications scientist, in which he provides support both in Spain and beyond, he enjoys speaking at national conferences and demonstrating the latest advances in MRI. He has also participated in numerous system tests for MR headquarters, a collaboration that he finds very motivating and useful for keeping up to date with the latest developments.

Apart from work, Alberto's passions in life are his family and cooking. He likes to spend as much time as possible with his family, and he loves trying out new dishes – always with a nice cold beer on the side.

Madrid, Spain

Contact

Jose Alberto Cruces Dopico
SHS EMEA SEU ESP CS TC&APP DI&AT
Calle Mahonia, 2
28043 Madrid
Spain
josealberto.cruces@siemens-healthineers.com

My favorite feature …

… is the Echo Spacing (ES) parameter. Learning how to control and modify the ES is key to avoiding artifacts on TrueFISP sequences, such as in cardiac cine imaging, especially at 3 Tesla.

At 3T, it is very important to manually accurately position the shimming volume to the patient's heart during a cardiac MR examination. However, flow or banding artifacts can still appear in sensitive sequences like TrueFISP, depending on the patient's morphology, physiology, and pathology, and the TrueFISP sequences are particularly sensitive to this type of artifact. When this happens, I always turn to the ES parameter in the Sequence tab. Adjusting the ES value to below 3 ms (e.g., 2.8–2.9 ms) helps remove the undesired artifacts in most cases. To do

this, you can adjust the RF Pulse Type, most times using the Fast option and allowing Asymmetric Echo, while increasing the Readout BW. Also choosing a higher gradient mode (e.g., from Fast to Performance) can decrease the ES as shown in Figure 2. Don't forget to keep an eye on the signal-to-noise ratio and the desired flip angle when applying these changes to the sequences, to make sure that image quality and contrast are preserved.

Acknowledgments
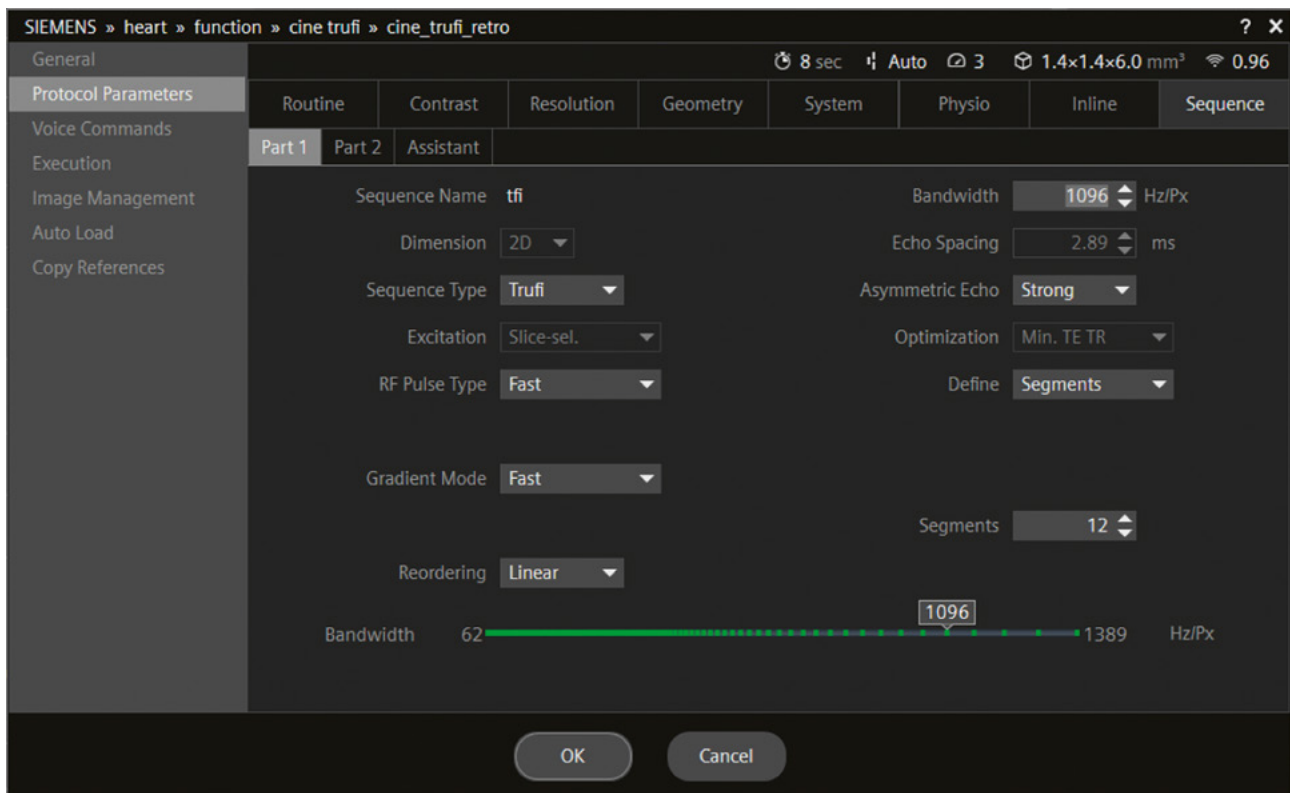
1 Standard gradients.
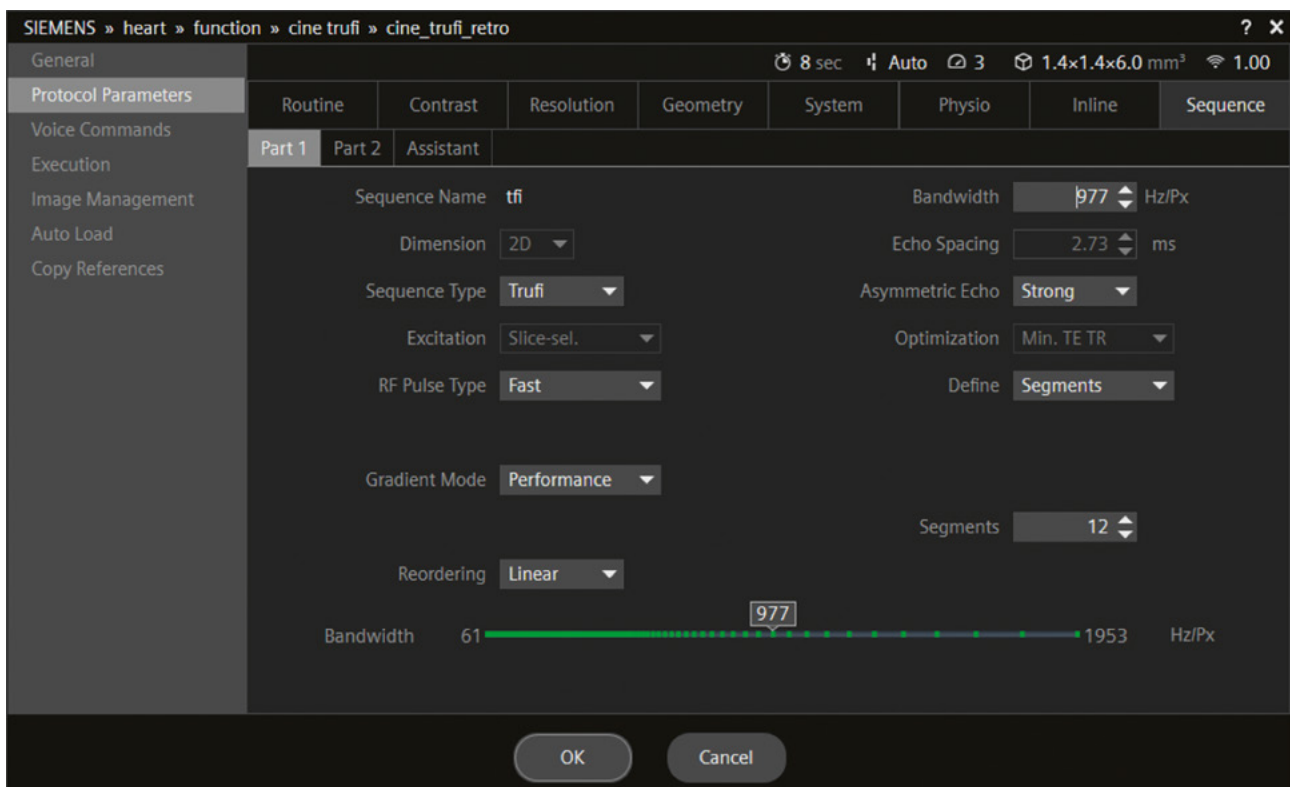
2 High-performance gradients.

Cardiac Amyloidosis – A Heartfelt Diagnosis

Gwendolyn Vuurberg, M.D., Ph.D.[1,4]; Victoria von Beckerath, M.D.[2]; Paul M. Hendriks, M.Sc., M.D.[3]

[1]Department of Radiology and Nuclear Medicine, Rijnstate Hospital, Arnhem, Netherlands
[2]Department of Radiology and Nuclear Medicine, Radboudumc, Nijmegen, Netherlands
[3]Department of Cardiology, Erasmus University Medical Center, Rotterdam, Netherlands
[4]Editorial board, Compendium Medicine

Abstract

When a patient presents at the cardiac care unit with symptoms of heart failure, the clinical workup includes multimodal imaging. In this case of a 72-year-old man, conventional radiography and echocardiography confirmed heart failure with a reduced left ventricular ejection fraction. The combination of an MRI, nuclear imaging, and a myocardial biopsy was needed to differentiate between an ischemic and non-ischemic origin of the newly diagnosed cardiomyopathy, and to identify the underlying condition.

Case information

A 72-year-old male with no history of cardiac disease presented at the cardiac care unit (CCU) in October 2022 with orthopnea and no palpitations or chest pain. Physical examination indicated a blood pressure of 140/109, and an irregular pulse of 157/min. Chest X-ray revealed limited bilateral pleural effusion and increased cardiothoracic ratio. The ECG showed de novo atrial fibrillation (AF) with normal ventricular response and diffuse low voltages. Blood tests indicated an increased NT-proBNP of 3,200 pg/mL (normal value < 450) and increased light protein chains. The patient was admitted with acute decompensated heart failure and treated with intravenous diuretics. Transthoracic echocardiography (TTE) during hospitalization revealed a reduced left ventricular ejection fraction (LVEF) of 30 – 35%, moderate mitral valve regurgitation, no thickening of the heart valves, and normal wall thickness without ventricular dilatation. Right ventricular systolic pressure was significantly elevated. After recompensation, the patient was started on heart failure medication and discharged in good clinical condition.

Eight weeks after discharge, no echocardiographic improvement was observed following the initiation of heart failure therapy, and coronary angiography was normal. Cardiac MRI was performed to further differentiate the etiology of the de novo heart failure.

This article is written in the concise Compendium Medicine style, using *bells* to outline important warning signs and clinical symptoms, *light bulbs* for interesting facts, and a *condition summary* using the first letter of each indicated step in the clinical process/patient follow-up (see the abbreviation list).

Abbreviations

|	
ACM	Arrhythmogenic cardiomyopathy
AF	Atrial fibrillation
AL	Light chain amyloidosis
ATTR	Transthyretin amyloidosis
bSSFP	balanced steady state free precession
CA	Cardiac amyloidosis
CAG	Coronary angiography
CCU	Cardiac care unit
CM	Cardiomyopathy
CTR	Cardiothoracic ratio
D	Definition
DDx	Differential diagnosis
Dx	Diagnostics
E	Epidemiology
Et	Etiology
HFrEF	Heart failure with a reduced ejection fraction
Hx	Patient history
IV	Intravenously
LGE	Late gadolinium enhancement
OPT	Optimal pharmacological therapy
P	Prognosis
PE	Physical examination
SPECT	Single-photon emission computed tomography
Tx	Treatment
!	Watch out / don't forget

Diagnostic imaging

Cardiac MRI

This case concerns heart failure with a reduced ejection fraction (HFrEF) based on the performed echocardiography in combination with de novo AF. An MRI with contrast was indicated to differentiate between an ischemic and non-ischemic origin of the cardiomyopathy (CM).

In January 2023, a cardiac MRI was performed. Images were acquired on a 1.5-Tesla MAGNETOM Avanto Fit (Siemens Healthineers, Erlangen, Germany). First, balanced steady state free precession (bSSFP) cine images were acquired. Then 25 mL Dotarem IV (Guerbet, Villepinte, France) was administered, and the delayed enhancement images were acquired. Both cine and late gadolinium enhancement (LGE) images were acquired in standard short-axis and long-axis views.

MRI confirmed a reduced LVEF of 45%. The four-chamber view (Fig. 1) revealed dilated atria, dilation of the mitral annulus, and lipomatous hypertrophy of the atrial septum. Wall movement and pericardium were normal. Apart from the mitral valve thickening, there were no evident valvular abnormalities. Administration of intravenous contrast revealed subendocardial LGE of the mid-to-apical right septal side and left side of the inferior ventricular septum, partial LGE of the papillary muscles,
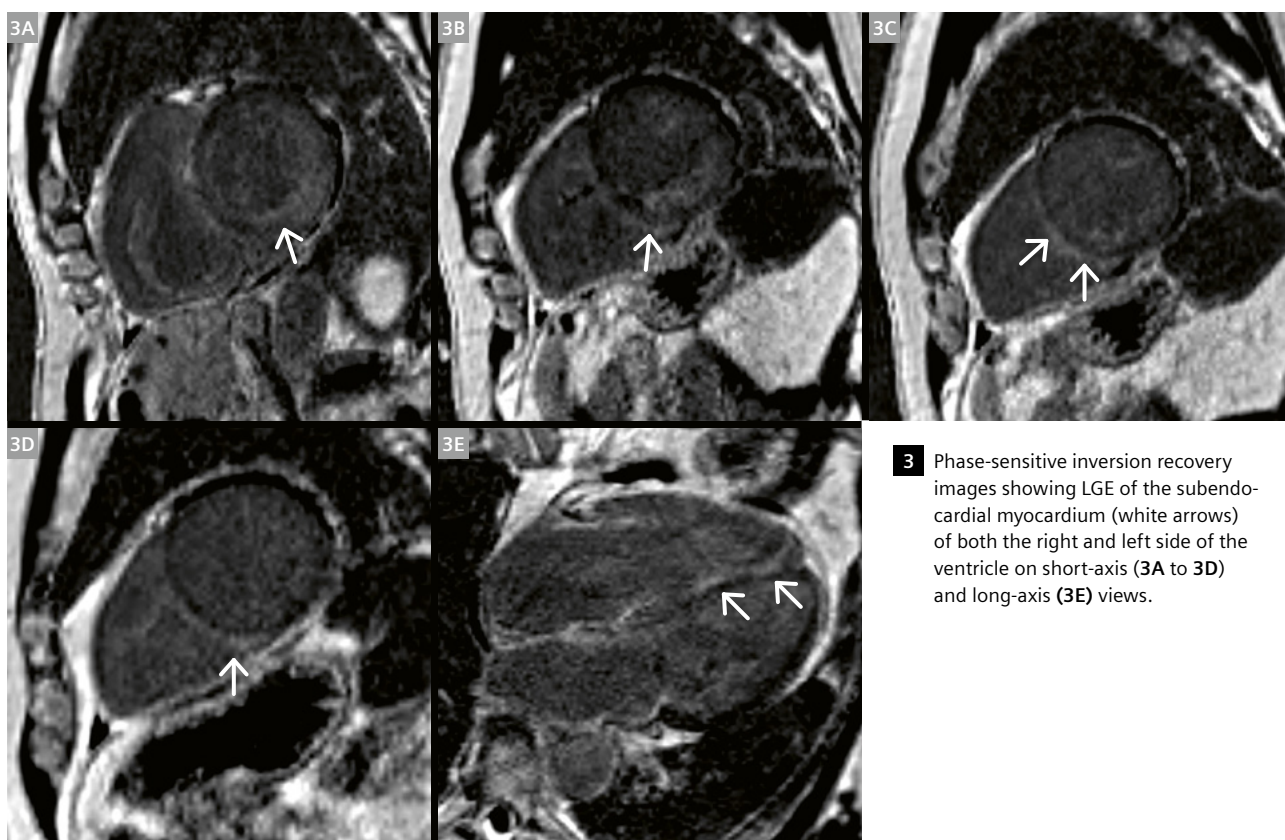
and LGE of the atrial wall (left more than right), see Figures 2 and 3. The pericardium was normal on both pre- and postcontrast images.
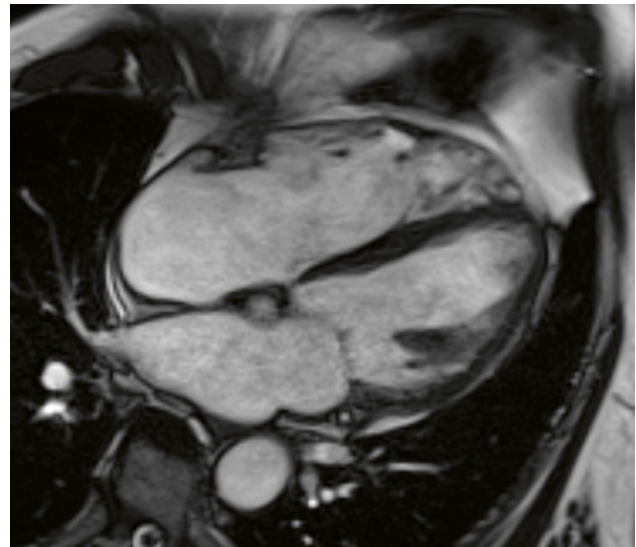
1 Four-chamber view showing dilated atria.
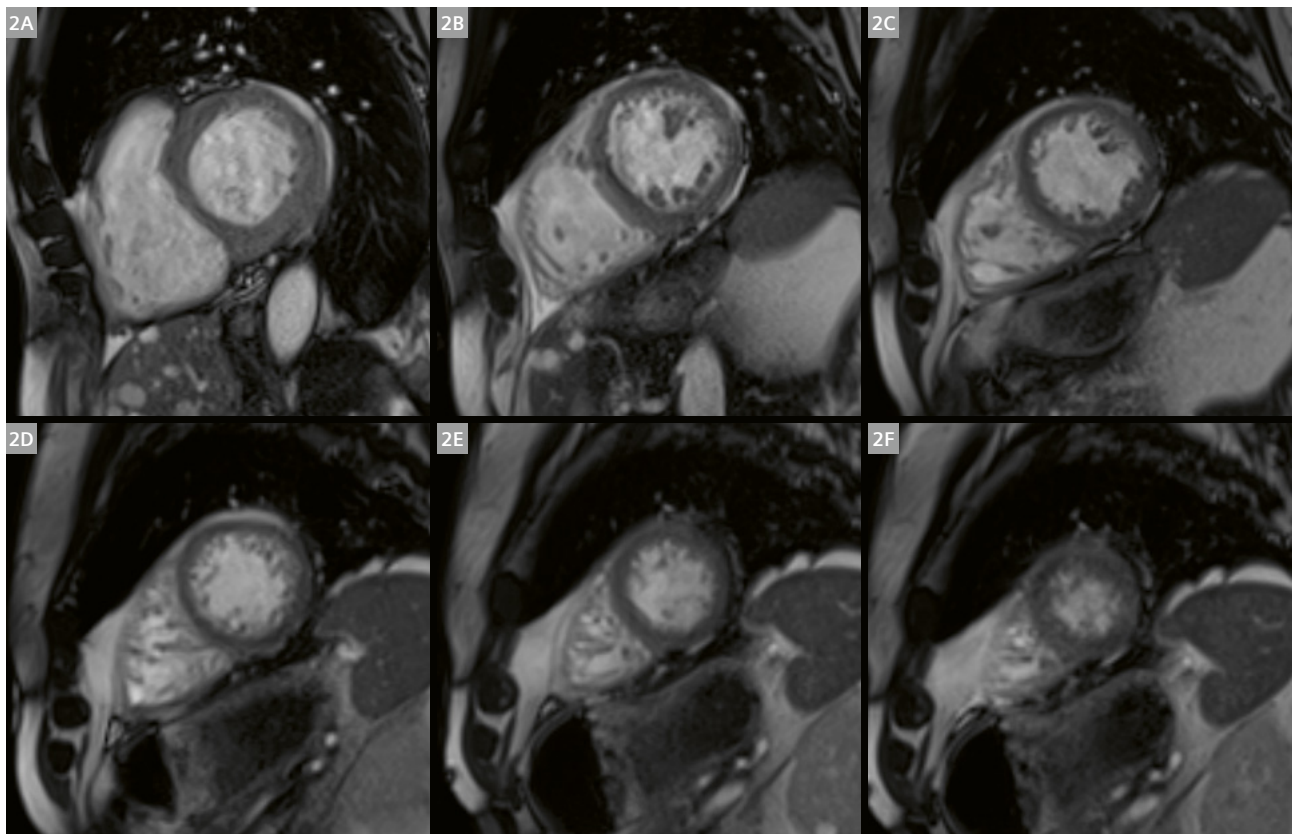
2 Short-axis cine series (base to apex, sagittal plane); (**2A** to **2F**) showing no focal thickening or thinning of the myocardium.

3 Phase-sensitive inversion recovery images showing LGE of the subendo-cardial myocardium (white arrows) of both the right and left side of the ventricle on short-axis (**3A** to **3D**) and long-axis **(3E)** views.

Clinical dilemma

Subendocardial enhancement may be seen in subendocardial infarction, but also in cardiac amyloidosis and systemic sclerosis. Depending on the type of findings, ischemic injury may be more or less likely. In this case, LGE not matching the coronary supply area, circular aspect, and involvement of the right side of the septum made ischemic injury less likely.

The use of contrast in MRI enables visualization of both normal myocardium and injured myocardium. Injured myocardium often shows late enhancement after 10 to 15 minutes, also known as late gadolinium enhancement (LGE). Delayed enhancement is often the result of regional differences in the extracellular volume with differences in uptake and washout due to issues such as edema, necrosis, or fibrotic tissue. The distinct pattern of LGE (e.g., subendocardial, mid-wall, or epicardial) and the location may, together with the clinical presentation, aid in defining a differential diagnosis [7].

In this case, the MRI showed subendocardial LGE. Subendocardial LGE is specifically seen in ischemic cardiac events and indicates fibrosis, as the ischemic wave front starts from the subendocardium, but can also occur in systemic sclerosis and cardiac amyloidosis [4]. The combination of extensive delayed enhancement of the septum on both the right and left ventricular side, papillary muscle, and atrial wall, not corresponding to ischemic injury or coronary infarction, increased the suspicion of amyloidosis.

Nuclear imaging

Various forms of amyloidosis can be differentiated. In instances of cardiac involvement, the predominant types are transthyretin amyloidosis (ATTR) wild type, hereditary ATTR, and light chain (AL) amyloidosis. In cases of clinically suspected cardiac ATTR amyloidosis, nuclear imaging with 99mTc-labeled bone-seeking agents is an important non-invasive diagnostic tool for confirming the diagnosis, and thereby in some cases replacing the earlier required myocardial biopsy [9]. Furthermore, myocardial uptake on bone scans can occasionally also be seen in AL amyloidosis.

Scans should be obtained 2 to 3 hours after administration of the radiotracer, and planar images or SPECT/CT of the chest are recommended. Whole-body planar can optionally be performed and can be helpful in identifying signs of systemic transthyretin amyloidosis (ATTR), e.g., uptake of the radiotracer in the shoulder and hip girdles.
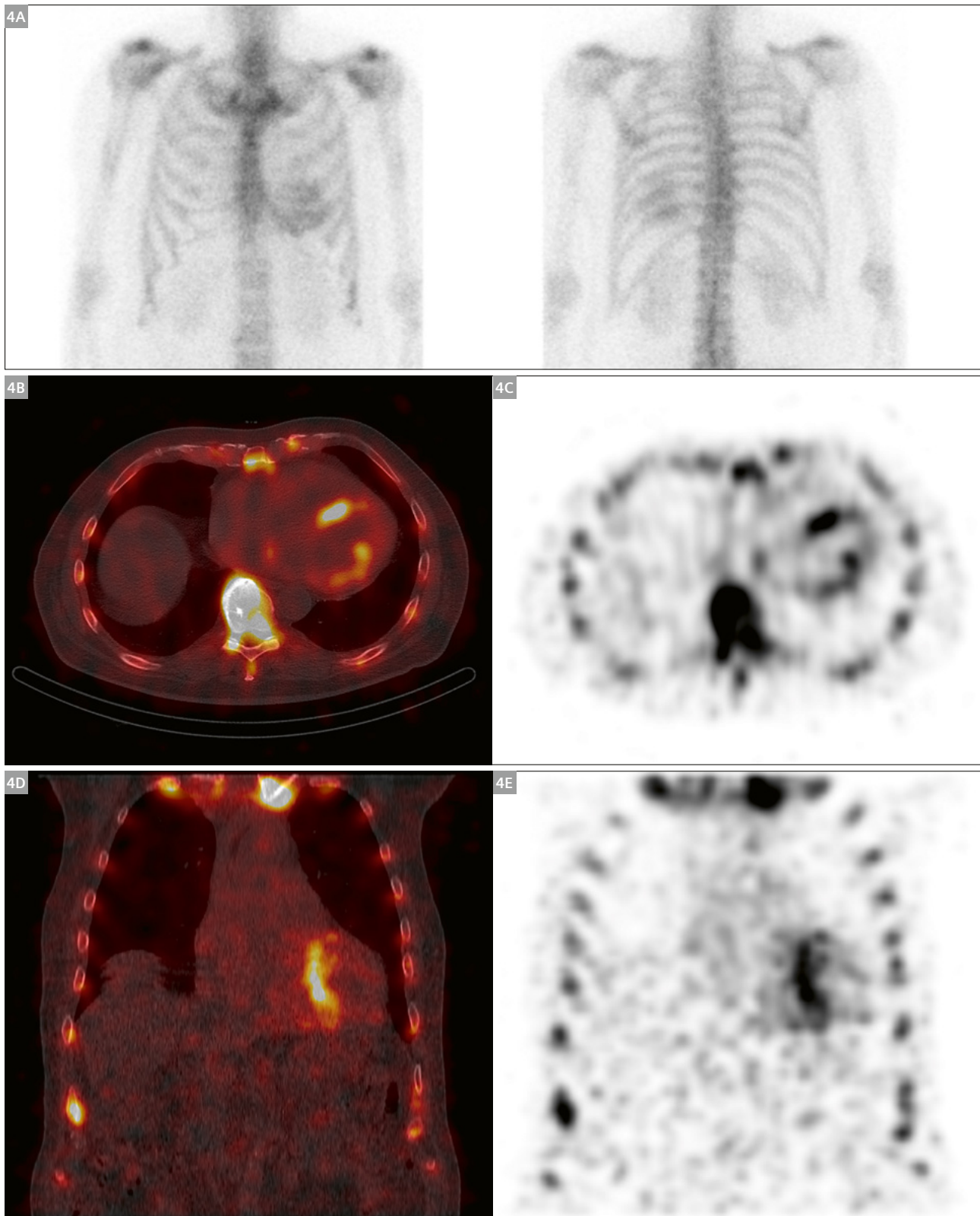
4 Tc-99m-HDP SPECT:
(4A), planar bone scintigraphy anterior (left) and posterior (right) view; (4B, 4C) axial fusion reconstructions and scintigraphy;
(4D, 4E), coronal fusion reconstructions and scintigraphy.

For this patient, images were acquired on a Symbia T16 SPECT/CT (Siemens Healthineers, Hoffman Estates, IL, USA) 4 hours after administration of approximately 500 MBq ^{99m}Tc-HDP (hydroxybiphosphonate). Static planar whole-body images from anterior and posterior were acquired, as were SPECT/CT images of the thorax.

Increased uptake was seen in the wall of the left ventricle, especially in the septum and basal wall (Fig. 4). The ratio of the counts in the affected myocardium compared to the contralateral lung parenchyma on the same level was > 1.5, a finding suggestive of ATTR amyloidosis and less suggestive of AL amyloidosis [8]. Cardiac uptake can furthermore be evaluated visually and scored according to the Perugini scale, with a grade 2 or 3 for ATTR.

> **Perugini grading scale** for cardiac amyloidosis:
> - 0: no cardiac uptake, normal rib uptake
> - 1: cardiac uptake < rib uptake
> - 2: cardiac uptake = rib uptake
> - 3: cardiac uptake > rib uptake / absent rib uptake

Case summary

This patient received an MRI to assist in the differential diagnosis for newly diagnosed heart failure and to differentiate between ischemic and non-ischemic CM. The visualized subendocardial enhancement raised suspicion of cardiac amyloidosis. The combination of the MR findings indicated the need for a bone scan for cardiac amyloidosis. The subsequent bone scan showed increased uptake in the myocardium (Perugini grade 2 or 3).

Pathophysiology
Systemic amyloidosis is characterized by extracellular deposition of insoluble amyloid fibrils. While there are many different types of amyloidosis, cardiac amyloidosis (CA) is caused in more than 95% of cases by immunoglobulin light chain amyloidosis (AL) and transthyretin-related amyloidosis (ATTR). Excessive production and malformation of antibody light chains is the cause of AL-CA, whereas ATTR involves a misfolding of the liver-derived protein transthyretin. ATTR can be hereditary or occur as wild type.

Cardiac amyloid fibril deposition leads to diffuse wall thickening, possibly mimicking hypertrophic CM, and to late gadolinium enhancement on MRI. Ventricular wall thickening results in progressive restrictive ventricular filling. LVEF can be less reliable for diagnosing CA, as low end-diastolic volumes can result in low stroke volume and thus low cardiac output while LVEF can still be preserved. Amyloid deposition primarily affects diastolic function, and additional systolic dysfunction is only seen in a late stage. The intra-atrial septum is often involved, leading to poor atrial function and predisposing the patient to atrial fibrillation. Thickening of the valvular leaflets is often associated with mild-to-moderate regurgitation. Amyloid deposition in the conduction system can lead to various conduction and bundle branch blocks. Coronary involvement usually affects small intramural vessels, leading to ischemia with normal aspects of the large coronary arteries. Pericardial effusion can be observed, but is usually limited.

Patients often present with heart failure with preserved ejection fraction (HFpEF) accompanied by exertional dyspnea or peripheral edema. General symptoms of fatigue and weakness are often attributed to advancing age. Atrial fibrillation (AF) and conduction abnormalities can be the first presentation. In particular, AF with rapid ventricular response is not well tolerated due to the restrictive filling pattern. Non-cardiac symptoms often precede cardiac involvement such as carpal tunnel syndrome (often bilaterally), spinal stenosis, neuropathy, proteinuria, and gastrointestinal symptoms.

> **Cardiac amyloidosis red flags**
> Echocardiographic concentric LV thickening without signs of high voltages on the ECG, and characteristic LGE patterns on MRI.

Case follow-up
The neurologist found no autonomous or peripheral neuropathy. Based on the MRI and SPECT scan discussed above, the patient was referred to the hematologist for further investigation of the suspected amyloidosis. A smoldering multiple myeloma was diagnosed with increased light chain proteins in the blood, but no signs of AL amyloidosis were found in the myocardial biopsy, crystal crest biopsy, or fat pad biopsy. Further immunohistochemical characterization was more suggestive of ATTR-CA, which correlates better with the findings on the bone scan. Genetic testing for hereditary ATTR showed no underlying genetic defect. The patient was therefore diagnosed with wild-type ATTR-CA and treated accordingly.

The statements described herein are based on results that were achieved in the author's unique setting. Since there is no "typical" hospital and many variables exist (e.g., hospital size, case mix, level of IT adoption) there can be no guarantee that other users will achieve the same results.

Cardiac amyloidosis

D Definition

Cardiac amyloidosis, also known as stiff heart syndrome, is a systemic infiltrative disease. It is characterized by extracellular insoluble protein deposition and is one of the leading causes of restrictive cardiomyopathy [6].

E Epidemiology

- AL subtype incidence of 1:100,000 and prevalence of 17:100,000; ATTR subtype incidence of 3.6:100,000 [10]
- ↑ due to ↑ survival and ↑ diagnostic rates

Et Etiology

- Extracellular deposition of the toxic component amyloid → ventricular wall thickness ↑ → ventricular stiffness → ventricular diastolic dysfunction
- Types of amyloidosis (1) AL amyloidosis (deposition of AL fibrils created by abnormal plasma cells, e.g., in patients with multiple myeloma), (2) wild-type ATTR amyloidosis (wtATTR, deposition of liver-produced transthyretin), (3) hereditary ATTR amyloidosis (hATTR)

Hx Patient history

Fatigue, malaise, (exertional) dyspnea, orthopnea, palpitations, chest pain, syncope, lower limb swelling, abdominal distention (ascites)

PE Physical examination

Fine lung crackles, pedal edema, jugular venous pressure ↑, ascites, orthostatic hypotension, hepatomegaly, neuropathy, periorbital purpura

DDx Differential diagnosis

Restrictive CM, cardiac hypertrophy (hypertrophic cardiomyopathy, arterial hypertension induced cardiac hypertrophy)

Dx Diagnostics

- Lab: (NT-pro)BNP ↑, Troponin T or I ↑/=, serum free light chain ↑ (AL-CA), M-protein spike on immunofixation (AL-CA)
- ECG: low voltages (no signs of hypertrophy), Q-waves early precordial leads, conduction abnormalities (AV block, bundle branch block)
- Echocardiography: LV and RV wall thickness ↑ (usually symmetric), septal wall thickness ↑, heart valve thickness ↑, ventricular dimensions =, biatrial dilatation ↑, LVEF =/↓, diastolic dysfunction, septal and lateral tissue doppler velocity ↓, longitudinal strain speckle tracking ↓, apical sparing in strain
- Cardiac MRI: native T1 mapping time ↑, LGE diffuse and subendocardial not following coronary distribution. Structural findings similar to echocardiography
- Bone scintigraphy: myocardial ^{99m}Tc-HDP uptake ↑ (ATTR-CA > AL-CA)
- Myocardial biopsy: confirmation of diagnosis and subtyping
- Fat pad biopsy: amyloid infiltration, lower sensitivity than myocardial biopsy
- Genetic analysis: differentiating wild-type and hereditary ATTR

Tx Treatment

- Patient education regarding disease and prognosis
- Pharmacological AL treatment: chemotherapy
- Pharmacological ATTR treatment: TTR synthesis inhibitors, TTR tetramer stabilizers, fibril disruptors
- Pharmacological treatment for heart failure
- Potential heart and/or liver transplantation in selected cases after good hematologic response

P Prognosis

Life expectancy
(1) AL-CA: 9 to 24 months,
(2) wtATTR amyloidosis: 5 to 7 years,
(3) hATTR 7 to 10 years

! Watch out / don't forget

- Increased risk of digoxin-toxicity in CA
- Non-dihydropyridine calcium antagonists are *contraindicated*
- Associated pathology: (bilateral) carpal tunnel syndrome, autonomous or peripheral neuropathy, spinal stenosis, nephrotic syndrome

References

1 Tanaka H. Illustrative review of cardiac amyloidosis by multi-modality imaging. Heart Fail Rev. 2023;28(1):113–122.
2 Wu Z, Yu C. Diagnostic performance of CMR, SPECT, and PET imaging for the detection of cardiac amyloidosis: a meta-analysis. BMC Cardiovasc Disord. 2021;21(1):482.

3 van Es W, van Heesewijk H, Rensing B, van der Heijden J, Smithuis R. Ischemic and non-ischemic cardiac myopathy. 2009. (Accessed December 5, 2023). https://radiologyassistant.nl/cardiovascular/cardiomyopathy/ischemic-and-non-ischemic-cardiomyopathy

4   Satoh H, Sano M, Suwa K, Saitoh T, Nobuhara M, Saotome M, et al. Distribution of late gadolinium enhancement in various types of cardiomyopathies: Significance in differential diagnosis, clinical features and prognosis. World J Cardiol. 2014;6(7):585–601.

5   El-Feky M. Cardiac amyloidosis. Radiopaedia.org. 2010. Accessed December 5, 2023. https://doi.org/10.53347/rid-12599.

6   Shams P, Ahmed I. Cardiac Amyloidosis. [Updated 2023 Jul 30]. In: StatPearls [Internet]. Treasure Island (FL): StatPearls Publishing; 2023 Jan. Accessed December 5, 2023. https://www.ncbi.nlm.nih.gov/books/NBK580521/.

7   Feger J. Late gadolinium enhancement. Radiopaedia.org. 2020. Accessed December 5, 2023. https://doi.org/10.53347/rid-79068.

8   Bokhari S, Castaño A, Pozniakoff T, Deslisle S, Latif F, Maurer MS. 99mTc-pyrophosphate scintigraphy for differentiating light-chain cardiac amyloidosis from the transthyretin-related familial and senile cardiac amyloidosis. Circ Cardiovasc Imaging. 2013;6(2):195–201.

9   Dorbala S, Bokhari S, Glaudemans AWJM, Miller E, Bullock-Palmer R, Slart RHJA. 99mTechnetium-3, 3-diphosphono-1, 2-propanodicar-boxylic acid (DPD) and 99mTechnetiumhydroxymethylene diphosphonate (HMDP) Imaging for transthyretin. ASNC and EANM Cardiac Amyloidosis Practice Points. 2019. Accessed December 5, 2023. https://www.eanm.org/content-eanm/up-loads/2019/10/19110-ASNC-AND-EANM-Amyloidosis-Practice-Points-WEB.pdf.

10   Damy T, Bourel G, Slama M, Algalarrondo V, Lairez O, Fournier P, et al. Incidence and survival of transthyretin amyloid cardiomyo-pathy from a French nationwide study of in- and out-patient databases. Orphanet J Rare Dis. 2023;18(1):345.
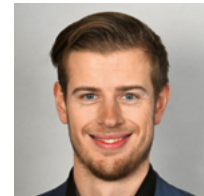
Contact

Gwendolyn Vuurberg, M.D., Ph.D.
Rijnstate Hospital
Wagnerlaan 55
6815 AD Arnhem
Netherlands
g.vuurberg@compendiummedicine.com

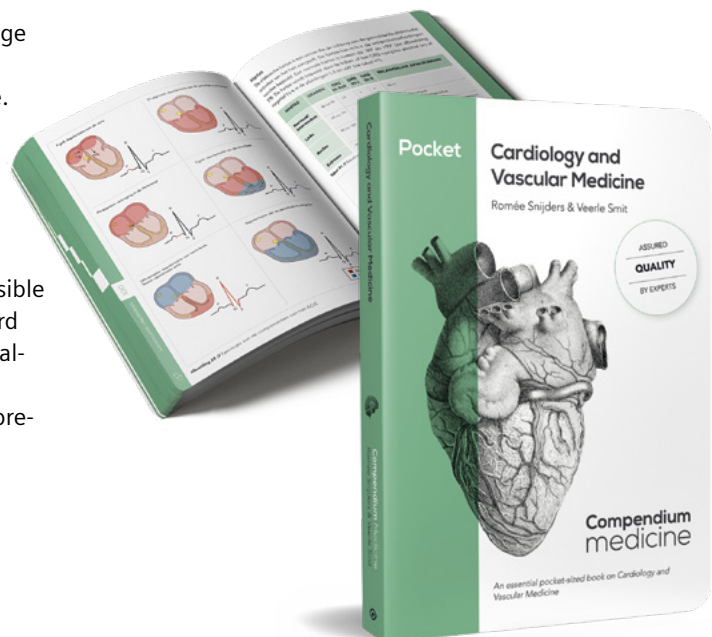Gwendolyn Vuurberg   Victoria von Beckerath   Paul M. Hendriks

CMR and Advanced Cardiac Imaging at Vannini Hospital: The Heart Imaging Team

Massimiliano Danti[1], Luca Arcari[2], Federica Ciolina[1], Giovanni Camastra[2]

[1]Radiology Unit, Madre Giuseppina Vannini Hospital, Rome, Italy
[2]Cardiology Unit, Madre Giuseppina Vannini Hospital, Rome, Italy

Introduction

Cardiovascular imaging with computed tomography (CT) and cardiovascular magnetic resonance (CMR) have seen a notable increase in indications and requests in recent years. This shows clearly when comparing clinical indications available in 2004 [1] with an update published by the Society for Cardovascular Magnetic Resonance (SCMR) [2], and by looking at the more recent European Society of Cardiology guidelines for acute coronary syndromes [3] and cardiomyopathies [4] in which cardiac CT and CMR both have a relevant role within the diagnostic work-up and prognostic stratification. Amidst the increasing importance of these techniques in the clinical arena, the need has emerged to expand training in advanced cardiac imaging and to boost the sharing of competencies between the different actors at play, including both radiologists and cardiologists [5, 6]. Continuing medical education, training, and certification of competencies remain of utmost importance, with the aim of delivering appropriate guidelines-directed diagnostic procedures to the highest share of eligible patients. Here, we summarize the approach to advanced cardiac imaging as practiced at our center, Madre Giuseppina Vannini Hospital in Rome, Italy, a

first-level community hospital. Managing a relatively high volume of unselected patients, close collaboration between cardiologists and radiologists, and continuous optimization of resources are mandatory to effectively continuing our activities.

The Heart Imaging Team

At our hospital, cardiologist-radiologist collaboration started about twenty years ago with the implementation of cardiac CT and CMR services. During this time, we developed and put into practice the concept of a pragmatic multidisciplinary approach quite conventionally in the form of a "heart team" made up of cardiologists and cardiac surgeons [7]. Our Heart Imaging Team (HIT) works in concert to provide the most appropriate use of advanced cardiac imaging, including discussion of indications, running of the service, and interpretation of reported results in the clinical context of the patient. The high quality of the CMR service is testified by the level 3 EACVI certification held by team members and the ESC accreditation of our CMR laboratory [8]. Our team consists of four physicians: two cardiologists
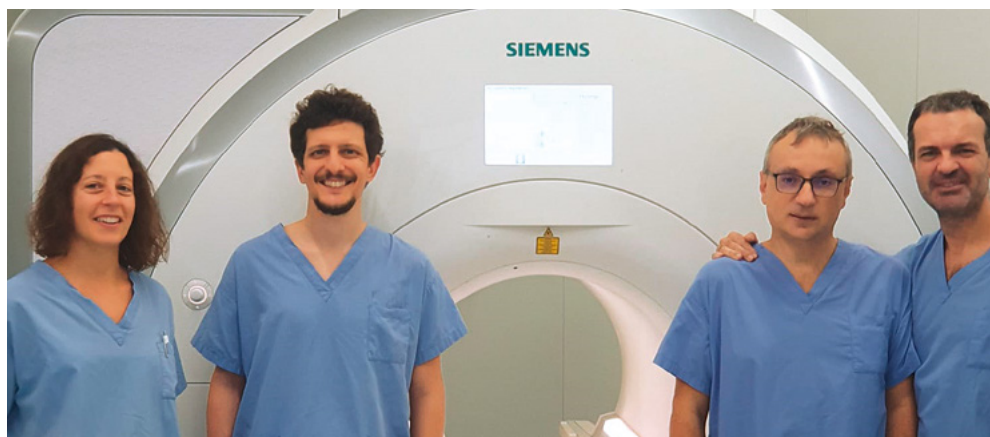
1 The Heart Imaging Team of Vannini Hospital (from left to right): Federica Ciolina, Luca Arcari, Giovanni Camastra, Massimiliano Danti.

and two radiologists, all working under the supervision of their respective unit directors in cardiology and radiology. The decision to perform CT or CMR procedures is made both by internal (HIT) or external referring physicians. However, the HIT provides support through a dedicated cardio-radiologic outpatient service where the requests for an advanced cardiac imaging examination from external referring physicians are critically reviewed. In this way, we ensure to maximize the appropriateness of indications. Even though each member of the HIT is an independent and expert user who can autonomously perform and report advanced cardiac imaging examinations, we strive to guarantee the presence of at least two HIT members, one cardiologist and one radiologist, when scans are performed. By doing so, we aim to exploit specific expertise, for example regarding the appropriate evaluation of extra-cardiac findings [9] (Fig. 1) and the tailoring of the scan to the special clinical characteristics of the patient [10]. Indeed, we pay great attention to the clinical background of our patients, where the result of the imaging examination is often just one piece of a more complex puzzle. The review of any relevant clinical documentation such as electrocardiograms, echocardiograms, and coronary angiograms is performed before execution/reporting of the examination. Finally, we are keen to share feedback with referring physicians and to discuss the clinical implications of the imaging findings. Overall, it is our opinion that this kind of multidisciplinary approach could contribute to improving the patients' care.

Optimizing resources

Optimizing the available resources is essential in our daily clinical practice. Indeed, our community hospital serves a densely populated, multicultural, and diverse neighborhood in the city of Rome, providing access to patients through a dedicated emergency department and offering, among others, surgical and orthopedic health services. Our CMR service shares the infrastructure with these other providers. In this context, the ability to perform a quick examination is essential. Our standard CMR protocol can be carried out in approximately 30 minutes (Table 1) and provides the relevant information needed for the diagnosis of the main pathologies encountered in clinical practice. This approach is in line with the more recent SCMR recommendations [11]. Moreover, correct patient preparation and briefing before the scan can help improve the quality of the images and reduce the duration of the examination; breathing instructions should be clearly understood and reproduced by the patient, the feeling of contrast injection should be anticipated. The protocol reported in Table 1 can be further personalized for specific patient needs. For example, flow imaging can be added if valvular heart disease is present, or contrast agent administration can be avoided if tissue mapping is sufficient to reach a diagnosis (Fig. 2) as may be the case with cardiac amyloidosis [12]. Reducing the scan time can improve patient adherence to the breathing instructions, result in better diagnostic imaging quality and better access to care in the context of limited

|	Cine-bSSFP	TIRM	T1 MAPPING	T2 MAPPING	PERFU-SION	Cine-bSSFP	T1 SCOUT	T1 LGE	T1 MAPPING POST
Acquisition time (s)	6 per slice	12 per slice	11 per slice	8 per slice	60	6 per slice	28 per slice	12 per slice (high-res)	11 per slice
Slice thickness (mm)	8	8	8	8	8	8	8	8	8
Gap	25%	50%	150%	150%	90%	25%	20%	20%	150%
Matrix	256 × 143	256 × 143	256 × 143	160 × 75	160 × 75	256 × 143	192 × 78	256 × 160	256 × 143
TE (ms)	1.21	52	1.8	1.8	1.18	1.21	1.12	3.19	1.8
TR (ms)	51.3	593	306.2	213	177.70	51.3	23	635	306.2
Flip angle	70°	180°	35°	70°	12°	70°	50°	25°	35°
Planes	4-chamber 2-chamber 3-chamber	4-chamber Basal-SAX Mid-SAX Apical-SAX	4-chamber Basal-SAX Mid-SAX Apical-SAX	4-chamber Basal-SAX Mid-SAX Apical-SAX	4-chamber Basal-SAX Mid-SAX Apical-SAX	SAX	Mid-SAX	SAX (overview) 4-chamber (high-res) 2-chamber (high-res) 3-chamber (high-res)	4-chamber Basal-SAX Mid-SAX Apical-SAX

Table 1: Our standard CMR protocol.

resources. A special situation is that of patients with suspected myocardial ischemia undergoing CMR stress perfusion imaging. In these cases, the clinical question can be evaluated with an abbreviated protocol lasting approximately 20 minutes (Table 2) [13]. In these patients, except for those where scar imaging is needed to identify ischemic necrotic myocardium, tissue characterization is less important; nevertheless, we strive to perform T1 and T2 mapping in all patients given the known prognostic relevance of this

evaluation in patients with coronary artery disease [14]. In our opinion, rest perfusion can be avoided in most of the cases. Indeed, literature suggests that, in the presence of an expert operator, it does not improve the diagnostic accuracy of stress imaging by itself (plus LGE) [15] (Fig. 3). When stress perfusion CMR is performed, at least two members of the HIT are present at the scanner. One stands at the control station to guide perfusion imaging acquisition and contrast media administration, the other is in the
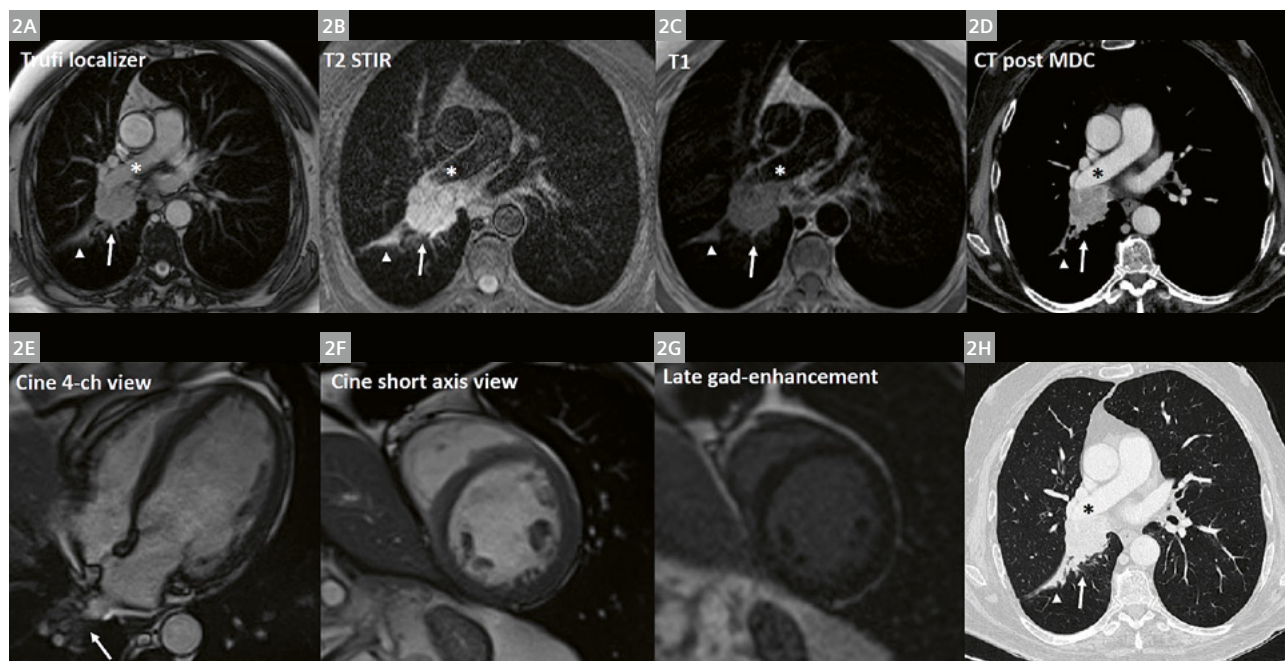
2 Images from a 64-year-old male with left bundle branch block and non-ischemic dilated cardiomyopathy. **(2A)** Trufi localizer showed a right pulmonary hilar mass (arrow) close to the right pulmonary artery (asterisk) with linear consolidation in the lung parenchyma (arrowhead). T2 STIR **(2B)**, and T1-weighted images **(2C)** confirm the solid mass. **(2E)** Cine 4-chamber view shows left ventricle dilatation and tissue close to right inferior pulmonary vein (arrows). **(2F)** Short-axis view confirmed the mild left ventricle dilatation without signs of fibrosis on late gadolinium enhancement image **(2G)**. **(2D)** Portal phase mediastinal view and **(2H)** lung window confirmed the presence of a right hilar mass (arrows) infiltrating right pulmonary artery (asterisk) and determining partial atelectasia of the right inferior lobe (arrowhead).
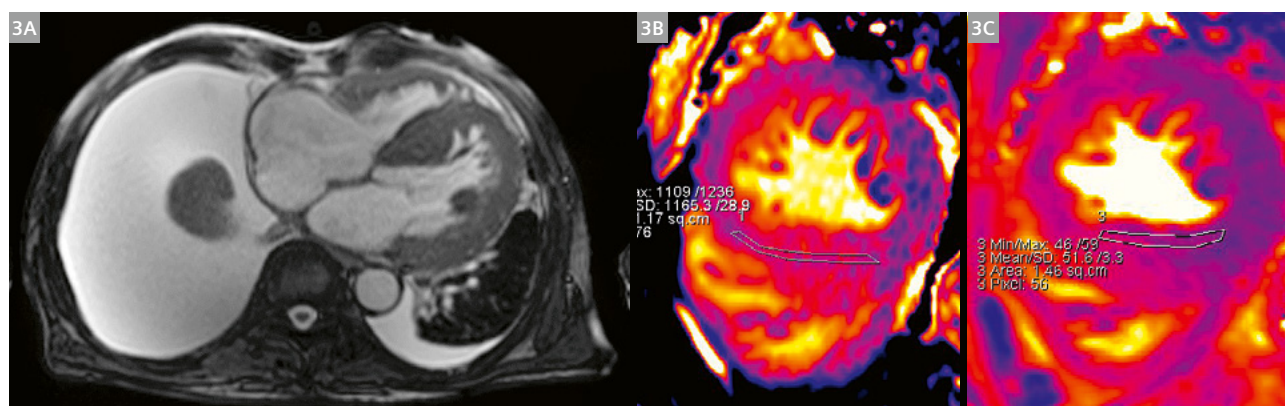

3 A 92-year-old patient hospitalized for heart failure underwent CMR due to suspected amyloidosis. TrueFISP images show left ventricular hypertrophy and large pleural effusion **(3A)**. The non-contrast CMR with tissue mapping revealed relevant increase of native T1 affecting the hypertrophied interventricular septum **(3B)** and mild increase of T2 values **(3C)** indicating concomitant mild myocardial edema. CMR findings are consistent with cardiac amyloidosis. In-center normality range for native T1 is 970 ± 20 msec and for T2 is 46 ± 2 msec.

scanner room to administer the stress agent, monitor patient reactions and vital signs, and treat any side effects should they develop. Adenosine as a pharmacological stress agent can cause several non-severe side-effects, such as flushing, chest pain, palpitations, and breathlessness, for which patients should be briefed before the examination to improve adherence to breathing instructions. The patient is required to sign a specific informed consent form for stress-perfusion imaging.

## Implementing a clinical and research workflow

The presence of a HIT and the close collaboration with the hospital clinics where the two HIT cardiologists also serve as consultants for the ward, echo lab, and emergency departments, leads to the smooth integration of the radiological data with the patient's subsequent management, including treatment changes and planning of further medical procedures. One typical example of the impact that a CMR examination can have is that of patients with myocardial infarction with non-obstructive coronary artery disease (MINOCA) [16], for which the etiology is unclear after first-level examinations. In this context, CMR can provide relevant information to drive the diagnosis and subsequent treatment [17]. The presence of a scar, whether ischemic or non-ischemic, can inform the clinician about further treatments and specific follow-ups to be performed (Fig. 4).
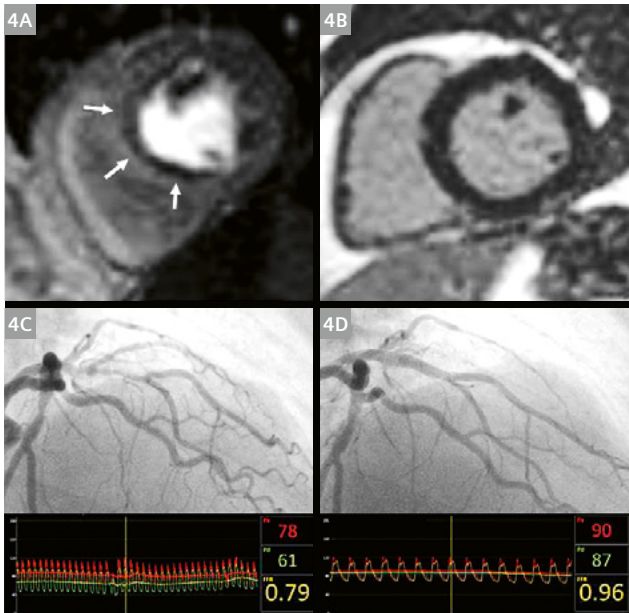
4 First-pass perfusion imaging in a patient with effort angina shows a subendocardial defect affecting the subendocardium of interventricular septum at mid-left ventricular level **(4A)**. LGE imaging shows absence of replacement fibrosis **(4B)**. The patient underwent coronary angiography with fractional flow reserve revealing a significant stenosis (FFR 0.79) of the left anterior descending artery **(4C)**, which was effectively treated with angioplasty and stent implantation (FFR 0.96) **(4D)**.

|	Cine-bSSFP	PERFUSION (test)	PERFUSION (stress)	Cine-bSSFP	T1 SCOUT	T1 LGE	PERFUSION (rest – optional)
Acquisition time (s)	6 per slice	10	60	6 per slice	28 per slice	12 per slice (high-res)	60
Slice thickness (mm)	8	8	8	8	8	8	8
Gap	25%	90%	90%	25%	20%	20%	150%
Matrix	256 × 143	160 × 75	160 × 75	256 × 143	192 × 78	256 × 160	256 × 143
TE (ms)	1.21	1.18	1.18	1.21	1.12	3.19	1.8
TR (ms)	51.3	177.70	177.70	51.3	23	635	306.2
Flip angle	70°	12°	12°	70°	50°	25°	35°
Planes	4-chamber 2-chamber 3-chamber	Basal-SAX Mid-SAX Apical-SAX	Basal-SAX Mid-SAX Apical-SAX	SAX	Mid-SAX	SAX (overview) 4-chamber (high-res) 2-chamber (high-res) 3-chamber (high-res)	Basal-SAX Mid-SAX Apical-SAX

Table 2: Abbreviated protocol.
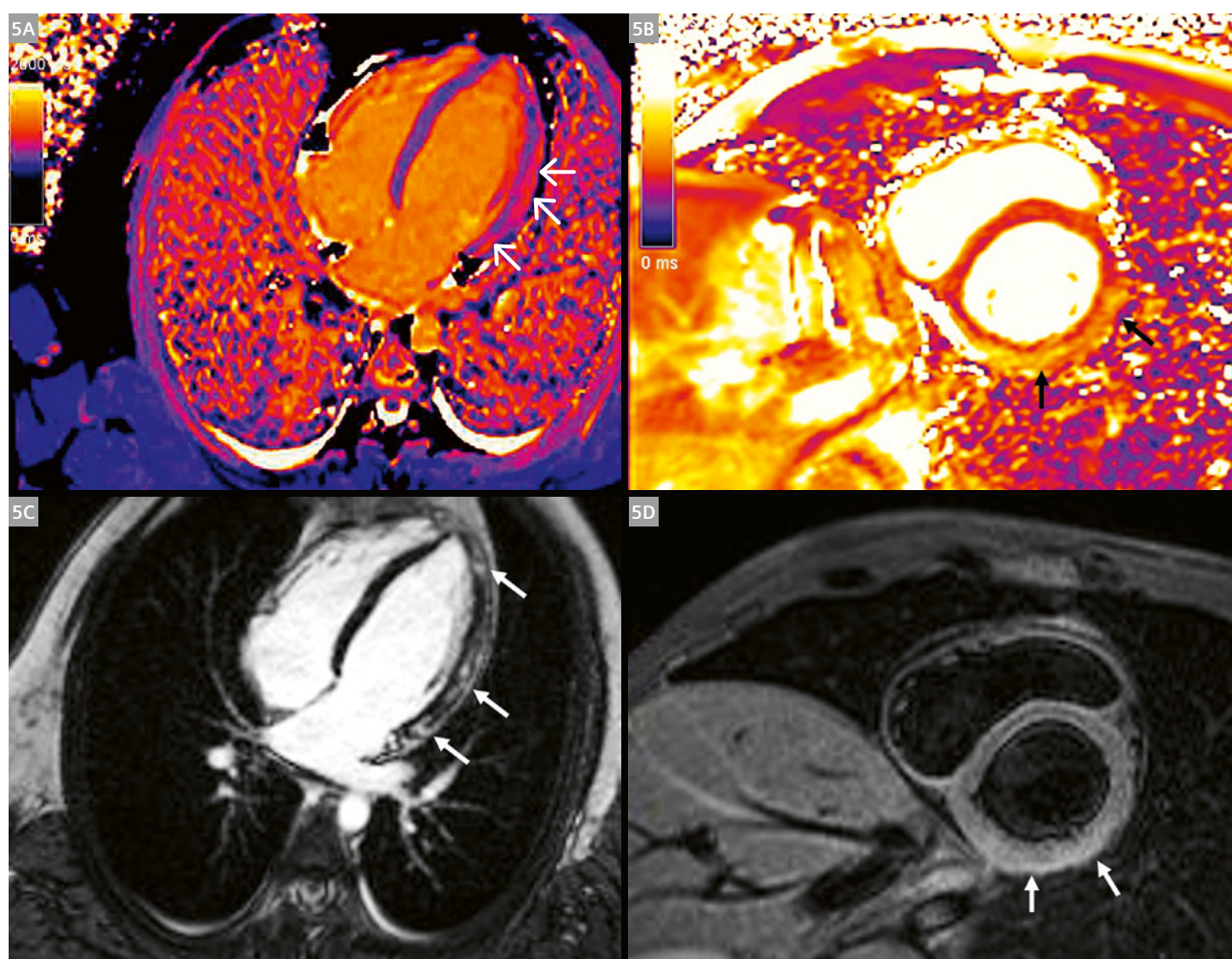
5 Images from a patient in his thirties, presented to the emergency department after complaining of chest pain and fever. ECG consistent with inferior STEMI. Urgent coronary angiography revealed patent coronary arteries; troponin T rose to 1130 pg/mL (normal value below 14 pg/mL). CMR examination was performed a few days later. Native T1 (4-chamber long-axis view in **5A**) and T2 (basal short-axis view in **5B**) revealed increased signal intensity in the lateral to inferior left ventricular wall (arrows). Bottom panels represent LGE imaging **(5C)** and T2 STIR imaging **(5D)** in the same view as the upper panel; areas of increased signal intensity are indicated by the arrows. The presence of non-ischemic LGE (patchy sub-epicardial and intra-myocardial) plus myocardial edema is consistent with a diagnosis of acute myocarditis.

This comprehensive approach to advanced cardiac imaging used in our institution, from the indications to the execution, reporting, and clinical impact of these procedures, makes it possible to collect relevant data for research purposes. This activity is also supported by the availability of relatively recent quantitative tools for tissue characterization, such as T1 and T2 mapping. Prospective and standardized collection of this data is performed on consecutive patients, especially that pertaining to some specific subgroups of diseases, such as myocarditis [18] (Fig. 5) and takotsubo syndrome [19] (Fig. 6). Notably, the analysis of mapping data is made in accordance with

indications from expert consensus [20] and by using standardized and reproducible methods [21] (Fig. 2). Finally, we often undervalue the amount of information acquired during a CMR scan. Indeed, even with standard T1 and T2 mapping acquisition, a large volume of extracardiac data pertaining to the lungs, spleen, and liver is collected and can be further analyzed [22, 23]. To this extent, the implementation of artificial intelligence-based technology could boost analysis of images and potentially very large datasets [24] and further improve the role of tissue characterization in magnetic resonance imaging as a pivotal diagnostic examination in a wide range of cardiac and non-cardiac pathologies.
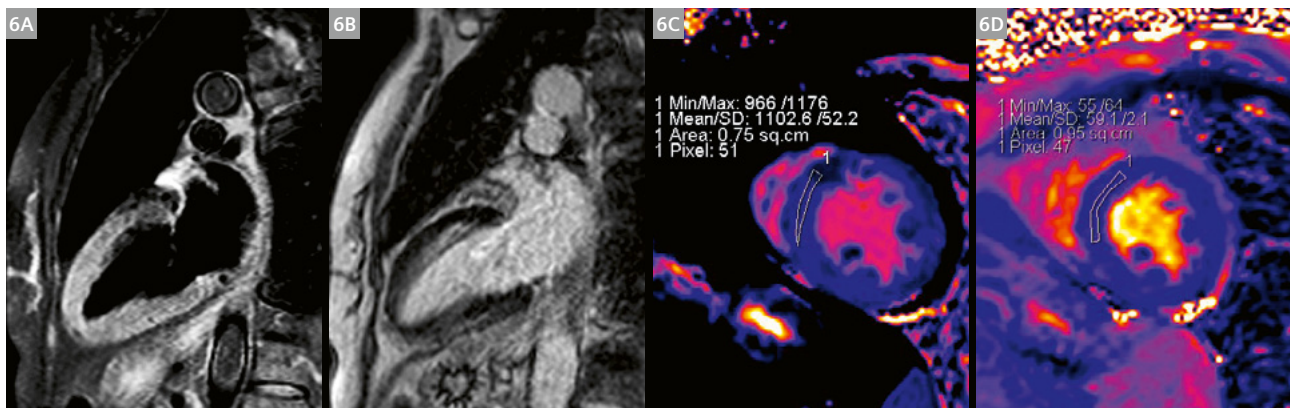
6 CMR of a patient with suspected takotsubo syndrome, confirming the clinical suspicion. T2-STIR sequence of 2-chamber view shows increased signal at mid-apical level consistent with myocardial edema (arrows in **6A**). LGE imaging in the same plane excludes the presence of replacement fibrosis **(6B)**. Quantitative analysis with native T1 **(6C)** and T2 **(6D)** mapping is performed at mid-septal level from short-axis view, as indicated by expert consensus. The parametric evaluation of myocardial edema offers more accurate diagnostic and, potentially, prognostic information in this setting [19].

Summary

A high-quality CMR service can be effectively deployed in the context of a first-level setting of care, in accordance with current clinical practice guidelines. To enhance the clinical relevance of imaging findings, a multimodality (imaging) and multispecialty (physicians) approach is essential. This requires appropriate training, infrastructure availability, and close collaboration between the professionals involved.

References

1   Pennell DJ, Sechtem UP, Higgins CB, Manning WJ, Pohost GM, Rademakers FE, et al. Clinical indications for cardiovascular magnetic resonance (CMR): Consensus Panel report. Eur Heart J. 2004;25(21):1940–1965.

2   Leiner T, Bogaert J, Friedrich MG, Mohiaddin R, Muthurangu V, Myerson S, et al. SCMR Position Paper (2020) on clinical indications for cardiovascular magnetic resonance. J Cardiovasc Magn Reson. 2020;22(1):1–37.

3   Byrne RA, Rossello X, Coughlan JJ, Barbato E, Berry C, Chieffo A, et al. 2023 ESC Guidelines for the management of acute coronary syndromes. Eur Heart J. 2023;44(38):3720–3826.

4   Arbelo E, Protonotarios A, Gimeno JR, Arbustini E, Barriales-Villa R, Basso C, et al. 2023 ESC Guidelines for the management of cardiomyopathies. Eur Heart J. 2023;44(37):3503–3626.

5   Westwood M, Almeida AG, Barbato E, Delgado V, Dellegrottaglie S, Fox KF, et al. Competency-based cardiac imaging for patient-centred care. A statement of the European Society of Cardiology (ESC). Eur Heart J. 2023;10:1–10.

6   Choi AD, Thomas DM, Lee J, Abbara S, Cury RC, Leipsic JA, et al. 2020 SCCT Guideline for Training Cardiology and Radiology Trainees as Independent Practitioners (Level II) and Advanced Practitioners (Level III) in Cardiovascular Computed Tomography: A Statement from the Society of Cardiovascular Computed Tomography. J Cardiovasc Comput Tomogr. 2021;15(1):2–15.

7   Young MN, Kolte D, Cadigan ME, Laikhter E, Sinclair K, Pomerantsev E, et al. Multidisciplinary heart team approach for complex coronary artery disease: Single center clinical presentation. J Am Heart Assoc. 2020;9(8):e014738.

8   https://www.escardio.org/Education/Career-Development/Accreditation/EACVI-Laboratory-accreditation/eacvi-cmr-accredited-laboratories (accessed November 10, 2023).

9   Rodrigues JCL, Lyen SM, Loughborough W, Amadu AM, Baritussio A, Dastidar AG, et al. Extra-cardiac findings in cardiovascular magnetic resonance: What the imaging cardiologist needs to know. J Cardiovasc Magn Reson. 2016;18(1):1–21.

10 Quarta G, Aquaro GD, Pedrotti P, Pontone G, Dellegrottaglie S, Iacovoni A, et al. Cardiovascular magnetic resonance imaging in hypertrophic cardiomyopathy: the importance of clinical context. Eur Hear Journal Cardiovasc Imaging. 2018;19(6):601–610.

11 Raman SV, Markl M, Patel AR, Bryant J, Allen BD, Plein S, et al. 30-minute CMR for common clinical indications: a Society for Cardiovascular Magnetic Resonance white paper. J Cardiovasc Magn Reson. 2022;24(1):1–11.

12 Baggiano A, Boldrini M, Martinez-Naharro A, Kotecha T, Petrie A, Rezk T, et al. Noncontrast Magnetic Resonance for the Diagnosis of Cardiac Amyloidosis. JACC Cardiovasc Imaging. 2020;13(1 Pt 1):69–80.

13 Hendel RC, Friedrich MG, Schulz-Menger J, Zemmrich C, Bengel F, Berman DS, et al. CMR First-Pass Perfusion for Suspected Inducible Myocardial Ischemia. JACC Cardiovasc Imaging. 2016;9(11):1338–1348.

14 Puntmann VO, Carr-White G, Jabbour A, Yu CY, Gebker R, Kelle S, et al. Native T1 and ECV of Noninfarcted Myocardium and Outcome in Patients With Coronary Artery Disease. J Am Coll Cardiol. 2018;71(7):766-778.

15 Villa ADM, Corsinovi L, Ntalas I, Milidonis X, Scannell C, Di Giovine G, et al. Importance of operator training and rest perfusion on the diagnostic accuracy of stress perfusion cardiovascular magnetic resonance. J Cardiovasc Magn Reson. 2018;20(1):1–10.

16 Hausvater A, Smilowitz NR, Li B, Redel-Traub G, Quien M, Qian Y, et al. Myocarditis in Relation to Angiographic Findings in Patients With Provisional Diagnoses of MINOCA. JACC Cardiovasc Imaging. 2020;13(9):1906–1913.

17 Dastidar AG, Baritussio A, De Garate E, Drobni Z, Biglino G, Singhal P, et al. Prognostic Role of CMR and Conventional Risk Factors in Myocardial Infarction With Nonobstructed Coronary Arteries. JACC Cardiovasc Imaging. 2019;12(10):1973–1982.

18 Aquaro GD, Perfetti M, Camastra G, Monti L, Dellegrottaglie S, Moro C, et al. Cardiac MR With Late Gadolinium Enhancement in Acute Myocarditis With Preserved Systolic Function: ITAMY Study. J Am Coll Cardiol. 2017;70(16):1977–1987.

19 Arcari L, Camastra G, Ciolina F, Limite LR, Danti M, Sclafani M, et al. Myocardial oedema contributes to interstitial expansion and associates with mechanical and electrocardiographic changes in takotsubo syndrome: a CMR T1 and T2 mapping study. Eur Heart J Cardiovasc Imaging. 2023;24(8):1082-1091.

20 Puntmann VO, Valbuena S, Hinojar R, Petersen SE, Greenwood JP, Kramer CM, et al. Society for Cardiovascular Magnetic Resonance (SCMR) expert consensus for CMR imaging endpoints in clinical research: Part i - Analytical validation and clinical qualification. J Cardiovasc Magn Reson. 2018;20(1):67.

21 Dabir D, Child N, Kalra A, Rogers T, Gebker R, Jabbour A, et al. Reference values for healthy human myocardium using a T1 mapping methodology: results from the International T1 Multi-center cardiovascular magnetic resonance study. J Cardiovasc Magn Reson. 2014;16(1):69.

22 Camastra G, Arcari L, Ciolina F, Danti M, Ansalone G, Cacciotti L, et al. Characterization of COVID-19-Related Lung Involvement in Patients Undergoing Magnetic Resonance T1 and T2 Mapping Imaging: A Pilot Study. J Imaging. 2022;8(12):314.

23 Chacko L, Boldrini M, Martone R, Law S, Martinez-Naharrro A, Hutt DF, et al. Cardiac Magnetic Resonance-Derived Extracellular Volume Mapping for the Quantification of Hepatic and Splenic Amyloid. Circ Cardiovasc Imaging. 2021;14(4):E012506.

24 Hunter DJ, Holmes C. Where Medical Statistics Meets Artificial Intelligence. N Engl J Med. 2023;389(13):1211–1219.

Contact

Giovanni Camastra, M.D.
Cardiology Unit
Madre Giuseppina Vannini Hospital
Via di Acqua Bullicante, 4
00177 Roma RM
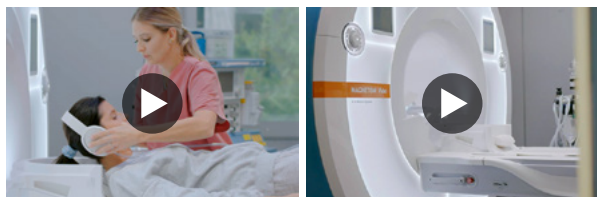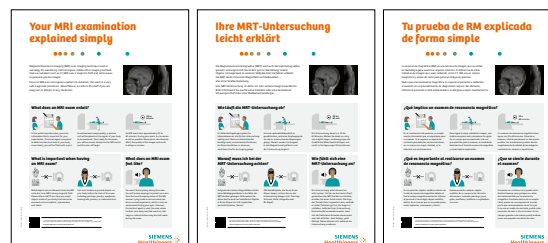Italy
gcamastra@virgilio.it

MRI Patient Education Toolkit

www.magnetomworld.siemens-healthineers.com/toolkit/mri-patient-education

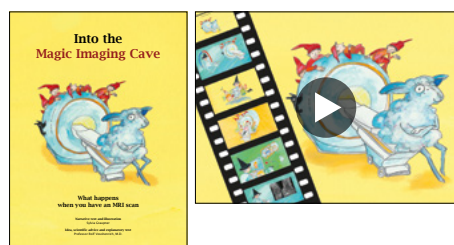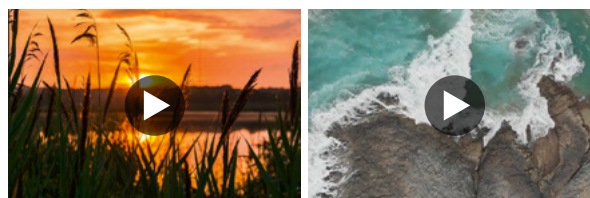## Patient Education Video

Patient Education Poster

## Children's Book and Movie

Patient Meditation

Meet Siemens Healthineers

Siemens Healthineers: Our brand name embodies the pioneering spirit and engineering expertise that is unique in the healthcare industry. The people working for Siemens Healthineers are totally committed to the company they work for, and are passionate about their technology. In this section we introduce you to colleagues from all over the world – people who put their hearts into what they do.

MunYoung Paek

MunYoung Paek graduated from Inje University in South Korea in 2000, majoring in computer science. Following her undergraduate studies, she pursued a specialization in MRI at the university's Graduate School of Medical Imaging Science. After earning her master's degree in 2002, she joined a Korean company that was developing a low-field 0.32T MRI system. This company was spun off from the medical device division of another domestic company, and developed the MRI scanner with its own technology, from hardware to software. For over eight years, MunYoung worked as a sequence developer in the R&D team, designing and developing routine MRI sequences for each body part, including b-SSFP in cardiac MRI. She joined Siemens Healthineers Korea in late 2010 and is currently a senior MR scientist responsible for research collaborations in cardiovascular and oncology MRI.

Seoul, South Korea
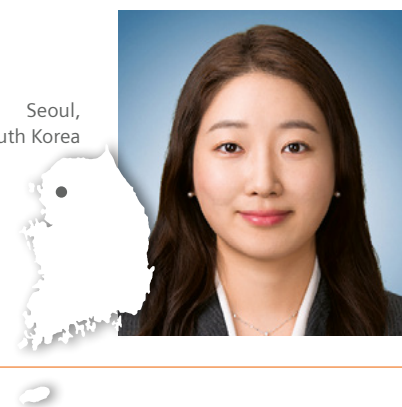
How did you first come into contact with MRI?

I first encountered cell and diagnostic scanner images while majoring in computer science and participating in research activities in a medical image processing laboratory. Perhaps it was fate, but as I approached graduation, the Graduate School of Medical Imaging Science was established through a collaboration between Computer Science and Biomedical Engineering. Intrigued by this interdisciplinary opportunity, I enrolled in the school to delve deeper into this field. This was where I met my supervisor, who had deep roots in MRI academia, and my journey into the world of MRI began.

What do you find motivating about your job?

My motivation has changed over time. In the early days of development, I was proud to be an engineer in a field that is rare in Korea, and proud that the sequences I made were being commercialized in the MRI scanner. Joining Siemens Healthineers has greatly expanded my horizons and has supported a variety of clinical research activities conducted by leading partners. My current motivation is the belief that I can have some meaningful impact in helping patients receive more accurate diagnoses in the future. When I hear that a disease was missed even after someone underwent MRI, I feel sad. This is because anyone can unexpectedly become a patient. These thoughts strengthen my commitment to helping advance medical imaging for the benefit of patients.

What are the biggest challenges in your job?

I have dozens of ongoing projects every year, so I often find it challenging to maintain deep focus on each individual project. Finding a balance between the quantity and quality of projects is important. I believe that actively supporting both capable researchers and the clinical research activities of customers in a variety of settings plays an important role in contributing to academia and accelerating the advancement of the technology.

What are the most important developments in CMR?

I think the most important factor in CMR is speed. In order to reduce high costs and promote CMR scanning, fast scans such as brain MRI and cardiac CT must be performed. The speed refers to total table time, not just acquisition time. This begins with attaching the ECG leads to the chest, with the patient on the table. The BioMatrix Beat Sensor, which doesn't require ECG leads, can be used in all routine cardiac protocols beginning with versions VA51 and VA60, and that makes me excited to think about the changes to the new cardiac MR scanning environment. myExam Cardiac Assist (formerly Cardiac Dot Engine) has already established itself as a reliable and essential tool for radiology technicians, thanks to its convenience during CMR scans. I believe that other technological developments such as Compressed Sensing acceleration, single-shot free-breathing techniques, deep learning image reconstruction, 3D imaging, and AI-assisted workflows will help to gradually increase the proportion of CMR exams.

What would you do if you could spend a month doing whatever you wanted?
Even just imagining that makes me happy. This is because I have worked without a gap for the past 21 years. I have so many things on my bucket list that I want to do, but I must choose only those that require a month. First, I want to train my body and mind by practicing yoga in Bali for a month. Alternatively, I would sign up for a 4-week mud-house building program in Korea. If it's a work-related opportunity, I would like to visit centers that perform and interpret MRI remotely (WeScan), which is challenging to introduce in South Korea because of our domestic health-care system. I'm also interested in visiting regions around the world where mobile MRI scanners are in operation.

Daniel Giese, Ph.D.

Daniel Giese studied physics and biomedical engineering in Germany at the Karlsruhe Institute of Technology (KIT), and in Grenoble, France, at the école nationale supérieure de physique, électronique et matériaux (ENSPG) and at Université Joseph Fourier (UJF) de Grenoble. After writing his diploma thesis in cardiovascular MR imaging in Freiburg, Germany, in 2008 (under Professor Hennig), he pursued a Ph.D. at King's College London (KCL), UK (under Professor Kozerke and Professor Schaeffter). This included a 1.5-year research stay at ETH Zürich in Switzerland. After a postdoc at KCL, Daniel moved to the University of Cologne, Germany, in 2013, where he later led an independent research group in MRI physics and obtained his Habilitation (postdoctoral lecturing qualification). He joined Siemens Healthineers in December 2018 as an application developer in the CMR Predevelopment Team, remaining active as a researcher while contributing to several widely used research packages. As Senior Key Expert he is responsible for driving a variety of predevelopment activities, including CMR at 0.55T.

Erlangen, Germany

How did you first come into contact with MRI?
My studies in Grenoble included several compulsory internships. I really wanted to go abroad and was fortunate to win a research internship at the University of Queensland in Brisbane, Australia, where I worked in Professor Graham Galloway's lab. My project consisted of building a torso coil for a human 4T system. I was incredibly impressed when I was able to acquire images (in a phantom) with a receiver coil that we had built and soldered from copper wires and some electronic modules within a few weeks. This was 2006 and it sparked my desire to continue working in the field of MRI.

What do you find motivating about your job?
Working in the cardiac MRI predevelopment group at Siemens Healthineers allows me to make a real impact in CMR. The interval between having an idea and seeing results in patients around the globe is as short as I can imagine it could ever be. This is partially because of the infrastructure, tools, and knowledgeable colleagues at Siemens Healthineers. But it's also thanks to our collaboration partners, who are highly motivated to try out new methods and give us feedback. This is crucial for bringing novel ideas into clinical routine. Another very motivating aspect of my job is my continuing active involvement in research societies such as SCMR, and the possibility to supervise and support talented young students during their studies and research projects.

What are the biggest challenges in your job?
The biggest challenge is managing my time effectively. I cannot convert every idea into reality. Although I do write down all my ideas in a notebook, I can only pursue a fraction of them. Another challenge is that my desire to try and understand the basic physics might slow down the successful completion of some projects.

What are the most important developments in CMR?
I think the most important acquisition and reconstruction developments in CMR are related to handling motion and acquiring quantitative images. Breathing and cardiac motion remain two of the biggest challenges in CMR, especially given the main assumption that ECG and breathing cycles are periodical. These assumptions, combined with the intrinsically long acquisition process in MRI, make the field of motion handling very active. From the development and introduction of the MR navigator in the early 1980s, to novel multidimensional and self-gating

approaches combined with motion-compensated reconstruction algorithms and deep-learning approaches, the sector has made an incredible leap toward unprecedented image quality. In a world where AI is increasingly used to interpret data, I think quantitative imaging is compulsory. Quantitative imaging goes together with a standardized acquisition, which is simplified by automation to reduce variance. In summary: fast, motion-robust, accurate, and quantitative CMR is the future.

What would you do if you could spend a month doing whatever you wanted?

I lived in Sub-Saharan Africa (Guinea, Niger, and Zimbabwe) until the age of 12. I'd like to revisit many of the places from my childhood with my family. And since one of the reasons I'm in my current job is to improve access to care, I am convinced that a trip like this would also allow me to add new ideas to my notebook – so I can keep working on predevelopment projects in this exciting field.

Get to know us

Michaela Schmidt

Erlangen,
Germany

Peter Speier, Ph.D.

Erlangen,
Germany

Solenn Toupin, Ph.D.

Bordeaux,
France

Dominik Nickel, Ph.D.

Erlangen,
Germany

Carmel Hayes, Ph.D.

Erlangen,
Germany

Find more portraits
of our colleagues
around the world!

www.magnetomworld.siemens-healthineers.com/meet-siemens-healthineers

The entire editorial staff at King's College London, UK, and at Siemens Healthineers extends their appreciation to all the radiologists, technologists, physicists, experts, and scholars who donate their time and energy – without payment – in order to share their expertise with the readers of MAGNETOM Flash.

Note in accordance with § 33 Para.1 of the German Federal Data Protection Law: Despatch is made using an address file which is maintained with the aid of an automated data processing system.

MAGNETOM Flash is sent free of charge to Siemens Healthineers MR customers, qualified physicians, technologists, physicists and radiology departments throughout the world. It includes reports in the English language on magnetic resonance: diagnostic and therapeutic methods and their application as well as results and experience gained with corresponding systems and solutions. It introduces from case to case new principles and procedures and discusses their clinical potential. The statements and views of the authors in the individual contributions do not necessarily reflect the opinion of the publisher.

The information presented in these articles and case reports is for illustration only and is not intended to be relied upon by the reader for instruction as to the practice of medicine. Any health care practitioner reading this information is reminded that they must use their own learning, training and expertise in dealing with their individual patients. This material does not substitute for that duty and is not intended by Siemens Healthcare to be used for any purpose in that regard. The drugs and doses mentioned herein are consistent with the approval labeling for uses and/or indications of the drug. The treating physician bears the sole responsibility for the diagnosis and treatment of patients, including drugs and doses prescribed in connection with such use. The Operating Instructions must always be strictly followed when operating the MR system. The sources for the technical data are the corresponding data sheets. Results may vary.

Partial reproduction in printed form of individual contributions is permitted, provided the customary bibliographical data such as author's name and title of the contribution as well as year, issue number and pages of MAGNETOM Flash are named, but the editors request that two copies be sent to them. The written consent of the authors and publisher is required for the complete reprinting of an article.

We welcome your questions and comments about the editorial content of MAGNETOM Flash. Please contact us at magnetomworld.team@siemens-healthineers.com

Manuscripts as well as suggestions, proposals and information are always welcome; they are carefully examined and submitted to the editorial board for attention. MAGNETOM Flash is not responsible for loss, damage, or any other injury to unsolicited manuscripts or other materials. We reserve the right to edit for clarity, accuracy, and space. Include your name, address, and phone number and send to the editors, address above.

MAGNETOM Flash is also available online:

www.siemens-healthineers.com/magnetom-world

Not for distribution in the US

On account of certain regional limitations of sales rights and service availability, we cannot guarantee that all products included in this brochure are available through the Siemens sales organization worldwide. Availability and packaging may vary by country and is subject to change without prior notice. Some/All of the features and products described herein may not be available in the United States.

The information in this document contains general technical descriptions of specifications and options as well as standard and optional features which do not always have to be present in individual cases, and which may not be commercially available in all countries.

Due to regulatory reasons their future availability cannot be guaranteed. Please contact your local Siemens organization for further details.

Siemens Healthineers reserves the right to modify the design, packaging, specifications, and options described herein without prior notice. Please contact your local Siemens sales representative for the most current information.

Note: Any technical data contained in this document may vary within defined tolerances. Original images always lose a certain amount of detail when reproduced.